I&EC research
Industrial & Engineering Chemistry Research
pubs.acs.org/IECR
Review

A Review on Lignin Liquefaction: Advanced Characterization of Structure and Microkinetic Modeling

Evan Terrell, Lauren D. Dellon, Anthony Dufour, Erika Bartolomei, Linda J. Broadbelt, and Manuel Garcia-Perez*

Cite This: *Ind. Eng. Chem. Res.* 2020, 59, 526−555

ABSTRACT: Lignin liquefaction microkinetics is a move toward a more first-principles (i.e., ab initio)-based understanding at the molecular level in reaction engineering. While the microkinetic modeling of reactions to obtain kinetic rate parameters of chemical reactions have been widely used in the field of gas phase combustion and heterogeneous catalysis, this approach has not been as thoroughly developed in the area of biomass thermochemical reactions (e.g., lignin pyrolysis, hydrothermal liquefaction). The difficulties in establishing the structure of complex heterogeneous materials, like lignin, is perhaps the main challenge in developing rational microkinetic descriptions of biomass thermochemical reactions. In this manuscript, we review the current state of the art and the challenges to develop microkinetic models for lignin liquefaction technologies (e.g., pyrolysis, hydrothermal liquefaction, solvolysis). A general strategy for the development of microkinetic models for lignin liquefaction technologies is discussed. The first hurdle is to obtain sufficiently rich experimental data of lignin underlying polymeric structure and methodologies to use this data to build realistic lignin structural representations. Some analytical techniques for lignin structural characterization and their associated data, as well as a correlation for calculating the degree of macromolecular lignin branching, are discussed. The presence of small lignin oligomeric structures and the role of these structures in lignin pyrolysis is also addressed. The ways in which elementary deconstruction and repolymerization reactions occur within this structure to form a liquid intermediate and how these deconstruction products continue to interact with each other until they are removed from the liquid intermediate is thoroughly discussed. Further, experimental work with model compounds and the effect of reaction parameters (e.g., temperature, pressure, vapor residence time) are reviewed. Another major challenge to develop microkinetic models of lignin liquefaction is to describe product removal mechanisms (e.g., evaporation, solubilization, thermal ejection) from the liquid intermediate. Group contribution methods are presented for estimation of thermophysical parameters, like normal boiling point and heat of vaporization for model structures. Once the products have been removed from the liquid intermediate, they continue reacting in the aerosol droplets, in vapor phase, or in the solvent depending on the liquefaction technology studied. These "secondary reactions" need to be included in realistic microkinetic models. Based on this review, we can state that with careful implementation, high-quality microkinetic models can be developed to simulate thermochemical lignin liquefaction.

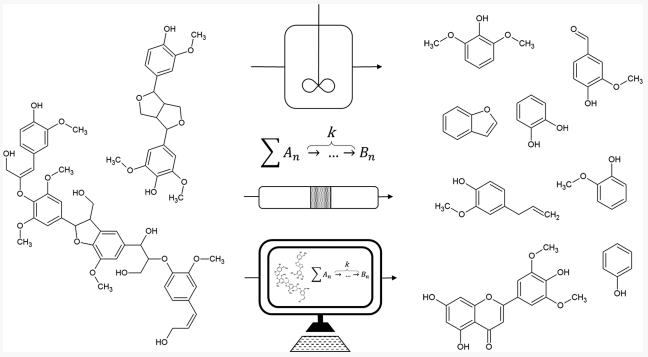

1. INTRODUCTION

With the growing demand for the utilization of lignocellulosic biomass, there is a corresponding increase in emphasis on the development of high-value products from biomass, specifically lignin, which is currently used most prominently as a low value fuel for process heat.[1] Lignin comprises approximately 15−30 wt % of woods and grasses, making it the second most abundant natural polymer in the world, behind cellulose.[1,2] Historically, lignin has inspired significant research, as it is a major byproduct of the pulp and paper industry, producing tens of millions of tons per year.[2,3] Lignin is also the primary byproduct of next-generation cellulosic biorefinery concepts that produce fuels and chemicals such as ethanol, butanol, olefins, succinic acid, acetic acid, glycerol, and sugar alcohols through fermentation technologies from cellulose.[4] Additionally, lignin is a major input into the coalification process and a significant geochemical precursor to coal.[5−7] Thus, a clear characterization of lignin depolymerization can have a strong impact on the foundational knowledge for bio- and thermochemical woody biomass conversion strategies. Due

Received: October 17, 2019
Revised: December 29, 2019
Accepted: December 29, 2019
Published: December 30, 2019

https://dx.doi.org/10.1021/acs.iecr.9b05744
Ind. Eng. Chem. Res. 2020, 59, 526−555

to these factors, there is a convincing need for continued research and development with respect to lignin biosynthesis, structural characterization, and implementation as a feedstock for the production of fuels, chemicals, and high-value materials.

Lignin is higher in carbon content, richer in aromatic subunits, and lower in oxygen content, rendering it particularly attractive for the production of fuels and chemicals.[8] Several technologies have been studied for the direct liquefaction of lignin, including fast pyrolysis (dry), solvolysis (organic solvents), and hydrothermal liquefaction (water). Fast pyrolysis is a promising technology for converting between 60 and 75 wt % of lignocellulosic materials into crude bio-oils.[9−12] While fast pyrolysis occurs under an inert environment, hydrothermal liquefaction utilizes water as a depolymerization reaction media, with temperatures and pressures between roughly 150−350 °C and 5−25 MPa, respectively.[13−15] Similarly, solvolysis systems use organic liquids, like alcohols, hydrocarbons, or oil refinery streams (such as vacuum gas oil and petroleum- or biomass-derived slurries/oils) to carry out thermochemical depolymerization reactions.[16−19] Close to 40 wt % of fast pyrolysis bio-oil could be further transformed into transportation fuels via hydrotreatment (i.e., hydrocracking and hydrodeoxygenation).[20,21] Pacific Northwest National Laboratory projected that a fast pyrolysis and bio-oil upgrading scheme can result in the production of 106 gallons of green gasoline and diesel per ton of biomass, with an estimated total annual yield of nearly 80 million gallons at a minimum selling price of $2.95 (adjusted to 2019 basis).[20,21] However, the presence of oligomeric pyrolytic lignin in fast pyrolysis oils (15−20 wt %) has been identified as one of the most important sources of catalyst-deactivating coke formation during bio-oil hydrotreatment.[22−24] The content of GC/MS-detectable monophenols in pyrolysis bio-oils is only between 1 and 4 wt % (Figure 1).[25,26,26,27]

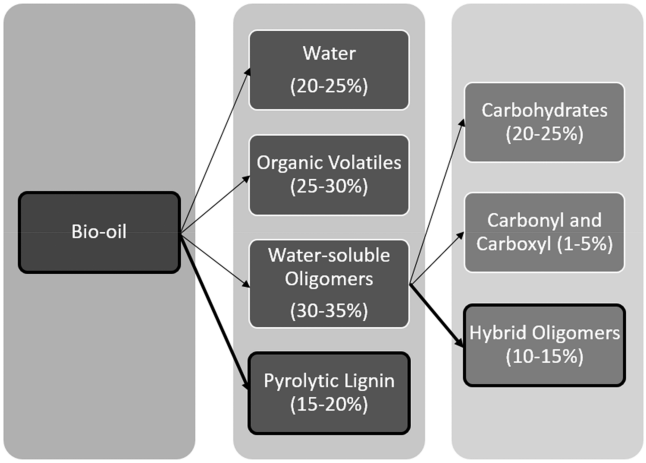

Figure 1. Breakdown of biomass-derived pyrolysis oil components.[26,27]

The mechanisms by which these oligomeric products are formed and removed from the reacting environment is a source of controversy.[28,29] There is little understanding of the relationship between the formation of these lignin oligomers and the characteristics of the original lignin.[30] Some experimental results promote the view that lignin oligomers are formed directly from the depolymerization of lignin[31−38] and subsequently removed from the liquid intermediate by evaporation or thermal ejection in the form of aerosols.[30,39−44] An alternative view suggests that lignin pyrolysis occurs through the formation of monophenols that further react to form oligomeric products.[28,45] The two outlooks are complementary, but the relative impact of these two pathways warrants further research.[28,29] Thus, it is critical to better understand the mechanism by which lignin monomeric and oligomeric products are formed and removed during the depolymerization of lignocellulosic materials and to identify strategies to enhance formation of high value monomeric products from lignin. Some main targeted compounds from lignin could be monomers, such as those given in Table 1.

To understand the mechanisms governing total product formation—such as various oligomer-yielding processes—it is necessary to take a generalized, holistic view of lignin thermochemical conversion. One emerging approach to achieve this is through the development of a microkinetic framework for describing thermochemical conversion. Microkinetic analysis has previously been used to study a wide array of subjects, including heterogeneous catalysis,[46,47] oxidation chemistry,[48−52] autoxidation,[53,54] and coal pyrolysis.[55−62]

Our overall goal is to review modeling and experimental research addressing components relevant to the creation of a microkinetic framework to describe lignin liquefaction reactions, with emphasis given to those methods that provide ready-to-use data for a computational lignin pyrolysis model. Because the chemical composition of lignin is ever-changing (in the plant, during extraction, and processing), there is a tendency to gradually form coal-like structures. Although there are several microkinetic models for coal pyrolysis (FG-DVC, FLASHCHAIN), in this review, we briefly use components of the Chemical Percolation Devolatilization (CPD) model developed for coal pyrolysis[65] as a source of inspiration for analysis of highly modified lignins.

2. MICROKINETIC FRAMEWORK

The information reviewed herein can be summarized in the physical models of lignin liquefaction (for pyrolysis and solvolysis) shown in Figure 2.[66−68] This model is used to guide our narrative. The reactions in solid phase lead to the formation of depolymerized oligomeric products that form a liquid intermediate. These reactions can also form small fragments which will be directly removed by evaporation in the case of pyrolysis or will be solubilized in the solvent in the case of solvolysis. The oligomeric materials will remain in the liquid intermediate until they further crack to form volatiles (in the case of pyrolysis), soluble compounds (in the case of solvolysis), or repolymerize to form char. These molecules can also be removed by thermal ejection in the form of aerosols in pyrolysis. Secondary reactions occur when depolymerization products leave the particle as gases or vapors in the aerosol droplets or when solubilized in the solvent (Figure 2).

Figure 3 summarizes a general strategy proposed for a microkinetic model of lignin liquefaction. Lignin pyrolysis microkinetics can be defined as an examination of elementary deconstruction reactions and physical steps that occur within a well-defined polymeric structure, as well as the relation of these deconstruction products to each other and their environment throughout the thermochemical conversion process (i.e., in the liquid intermediate, when removed from the liquid intermediate in vapor phase, as aerosol droplets, or in solution). As

https://dx.doi.org/10.1021/acs.iecr.9b05744
Ind. Eng. Chem. Res. 2020, 59, 526−555

Table 1. Some Lignin-Derived Monomers from Fast Pyrolysis and Their Molecular Weights and Experimentally Observed/Measured Normal Boiling Points (T_b)[36,42,63,64]

Name	Structure	Name	Structure
Guaiacol (124 g/mol) (T_b: 205 °C)	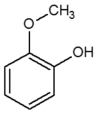	Creosol (138 g/mol) (T_b: 221 °C)	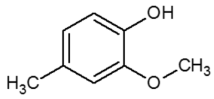
Phenol (94 g/mol) (T_b: 182 °C)	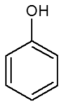	Eugenol (164 g/mol) (T_b: 254 °C)	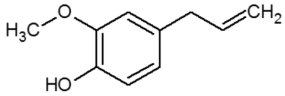
Syringol (154 g/mol) (T_b: 261 °C)	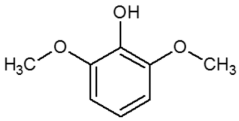	Vanillin (152 g/mol) (T_b: 285 °C)	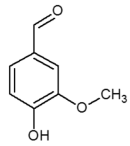
Catechol (110 g/mol) (T_b: 245 °C)	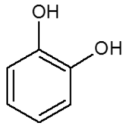	Anisole (108 g/mol) (T_b: 154 °C)	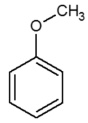

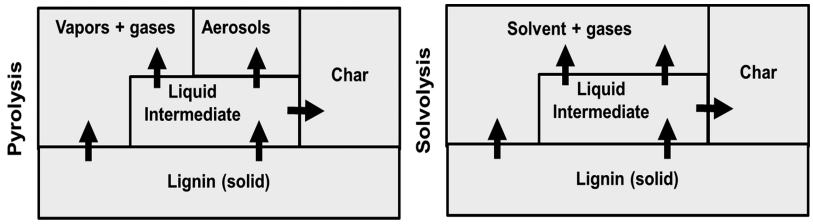

Figure 2. Physical model to describe liquefaction reactions in the presence (solvolysis) and absence (pyrolysis) of solvents.

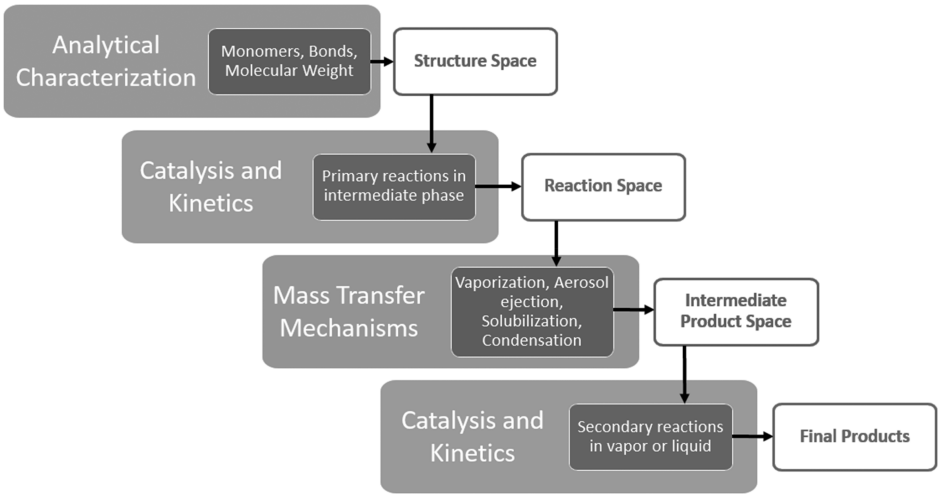

Figure 3. Microkinetic scheme of thermochemical lignin conversion.

such, a microkinetic approach is a move toward a comprehensive first-principles (i.e., *ab initio*) understanding of pyrolysis at the microscale and molecular level. The first major component of a microkinetic model is a well-defined lignin structure or library, which can be created from a comprehensive structural model.[3,69−71] In the case of the CPD model[65] to describe coal pyrolysis, the chemical structure of characterized coals was derived from the solid-state ^{13}C NMR measurements. In the CPD model, coal was described as a blend of small and large clusters. The small clusters can be

https://dx.doi.org/10.1021/acs.iecr.9b05744
Ind. Eng. Chem. Res. 2020, 59, 526−555

extracted using suitable solvents without breaking bonds. The large clusters are described as a large number of fused aromatic rings of different sizes connected by weak aliphatic bridges.[60] Properties characterizing a lignin structure include the distribution of monomers and interunit linkages, molecular weight distribution, and extent of branching. The presence of small oligomeric molecules within native lignin (i.e., potential conglomerates or clusters),[72−74] which could control the behavior of lignin during thermal depolymerization, also needs to be analyzed.

Next, the reaction kinetics are described by elucidating the elementary reactions for the thermal depolymerization of the input structure. In the case of the CPD model[65] for coal, the chemical reactivity of the bridges was critical to explain the formation of a reactive intermediate molecule, which can in turn break to form two side chains and condense to form a stable bridge with the concurrent release of gases. Finally, a description of how the primary intermediates ultimately transition—through solubilization, vaporization, or other mass transfer modes—into their final product form is determined. Because the products of lignin depolymerization change phases, these models have to take into account the removal mechanisms (e.g., evaporation, thermal ejection, solubilization, cross-linking, condensation), as well as the relevant heat transfer mechanisms that can have an effect on intraparticle phenomena during depolymerization.[75,76] This final transition phase can be quantified by a number of metrics, including vaporization rate governed by boiling point, oligomer formation rate governed by aerosol ejection intensity, or solubilization rate governed by solubility parameters. All these phenomena are controlled by the residence time and temperature of the biomass particle and the nature of its surrounding environment. In the case of the CPD model[65] for coal, the removal of volatiles is taken into account with a vapor pressure model combined with a flash distillation model. The microkinetic model should also include the secondary reactions in vapor phase, in aerosol droplets, and the reactions in the solvent. Each of these phenomena, in theory, can be well-described by different characteristic time expressions, governed by physical properties (e.g., length scale, viscosity, thermal conductivity), as shown by Dufour et al.[75] These secondary reactions are controlled by a second time scale (residence time of vapor, liquid, or aerosols in the reactor). This review focuses specifically on a microkinetic view of thermochemical lignin conversion. In light of this view, the central hypothesis of this review is that an explicit account of lignin structural characteristics and a detailed description of pyrolytic depolymerization and repolymerization phenomena together with the description of removal mechanisms (evaporation, thermal ejection, solubilization) and secondary reactions (in vapors, aerosol droplets, and solvents) will allow for the development of predictive models with the capacity to identify processing conditions to enhance desired thermochemical conversion products.

3. LIGNIN STRUCTURE OVERVIEW

Lignin, which serves as a continuous matrix for plant cell walls, is a polyphenolic material arising from free radical polymerization.[77,78] Its complexity has historically been attributed to its hyper-branched topology and diversity due to differences in biomass feedstock, isolation method, and characterization method.[71,72] To aid in the understanding of the structure and reactivity of lignin, it is often defined by four characteristics: monomer distribution, bond distribution, molecular weight distribution, and branching coefficient. The potential existence of native lignins being present as conglomerates (or clusters) of small molecules from monomers to oligomers, which can potentially influence its thermal behavior, also needs to be studied.[72−74] First, lignin is predominantly composed of three phenyl-propanoid monomers, shown in Figure 4: syringyl (S),

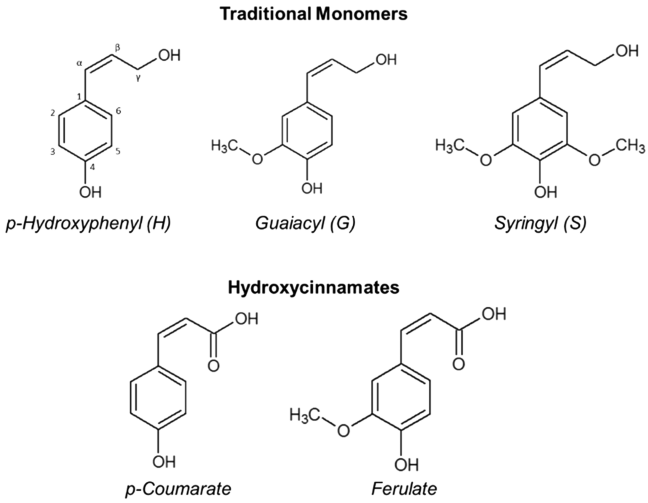

Figure 4. Representations of traditional lignin monomers and hydroxycinnamates, with labeling convention given on p-hydroxyphenyl; adapted from Dellon et al.[71]

guaiacyl (G), and p-hydroxyphenyl (H). Note that these units are often referred to as sinapyl, coniferyl, and p-coumaryl alcohol, respectively. A variety of other less common, though structurally similar, lignin units have also been identified, such as hydroxycinnamates (Figure 4), among others.[3,77,79,80] The monomer distribution varies significantly among the different types of feedstock. Softwood lignin (e.g., Douglas fir) predominantly contains G units, while hardwood lignin (e.g., hybrid poplar) comprises G and S units. Herbaceous biomass (e.g., grasses and crop residues) contains G and S units, with a higher percentage of H units and others, such as hydroxycinnamates.[80−83]

The well-known experimental fact, in nature, is that lignin is formed primarily from end-wise polymerization of H, S, and G units.[84] Other possible units (among a hypothetically ever-growing list) that can be incorporated to lignin structure are caffeyl alcohol, 5-hydroxy coniferyl alcohol, monolignol acetates, p-hydroxybenzoates, p-coumarates, ferulates, hydroxycinnamaldehydes, feruloyl amides, tricin, and hydroxystilbenes.[78] More specifically, these units are quasi-stochastically conjugated, through a variety of linkages, to produce a highly amorphous, three-dimensional polymer that is both physically and chemically heterogeneous.[85,86] These linkages include a variety of relatively weak interunit ether (β-O-4, α-O-4, and 4-O-5) and strong carbon−carbon bonds (β-1, β-5, 5-5, β-β).[71] The distribution of these bonds in a lignin molecule is a key characteristic and significantly contributes to the observed chemistry. The presence of these weak and strong bonds opens the door to a description of lignin structure by clusters—oligomeric units with ether and/or ester covalent links[87]—that could be used to describe lignin thermal behavior. The widely accepted polymerization process for lignin construction involves oxidative radicalization of phenols, followed by

https://dx.doi.org/10.1021/acs.iecr.9b05744
Ind. Eng. Chem. Res. 2020, 59, 526−555

combinatorial radical coupling.[84] The most common linkage that results from this process is β-O-4, accounting for approximately 60% of the total bond types.[88] Dimers from radical coupling are then dehydrogenated to form more phenolic radicals and are coupled with another lignin monomer. In this way, the overall lignin polymer unit grows one unit at a time, through end-wise coupling. Other polymerization routes include coupling between two lignin oligomers or through cross-linking reactions. Further information regarding polymerization and lignin biosynthesis can be found in excellent published reviews.[77,78,82,89,90] Lignin polymers are also defined by their molecular weight distribution, both number-average and weight-average, and their branching coefficient, which is defined as the number of monomers with three or more bonds divided by the total number of monomers.[91−94] Whether or not native lignin is actually branched is questionable, especially due to its proposed oligomeric nature.[72,87,95]

Structural representations of lignin have advanced significantly over the years. Early work proposed a single average representation of a lignin macromolecule for a single biomass source. This includes a representation of spruce lignin developed by Freudenberg,[96] a softwood model proposed by Sakakibara,[97] and a birch model presented by Adler.[98] Additionally, Glasser et al. developed a computational method for the generation of one average representation of a lignin molecule.[99] However, a single representation of a lignin molecule, matching bulk experimental values, does not consider the diversity among lignin molecules.[100] Alternatively, Faulon proposed a stochastic method to generate lignin representations whose average characteristics agree with experimental observables; in total he produced 10 random polymers each containing 27 monomers (although the possibility of nearly 1.5 million possible structural models is suggested).[101] Similarly, Yanez et al.[70] and Dellon et al.[71] developed a stochastic method for generating libraries of structural representations of lignin, both linear and hyperbranched, for any given feedstock with the four experimental characteristics discussed. Recently, this work has been extended by Vermaas et al. to computationally build three-dimensional lignin structures that are suitable for simulation and material property exploration.[3]

It is important to note that before lignin can be structurally characterized, it must be isolated from whole biomass. Two of the most commonly employed industrial methods are Kraft[88,102] and organosolv pulping.[103,104] As mentioned, different extraction or isolation methods yield unique lignin structures, even from the same feedstock, due to the chemical effects of the extraction process on the underlying lignin structure.[72,105] Among a variety of isolation methods, it is typically accepted that the Bjorkman method yields the least-altered lignin, often referred to as "milled wood lignin", that is among the most representative of the native material.[42,106,107] Methods discussed here to characterize lignin include Py-GC/MS, derivatization followed by reductive cleavage (DFRC), nuclear magnetic resonance (NMR) spectroscopy, and gel permeation chromatography (GPC). A more complete review of qualitative and quantitative assessment of lignin can be found in the excellent, in depth article from Lupoi et al.[108] Because lignin structure is always changing (in the plant, during extraction, and processing) a conceptual framework to describe the chemical structure of modified lignins should be developed. Coal structure based on ^{13}C NMR analyses used in the CPD model[60] is a good reference. In this model, coal was described as blend of small molecules extractable with solvents and macromolecules formed by clusters of fused aromatic rings with attached side chains connected by weak aliphatic bridges.[60] This abstract representation of coal structure is similar to the lignin representation described by Hou et al. as a set of single-ring aromatics with two attributes (type of propanoic side chain and the nature of methoxy phenol).[109] Chua et al. used THF extraction as a means to quantify low and high molecular weight lignin fractions.[110] The authors showed that most of the carbon residue formed is due to the high molecular weight fraction.

4. METHODS FOR QUANTIFICATION OF KEY CHARACTERISTICS

4.1. Monomer Distribution: Py-GC/MS and DFRC. Analysis of lignins with pyrolysis-GC/MS (Py-GC/MS) is a sufficiently robust, yet relatively simple thermo-degradative procedure to assess monomer percentages. In a typical Py-GC/MS procedure, the sample is pyrolyzed at a specified temperature and heating rate, and the products flow on to a gas chromatography column and are analyzed directly by GC/MS. Then, key structural characteristics of the monomeric products can be identified, so as to assign them to their primary origin monolignols (H, S, G units).[111−116] For example, phenol can originate from an H unit (zero $-OCH_3$), vanillin from a G unit (one $-OCH_3$), and syringol from an S unit (two $-OCH_3$). More origin monomer assignments are given in the Supporting Information, which although do not make up an exhaustive list, can be used as illustrative examples. These assignments are based on several previously reported results in literature.[111−117]

Care must be taken, however, to avoid incorrectly assigning Py-GC/MS-observed products to H, S, or G units when they could in fact be derived from hydroxycinnamates. This is especially true for grass lignin, for which a more appropriate monomer percent estimation could be achieved by disregarding p-hydroxycinnamate-derived vinyl compounds, including 4-vinylphenol, 4-vinylsyringol, and 4-vinylguaiacol.[115,116] Once all relevant Py-GC/MS products have been assigned to H/S/G monolignols, then the overall monomer percent can be determined from the relative abundance of each H, S, or G constituent peak in the GC/MS spectrum. The limitations of this method lie in uncertainty surrounding the presence of secondary reactions during Py-GC/MS, which can be due to reactor geometry or particle size, as well as variations in the reactivities of H, G, and S-type monomers.[112,117] Additionally, Py-GC/MS is only able to quantify volatile species during pyrolysis, so there is a distinct possibility that some important structural information can be overlooked due to the inability of this method to probe the nature of char-forming reactions and oligomeric products.

Another powerful tool for assessing the monomer distribution of a lignin sample is through the derivatization followed by reductive cleavage (DFRC) protocol, developed by Lu and Ralph.[118,119] In this method, lignins are first derivatized/solubilized using an acetyl bromide/acetic acid solution, and then, β-aryl ether bonds undergo reductive cleavage using zinc powder. The residue is then acetylated and dissolved in methylene chloride prior to analysis by GC/TCD/FID and/or GC/MS. Complete details of the full analytical procedure can be found in a series of papers by Lu and Ralph.[118,119] In one study using their method, Lu and Ralph

https://dx.doi.org/10.1021/acs.iecr.9b05744
Ind. Eng. Chem. Res. 2020, 59, 526−555

Table 2. Percentage of β-Linkages for Some Different Lignin Feedstocks from NMR Analysis

Feedstock (separation)	Type	ref	β-O-4[b]	β-5[c]	β-1[d]	β-β[e]
Black spruce (MWL[a])	Softwood	139	49	13	1	6
Norway spruce (MWL[a])	Softwood	139	45	11	1	3
Beech (MWL[a])	Hardwood	139	60	1	3	8
Paulownia fortunei (MWL[a])	Hardwood	126	62	11	3	12
Eucalyptus globulus (MWL[a])	Hardwood	128	69	3	3	18
Miscanthus (dioxane)	Grass	121	77	11	3	4
Wheat straw (MWL[a])	Grass	116	68	15	0	17

[a]Milled wood lignin; (b−e) the following are also known as. [b]β-aryl-ether. [c]Phenylcoumaran. [d]Spirodienone and diarylpropoane. [e]Resinol, as these are subunits containing the specified bonds.[120,123,140]

Table 3. Molecular Weight Characteristics and Monomer Distributions for Selected Feedstocks

Feedstock	ref	Type	M_n	M_w	PDI	H[a]	G	S
Spruce	147	Softwood	6400	23,500	3.67	2	98	0
Douglas fir	140	Softwood	2500	7400	2.96	6	94	0
Redwood	140	Softwood	2400	5900	2.46	5	95	0
White fir	140	Softwood	2800	8300	2.96	4	96	0
Pine	140	Softwood	4700	14,900	3.17	2	98	0
Hemlock[b,e]	91	Softwood	1800	20,690	11.5	–	–	–
Poplar[c]	147	Hardwood	4180	13,250	3.17	0	37	63
Poplar[d]	151	Hardwood	1310	3550	2.71	0	31	69
Beech	71	Hardwood	3690	5510	1.49	0	64	36
Birch[e]	71	Hardwood	1880	4600	2.45	0	50	50
Eucalyptus	140	Hardwood	2600	6700	2.58	2	15	83
Aspen[b,f]	152	Hardwood	2120	16,000	7.55	–	–	–
Cottonwood[b,e]	92	Hardwood	3700	23,540	6.36	–	–	–
Saltcedar[g]	153	Hardwood	2160	3750	1.74	2	37	61
Switchgrass	154	Grass	2070	5100	2.46	35	53	12
Alfalfa	145	Grass	4100	6000	1.46	5	56	39
Wheat straw[h]	116	Grass	1850	4210	2.28	6	64	30
Corn stover[h]	155, 156	Grass	19,070	22,680	1.19	4	35	61
Cotton stalk[g]	157	Grass	700	1520	2.17	1	59	40
Miscanthus	147	Grass	8300	13,700	1.65	4	52	44

[a]If only S:G ratio was provided, H was taken to be zero. [b]Monomer distributions not available in literature reference. [c]*P. euramericana*. [d]*P. tomentsa*. [e]Analytical instrument details unavailable in original reference. [f]DMSO solvent. [g]Refractive index detector. [h]DMF solvent

were able to successfully quantify the H/S/G ratio for six different feedstocks (pine, willow, aspen, kenaf, bamboo, bromegrass), and they report good agreement with separate thioacidolysis lignin monomer analysis, although with much higher overall molar yields for DFRC.[119] In a study using both py-GC/MS and DFRC, Del Río et al. reported good agreement between the two methods, with each giving an S/G ratio for their lignin of 0.5.[116]

4.2. Bond Type Distribution: NMR Spectroscopy. A commonly employed technique to assess lignin structure is NMR,[115,120−128] and a review of NMR lignin characterization is beyond our scope. However, further detailed reading can be found elsewhere.[129−133] NMR is capable of probing the nature of ^{1}H and ^{13}C nuclei in a given molecular structure, with 2D techniques, like heteronuclear single/multiple quantum coherence (HSQC/HMQC) NMR, allowing for the assessment of heteronuclear (e.g., C−H bonds), multiple-bond, or through-space correlations that may exist in a structure. NMR techniques are able to resolve lignin structural characteristics because different relevant lignin subunits—whether they be dimers containing specific interunit linkages (e.g., phenylcoumaran, resinol, spirodienone) or monomers themselves (i.e., H, S, G derivatives)—have different and identifiable chemical shifts within the NMR spectra (Supporting Information).[132] ^{13}C NMR chemical shift values for many lignin monomers, dimers, trimers, and tetrameters and bond types can be found in the NMR Database of Lignin and Cell Wall Model Compounds, available online,[133] and from Capanema et al.,[129] among numerous other sources. Some advantages of lignin analysis by NMR are the nondestructive and noninvasive nature of the technique, enhanced resolution from multidimensional methods, and unparalleled availability of structural information. However, NMR analysis does suffer from low-throughput, general lack of sensitivity, and high instrumentation cost.[108] The frequency of β-linkages in some NMR-analyzed lignin structures is given in Table 2. While these do not necessarily add up to 100% of all linkages in the structure, the β-linkages themselves generally account for the majority of all interunit lignin bonds. In addition to determining bond distributions, NMR, like Py-GC/MS and DFRC, is also capable of resolving lignin monomer percentages. Although not discussed in depth here, ^{31}P NMR is also a powerful and convenient tool for quantifying lignin monomers and other structural details regarding the nature of OH groups in the lignin sample.[134−136] Simulated ^{13}C NMR spectra are available in the Supporting Information, for example, resinol and phenylcoumaran structures.[137,138]

https://dx.doi.org/10.1021/acs.iecr.9b05744
Ind. Eng. Chem. Res. 2020, 59, 526−555

4.3. Molecular Weight: Gel Permeation Chromatography. The molecular weight characteristics (i.e., number-average (M_n) and weight-average (M_w) molecular weight) are important to the overall lignin structure, as the molecular weight distribution encodes the degree of polymerization of the polymeric structure. This is particularly important for establishing a termination criteria during computational structure generation.[70,71] Additionally, the ratio M_w/M_n, known as the polydispersity index (PDI), can be used in a correlation to determine the degree of branching, as presented in Section 4.4. One technique to measure molecular weight for lignin (and many other polymers) is through GPC. A typical GPC procedure involves dissolution of milligram quantities of lignin in a solvent like tetrahydrofuran (in spite of potentially limited solubility[141]), which is then injected into the GPC instrument at a flow rate of approximately 1 mL/min. Molecular weight data analysis is based on calibration with polystyrene standards, covering weights of magnitude roughly 10^2 to 10^6 Da.[141−146] A very good GPC protocol, with discussion of analytically important aspects of GPC measurements, can be found in a recent paper from Lange, Rulli, and Crestini.[141] Some advantages of GPC analysis are its broad molecular-weight range detection capabilities, low quantities of sample needed for analysis, and generally fast processing times, on the order of hours per sample.[147] However, the quality of the measurement depends on the calibration with appropriate standards, which is a nontrivial problem with GPC analyses of lignin. The most common standards used in the literature to calibrate lignin are polystyrene or polystyrenesulfonate (for lignosulfonate).[148−150] There are also discrepancies between GPC and mass spectrometry-based methods for measuring lignin molecular weights.[72] The GPC-derived molecular weight data for 20 different feedstocks, as well as their monomer distributions, are given in Table 3. The majority of these data were collected using GPC with UV detector and THF solvent.

4.4. Branching Coefficient Correlation. Unlike monomer distribution, bond type distribution, and molecular weight, which can be experimentally measured with various analytical techniques, to date, there is at present no clearly defined or widely accepted way to arrive at a value for the degree of branching in a lignin structure. Further, there is some disagreement in the literature as to whether lignin is even branched at all, with some sources reporting that lignin can be a linear molecule, at least more so than is typically conceptualized.[95,125,141,158]

The foundational work on the theoretical development of a so-called branching coefficient (α) for a polymer was given by Flory.[159,160] From Flory's work, Pla and Yan extended the concept of a branching coefficient to a lignin biopolymer.[93,94] The necessary inputs to their algorithm are the number-average molecular weight (M_n), the weight-average molecular weight (M_w), and the molecular weight of an average monomeric subunit (M_0). The final parameter, M_0, can be estimated or approximated from the monomer distribution, by assuming that H, G, and S units have weights of 150, 180, and 210 Da, respectively, or from carbon/hydrogen/oxygen elemental analysis. This is achieved by assuming an average $C_9H_xO_y$ formula for a lignin monomer and appropriately determining the relative proportions of hydrogen and oxygen from elemental analysis data.[161] For example, if a lignin sample has H:G:S of 5:45:50, then M_0 is 193.5 Da. If a sample has 60.0% C, 5.5% H and 35.5% O, then its average formula is $C_9H_{9.9}O_{3.8}$ with a weight of 180 Da.

Following the calculations described by Pla and Yan, one arrives at a system of nonlinear equations that can be solved numerically for two new governing parameters, which themselves are an input into a simple equation for α.[93] The calculated α value can be interpreted as the probability with which a given monomeric subunit of the lignin polymer is linked to more than two other subunits. Subunits with only one linkage can be thought of as terminal units. Single-linkage terminal units do not constitute an instance of branching when calculating branching probability. A "polymer" with only one-linkage subunits must necessarily be a dimer with $\alpha = 0$. Subunits with two linkages are linear, and any with more than two linkages are therefore instances of branching. A polymer featuring exclusively two-linkage subunits would be purely linear; i.e., $\alpha = 0$. In some cases, it is possible for numerical solution to converge on a negative value for cross-linking density, a governing parameter used for calculating α,[93] resulting in a calculated negative value for α. However, the minimum theoretical possible value for this governing parameter is zero, resulting in a calculated branching coefficient value of $\alpha = 0$. Additionally, probability in this case must be non-negative with a minimum possible value that has been shown to approach zero.[162,163] This limitation of the model arises when relying on numerical solution, and so here, negative calculated values for α are taken to be equal to zero; i.e., the polymer is linear.

In an attempt to systematically quantify the degree of branching, these calculations were carried out for the 20 feedstocks in Table 3. We found that there is a correlation between the reciprocal dispersity index (PDI^{-1}) and the calculated branching coefficient (α) for the analyzed feedstocks. This is depicted in Figure 5 and Table 4.

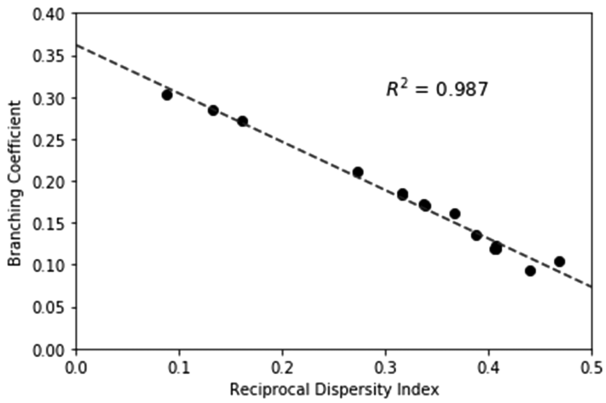

Figure 5. Correlation between the reciprocal dispersity index and branching coefficient (negative or zero calculated branching coefficient values omitted in the graph) [Data derived from references in Tables 3 and 4].

The trend shown in Figure 5 is an indication that more nonuniform lignin structures appropriately have a higher degree of branching. Lignin structures with PDI < 1.59 have $\alpha = 0$, of which three of five are grasses, and are therefore effectively linear polymers. PDI has a theoretical lower bound value of 1 and can be arbitrarily large. Therefore, PDI^{-1} is contained on the interval (0, 1). The correlation equation to find α is given in eq 1 and is calculated to have an upper bound of approximately 0.36, with a grand mean value of approximately 0.13 for the analyzed data.

https://dx.doi.org/10.1021/acs.iecr.9b05744
Ind. Eng. Chem. Res. 2020, 59, 526−555

Table 4. Dispersity Index and Branching Coefficients for Lignins of Selected Feedstocks

Feedstock	ref	Type	PDI	PDI^{-1}	α
Spruce	147	Softwood	3.67	0.27	0.21
Douglas fir	140	Softwood	2.96	0.34	0.17
Redwood	140	Softwood	2.46	0.40	0.12
White fir	140	Softwood	2.96	0.38	0.17
Pine	140	Softwood	3.17	0.32	0.18
Hemlock	91	Softwood	11.5	0.09	0.30
Softwood mean values			*4.45*	*0.30*	*0.19*
Poplar[a]	147	Hardwood	3.17	0.32	0.18
Poplar[b]	151	Hardwood	2.71	0.37	0.16
Beech	71	Hardwood	1.49	0.67	0.00
Birch	71	Hardwood	2.45	0.41	0.12
Eucalyptus	140	Hardwood	2.58	0.39	0.14
Aspen	152	Hardwood	7.55	0.13	0.29
Cottonwood	92	Hardwood	6.36	0.16	0.27
Saltcedar	153	Hardwood	1.74	0.57	0.00
Hardwood mean values			*3.50*	*0.38*	*0.15*
Switchgrass	154	Grass	2.46	0.41	0.12
Alfalfa	145	Grass	1.46	0.68	0.00
Wheat straw	116	Grass	2.28	0.44	0.09
Corn stover	155, 156	Grass	1.19	0.84	0.00
Cotton stalk	157	Grass	2.17	0.46	0.10
Miscanthus	147	Grass	1.65	0.61	0.00
Grass mean values			*1.87*	*0.57*	*0.05*

[a]*P. euramericana.* [b]*P. tomentsa.*

$$\alpha = f(\mathrm{PDI}^{-1}) = \begin{cases} -0.58 \times \mathrm{PDI}^{-1} + 0.36, & \text{if } \mathrm{PDI}^{-1} < 0.63 \\ 0, & \text{if PDI} \geq 0.63 \end{cases} \quad (1)$$

Further, it was found that among biomass types (i.e., hardwood, softwood, grass), there is a statistically significant difference ($p < 0.05$) in the means for reciprocal dispersity and branching coefficient between grass and softwood, with hardwood having intermediate values. Grass lignins tend to be more uniform (lower PDI) and linear (lower α), while softwood lignins tend to be more nonuniform (higher PDI) and branched (higher α). In general, the branching coefficient values for the analyzed data follow the trend: grass < hardwood < softwood. These results are summarized in Table 5. The relative reactivity and stability of bio-oils derived from these feedstock categories also differs.[164]

There is a relatively intuitive explanation for the more highly branched nature of softwood. It has been shown computationally that there is a strong correlation between higher branching coefficients and the prevalence of 5-5 linkages between lignin subunits.[71] Softwood lignins are made primarily of only guaiacyl units and have virtually zero syringyl units and very few p-hydroxyphenyl units (Table 3). It is physically impossible for a 5-5 linkage to occur on a syringyl lignin unit because the 5-position is occupied by a methoxy group (Figure 4). Therefore, lignin polymers with a higher guaiacyl monomer content than syringyl—as is the case for softwoods compared

Table 5. Kinetic Parameters for Pyrolysis of Different Model Compounds[a]

Substrate	Pyrolysis Products	$Log_{10}(A)$[b]	E_a[c]
Phenethylphenyl ether	1. Phenol, Styrene	11.1	188
	2. Styrene → Ethylbenzene, Toluene, Benzene	5.0	92
Guaiacol	1. Methane, Catechol	10.9	183
	2. Carbon monoxide, Phenol	11.5	198
Veratrole	1. Methane, Guaiacol	13.9	25
	2. Carbon monoxide, Methane, Phenol	14.1	244
	3. Carbon monoxide, Anisole	14.0	251
	4. Carbon monoxide, Cresol	11.2	206
Cinnamaldeyde	1. Carbon monoxide, Styrene	12.1	202
	2. Dimers	8.6	141
Salicyl alcohol	1. Water, o-Quinone methide	13.4	140
Cinnamyl alcohol	1. Cinnamaldhehyde	4.2	91
Syringol	1. Methane, Methoxycatechol	10.4	177
	2. Cabon monoxide, Guaiacol	11.1	190
Isoeugenol	1. Methane, Propenyl catechol	10.8	179
	2. Carbon monoxide, Propenyl phenol	11.3	193
Vanillin	1. Methane, Dihydroxybenzaldehyde	12.2	198
	2. Carbon monixde, Guaiacol	10.2	161
Acetophenone	1. Toluene, Carbon monoxide	10.9	236
	2. Benzene	9.6	211
o-Hydroxy-diphenylmethane	1. Toluene, Phenol	14.8	302
Phenyl ether	1. Benzene, Phenol	14.8	302
Cinnamic acid	1. Carbon Dioxide, Styrene	8.0	30
Ferulic acid	1. Carbon Dioxide, Vinylguaiacol	5.2	83
Anisole	1. Methane, Phenol	13.0	229
	2. Carbon monoxide, Benzene	14.5	255
	3. Cresol	7.9	169
Benzaldehyde	1. Benzene, Carbon monoxide	9.5	174

[a]Adapted from Klein and Virk.[5] [b]A = Pre-exponential factor, units s^{-1}. [c]E_a = Activation energy, units kJ/mol.

https://dx.doi.org/10.1021/acs.iecr.9b05744
Ind. Eng. Chem. Res. 2020, 59, 526−555

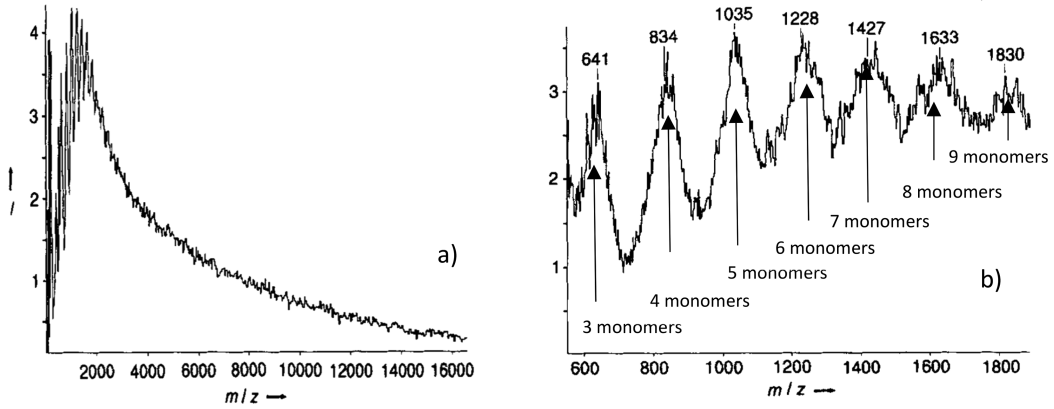

Figure 6. MALDI mass spectrum of birch lignin (a) whole spectrum and (b) fine structure in the range of 600 to 1830 Da; from Metzger et al.[173]

to both hardwoods and grasses—should exhibit more branching.

This explanation regarding 5-5 linkages is not valid when comparing the linearity of grasses (more linear) and hardwoods (more branched) alone. Grasses, like hardwoods, also have a higher syringyl content than softwood. However, grass lignins have a higher content of hydroxycinnamates (Figure 4), which can account for up to 3%−4% of the lignin content in addition to the "traditional" monolignols.[80] These constituents are not prevalent in woody biomass. There is evidence to suggest that ferulates can act as nucleation sites for lignin formation, and in the case of p-coumaric acid, Hatfield et al.[83] suggest two possible scenarios, quoted here directly: "(1) to act as a termination molecule for a developing lignin polymer and (2) to contribute to enhancing the linear or less reticulated nature of syringyl type lignin found in grasses". The prevalence of tricin and the nature in which the lignin-carbohydrate complex forms within grass lignins is also different from that in woody lignins.[165,166] Considering the contrasts between grass and hardwoods, it is postulated that these unique properties of grass lignins offer a phenomenological explanation for their more uniform (i.e., lower dispersity index) nature. This leads directly to a lower branching coefficient and more linearity in grass lignins.

4.5. Oligomeric Constituents Analyzed with Mass Spectroscopy. Several papers have been published on the use of mass spectroscopy to support lignin sequencing.[167−172] In a very important pioneering work, Metzger et al. used matrix-assisted laser desorption-ionization (MALDI) mass spectrometry to study milled wood lignin from birch and Chinese redwood lignin.[173] Figure 6 shows the molecular weight distribution of the lignin fragments/molecules from several hundreds to 16,000 Da with a center of gravity (M_n) close to 2600 Da, along with the fine structure of the mass spectrum.[173] The most interesting feature of this figure is the presence of clear peak divisions up to 2000 Da which can be assigned to oligomeric molecules (or lignin fragmentation clusters) covering from trimers (close to 600 Da) to 9-unit oligomers (close to 1830 Da). The authors estimated an average formula weight for birch lignin between 204 and 214 Da per phenylpropane unit of these oligomers. In the case of the Chinese redwood, the average formula weight for the phenyl propane unit was 190 Da, explainable by the almost exclusive presence of guaiacyl propane units in this lignin.[173]

Morreel et al. proposed for a first time a sequencing strategy for lignin oligomers using mass spectrometry. The authors observed 134 unique lignin oligomers from trimers to hexamers. Only 36 were completely sequenced.[169] Some of the oligomeric structure identified includethe following: Dimers (1) G(β-O-4)G, (2) G(β-5)G, (3) G(β-β)G. Trimers (1) G(β-O-4′)G(β-O-4′)G, (2) G(β-O-4′)S(β-5)G, (3) G(β-O-4′)S(β-β)G, (4) G(β-O-4′)S(β-5)$G^{glycerol}$, (5) G(β-O-4′)S(β- β)G, (6) S(β-O-4′)G(β-5)G, (7) G(β-O-4′)S(β-5)G′, (8) G(β-O-4′)S(β-5)G′, (9) G(β-O-4′)S(β-β)G, (10) G(β-O-4′)S(β-β′)S, (11) G(eβ-O-4′)S(β-β)S, (12) S(β-O-4′)S(β-β′)S, G(β-O-4′)S(β-5)V′. Tetramers (1) S(β-O-4′)S(β-β)S(β-O-4′)G, (2) S(β-O-4′)S(β-β′)S(β-O-4′)G, (3) G(β-O-4′)G(β-O-4′)G(β-β′)G, (4) G(β-O-4′)G(β-O-4′)G(β-5)G, (5) G(β-O-4′)G(β-β′)G(β-O-4′)G, (6) G(β-O-4′)G(β-5)G(β-O-4′)G, (7) G(β-5)G(β-O-4′)G(β-O-4′)G. Pentamers (1) G(β-O-4′)G(β-O-4′)G(β-O-4′)G(β-O-4′)G. Based on these results, the authors identified seven of the following lignin oligomer construction units: (1) G unit, derived from coniferyl alcohol, (2) S unit, derived from sinapyl alcohol, (3) G′ unit, derived from coniferaldehyde, (4) S′ unit, derived from sinapaldehyde, (5) V′ unit, derived from vanillin, (6) SP unit, derived from sinapyl p-hydroxybenzoate, and (7) $G^{glycerol}$ unit, derived from guiacyl-glycerol unit.[169] Kiyota et al. used commercially available enzymes, standards, and reagents to build a library of lignin oligomers. The authors synthesized several model lignin oligomers: Dimers (1) H(β-5)H, (2) H(β-β)H, (3) G(β-5)H, (4) G(β-5)G, (5) G(β-β)G, (6) G(β-O-4)G, (7) S(β-5)G, (8) S(β-5)G, (9) S(β-β)G, (10) S(β-O-4)G. Trimers (1) H(β-5)H(β-O-4)G, (2) G(β-5)G(β-5)G, (3) G(β-O-4)G(β-5)G, (4) G(β-O-4)G(β-O-4)G, (5) G(β-O-4)S(β-5)G, (6) S(β-O-4)G(β-5)G, (7) G(β-O-4)G(β-O-4)S, (8) S(β-O-4)S(β-5)G, (9) G(β-O-4)S(β-β)S, (10) S(β-O-4)G(β-O-4)S, (11) S(β-O-4)S(β−β)S, (12) S(β-O-4)S(β-O-4)S, (13) S(β-O*-4)S(β-β)S(β-O-4)Sb here.[73] Banoub et al., based on a review of mass spectroscopy data reported in the literature, concluded that lignin is composed of vast series of linear related oligomers, having different lengths covalently linked with cellulose and hemicellulose by either ether or ester covalent bonds, forming the network of vegetal matter. Essentially, they propose that what we call lignin is a blend of different length linear-related biosynthesized oligomers linked with cellulose or hemicellulose.[72,87]

5. KINETIC MODELING

Early kinetic models studied pyrolysis of whole lignin to develop empirical correlations capturing the rate of lignin conversion into volatile species. For example, Klein and Jegers

https://dx.doi.org/10.1021/acs.iecr.9b05744
Ind. Eng. Chem. Res. 2020, 59, 526−555

studied whole lignin pyrolysis using Kraft lignin to estimate rate constants for the decomposition of three catechol monomer and four guaiacol monomer species.[174] In similar work, Nunn et al. developed the kinetic rate constants for the evolution of several milled wood lignin pyrolysis products including CO, CO_2, H_2O, CH_4, and other light hydrocarbons.[175] More recently, Ojha et al. studied fast pyrolysis of alkali lignin with analytical pyrolysis and FTIR to derive global kinetic parameters.[176] The studies mentioned are limited by scope in that they can only estimate the rate parameters for a small number of species. In addition, developing empirical correlations from whole lignin is difficult due to the complex reaction pathways of the volatile components.

The advantage of using model compounds, which mimic specific components within a macromolecular lignin structure, lies in the fact that the pyrolysis of these molecules—typically dimers with specific bond types—provides a more simplified view of global parameters, thereby allowing for conjecture of more complicated reaction pathways or networks. Experimentally, several studies have utilized a range of model monomers or dimers containing various interunit linkages (e.g., β-O-4, α-O-4, β-1, 5-5) to assess their decomposition products and thereby deduce possible reaction pathways at the molecular level.[177−180] A similar approach has also been carried out in several *in silico* studies, rather than experimentally, through transition state theory and density functional theory.[181−185] There are, however, limitations to studies with model compounds as they can depart from the reality of using whole lignin. Nakamura et al. and Kotake et al. have shown that the temperatures of pyrolysis reactions of model compounds can differ from that of macromolecular lignin and among varying smaller compounds.[179,180] For example, a phenolic α-ether model becomes reactive in pyrolysis at 200 °C, β-ether and β-aryl at 250 °C, and coniferyl alcohol in the range of 250−300 °C.[179] Kotake et al. report that the formation of volatile products from primary lignin pyrolysis reactions in their experiments occurs at a much higher temperature than that of coniferyl alcohol.[180] Additionally, lignin model compounds (typically monomeric or dimeric) are incapable of reproducing the heavy oligomer yields that are known to exist from whole lignin pyrolysis, generated from evaporation and aerosol ejection as liquids.[36−42]

Kinetic models with a greater level of product speciation are advantageous in their applicability to different feedstocks and possibility to reaction engineer and optimize individual or groups of species of interest. Klein and Virk and co-workers developed a model with a greater level of mechanistic detail in which a lignin macromolecular structure is represented as a probability distribution of combinations of aromatic units and propanoid side chains, represented by different model substrates.[5,186,187] The kinetic parameters of these model substrate compounds undergoing pyrolysis reactions were then determined experimentally (Table 5) and used to mathematically simulate lignin pyrolysis. Similar work from Faravelli et al.,[188] Hough et al.,[189] and Furutani et al.[190] followed. Most recently, Yanez et al. developed a computational model by utilizing the data generated by lignin structural models previously discussed.[69] In their model, they assumed that four fractions of components are typically formed including gases, aqueous, char, and a complex fraction of aromatic species with diverse substitution patterns. Reaction families were specified based on experimental and theoretical studies, usually using model compounds. Kinetic parameters from the work of Klein and Virk were used as initial estimations. Their kinetic Monte Carlo simulation predicted yields of various fractions of lignin, within which species are distinguishable, in agreement with the experimental data provided by Patwardan et al.[191]

While the kinetic model developed by Yanez et al.[69] presents a significant stride for lignin pyrolysis modeling, the future holds an array of possible improvements. First, the kinetic model presented by Yanez et al. is only applicable for one biomass feedstock (wheat straw). However, recent work by Dellon et al. has extended the lignin structural model to account for all biomass feedstocks.[71] Thus, with the reaction families from the additional bonds, a compilation of an updated kinetic model, and the recent structural model can lead to predictions of yields for the pyrolysis of any biomass feedstock. In addition, though Patwardan et al.[191] achieved a high mass balance of 92%, the remaining fraction could include aerosols generated from nonvolatile lignin oligomers. Therefore, if experiments are done to quantify the aerosolization rate as a function of the pyrolysis conditions, the mass balance and results could be even further improved. Finally, there have been conflicting reports about the interactions among cellulose, lignin, and hemicellulose.[192] While some groups have found no interaction among the three components during pyrolysis, others claim that there is an interaction among the three components. Due to the controversy of this topic, it is worthwhile to revisit the lignin−cellulose and lignin−hemicellulose interactions for the purposes of lignin pyrolysis modeling.

Considering the zonal reactivity scheme for pyrolysis of lignin presented earlier in Figure 2 as an illustrative example, it is possible to derive sets of kinetic expressions that govern the pathways from one "zone" to another (e.g., liquid intermediate to char). These are summarized in eqs 2a−2e. Here, vapors can refer to water and light organic species (i.e., monomers) that are in the gas phase at pyrolysis temperature but may condense to liquid phase at room temperature. Heavy organics are the liquid-phase species (oligomers) collected as products through evaporation or aerosol ejection (a physical process, rather than chemical process). This type of lumping approach is commonly employed in kinetic studies, such as in work from Adam et al. (Kraft lignin pyrolysis),[193] Anca-Couce (general lignin pyrolysis),[194] and highly cited work from Ranzi et al. on chemical kinetics of biomass pyrolysis.[195] Results of the computational kinetic modeling of lignin from Yanez et al. and Hough et al. are also reported similarly as lumps.[69,189]

$$\text{Lignin} \xrightarrow{k_1} \text{Gas and vapors} \tag{2a}$$

$$\text{Lignin} \xrightarrow{k_2} \text{Liquid intermediate} \tag{2b}$$

$$\text{Liquid intermediate} \xrightarrow{k_3} \text{Gas and vapors} \tag{2c}$$

$$\text{Liquid intermediate} \xrightarrow{k_4} \text{Char} \tag{2d}$$

$$\text{Liquid intermediate} \xrightarrow{k_5} \text{Heavy organics} \tag{2e}$$

With this set of kinetic expressions, it then becomes possible to write a set of differential equations to describe the evolution of species throughout lignin pyrolysis. These are summarized in eqs 3a−3e. Ojha et al. report that first-order modeling is an acceptably good representation.[176] This (perhaps somewhat

https://dx.doi.org/10.1021/acs.iecr.9b05744
Ind. Eng. Chem. Res. 2020, 59, 526−555

limited) scheme is presented as it corresponds to Figure 2; however, other plausible pathways are certainly imaginable. For example, if reoligomerization in the gas phase is allowed, then a sixth reaction from "vapors + gases" to "char" would need to be incorporated. More detailed speciation within the specified zones or lumps is also commonly utilized, such as by Pu et al.[196] Here, "gases and vapors" is denoted by G, "liquid intermediate" by I, and heavy organics by A (for aerosols).

$$\frac{d(\text{Lignin})}{dt} = -(k_1 + k_2)(\text{Lignin}) \tag{3a}$$

$$\frac{d(G)}{dt} = k_1(\text{Lignin}) + k_3(I) \tag{3b}$$

$$\frac{d(I)}{dt} = k_2(\text{Lignin}) - (k_3 + k_4 + k_5)(I) \tag{3c}$$

$$\frac{d(\text{Char})}{dt} = k_4(I) \tag{3d}$$

$$\frac{d(A)}{dt} = k_5(I) \tag{3e}$$

The determination of time-resolved yields for various pyrolysis products, and subsequent calculation of lumped kinetic parameters, is achievable with current experimental and analytical capabilities.[197] However, the kinetic model of lignin pyrolysis from Hough et al. features ∼100 species and ∼400 reactions;[189] the model of Yanez et al. employs ∼1600 species and ∼4300 reactions.[69] It does not seem possible to imagine a scenario in which hundreds or thousands of kinetics-determining experiments can be realistically carried out in a lab setting.

Lab-scale methodologies for lignin liquefaction kinetics therefore seem to be limited to a lumped-model scale. Consequently, lumped kinetic parameters are composed of the hundreds or thousands of individual reactions featured in microkinetic models. This underscores the need for mechanistic computational study, which itself is still limited by computational resources. For the study of whole lignin liquefaction (or, in general, cracking and/or oligomerization of high molecular weight feedstocks), a *bona fide* first-principles approach may be beyond current capabilities.[198] To overcome this limitation, strategies such as the Single-Event MicroKinetic (SEMK) methodology can be considered.[198,199] In an SEMK approach, a full microkinetic model is reduced, on the basis that chemical transformations of a huge number of individual molecules are contained within transformations pertaining to a smaller number reactive moieties/families.[198,199] The kinetic parameters within these families should have very similar (or identical) values. Families used by Yanez et al. are (1) ether cleavage, (2) decarboxylation, (3) demethoxylation, (4) deacylation, (5) demethanation, (6) dealkylation, (7) aliphatic C−C cleavage, (8) aliphatic C−O cleavage of several types, (9) methoxyl group isomerization, (10) alcohol oxidation, (11) aldehyde oxidation, (11) hydrogen addition, and (12) char formation.[69] Families used by Hough et al. are (1) initiation reactions, (2) decomposition reactions, (3) molecular reactions, (4) substitutive addition reactions, (5) recombination reactions, (6) volatilization reactions, (7) char devolatilization reactions, and (8) hydrogen abstraction reactions.[189] To manage the experimental determination of kinetic parameters for ∼10 reaction families is reasonable. In this way, efficiency-minded computational approaches (e.g., SEMK) allow for the interplay between classical lab-based experimentation and *in silico* microkinetic modeling.

6. EFFECT OF REACTION PARAMETERS

6.1. Temperature. Most pyrolysis reactors typically operate within the temperature range of 400−600 °C, with maximum liquid yields (about 70%) from whole biomass pyrolysis occurring near 500 °C.[10,35,200] Research has also shown that lignin-derived oligomeric liquids, which are thought to be the primary products of lignin pyrolysis, also peak in the temperature range of 500−550 °C (Figure 7).[35,200] It is these oligomers which are largely responsible for the increase in liquid yields from fast pyrolysis of biomass between lower (350 °C) and higher (500 °C) temperature.[200]

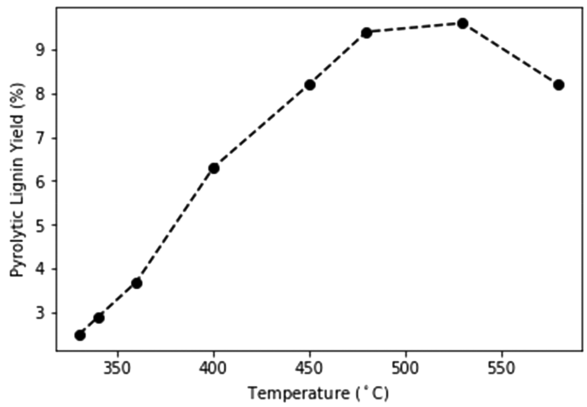

Figure 7. Lignin-derived oligomeric liquid (pyrolytic lignin) yields (reported on a dry biomass basis) from whole biomass pyrolysis as a function of temperature; adapted from Zhou et al.[35]

Further supporting evidence that lignin oligomers are primary pyrolysis products is provided by Zhou et al.[35] In their study, pyrolysis reactions took place in a vacuum atmosphere with rapid quenching of primary products, which could more readily evaporate due to low pressure.[35] Analysis of this quenched primary phase revealed the presence of lignin-derived oligomers, with a maximum oligomer yield at 530 °C, while the formation of monomers was attributed to secondary reactions. Overall, oil yield peaked at 480 °C, gas yields increased with temperature, and char yields decreased with temperature. When the collected pyrolytic (oligomeric) lignin was separately pyrolyzed again with Py-GC/MS, the yields of CO_2, acetone, and methoxylated phenols decreased with pyrolytic lignin production temperature, while alkylated phenols and char yields increased with temperature. The increase in char can be attributed to higher-temperature pyrolytic lignin having more fixed carbon and less volatile content than those samples produced at lower temperature,[35] while the other trends from Py-GC/MS are a result of decarboxylation, demethoxylation, and alkylation at higher temperatures.[35,201] GPC analysis of lignin pyrolysis oil revealed that a higher quantity of low molecular-weight species (monomer regime) were produced in lower temperature experiments compared to higher temperature, while at higher temperature there were more heavy products in an oligomer regime.[35]

https://dx.doi.org/10.1021/acs.iecr.9b05744
Ind. Eng. Chem. Res. 2020, 59, 526−555

In a pyrolysis study of two types of lignin, Jiang et al. report 600 °C as the temperature at which maximum yields of phenolic compounds were obtained from Py-GC/MS.[201] Ben and Ragauskas also report an optimal temperature of 600 °C for the pyrolysis of Kraft lignin. In this study, the yields of total pyrolysis oil and gas increased over their temperature range (400, 500, 600, 700 °C), while char yields decreased.[202] Kotake et al. reported a similar trend of increasing oil yields with temperature, although their studied temperature range was lower, at 250−350 °C.[203] All of these trends can be explained by considering the effect of temperature and how the lignin pyrolysis reactions initiate. The primary reactions involve cleavage of the ether linkages (such as β-O-4), producing radical oligomers while C−C bonds stay largely intact.[2,204] At low temperature (250 °C), the initial product environment is deficient in H-donor species, and these oligomers preferentially undergo condensation reactions (char); however, as reaction temperature increases (~350−400 °C), the initial product environment becomes richer in H-radicals (due to side-chain C−C cracking reactions) that can stabilize primary oligomers.[203,205] The primary oligomers can continue to react at even higher temperature (~450 °C), increasing the yield of monomers through further cracking of C−C bonds.[203,205] A further increase in reaction temperature (~550−600 °C) leads to the degradation of aromatic ring substituents.[206] In this case, secondary pyrolysis products made of catechols and pyrogallols evolve noncondensable carbon oxides (CO and CO_2), while cresols and xylenols tend to produce more CH_4 and H_2.[205] Further reading on more specific reaction mechanisms and pathways that occur during the pyrolysis of lignin can be found in a recent computational study from Jiang et al.,[207] experimental studies from Shrestha et al.[208] and Ansari et al.,[209] and in an excellent review by Kawamoto.[205]

With respect to computational microkinetic models, the role of temperature for a given reaction (or reaction family) follows familiar exponential dependence when using classical Arrhenius kinetics, as in the application of Klein and Virk's results[5] (Table 5) in modeling from Yanez et al.[69] Modified Arrhenius expressions for rate constants can also be used, as in eq 4. In this case, there is an additional nth order dependence of the rate with respect to temperature. Among the reaction families featured in modeling from Hough et al., for example, all are zeroth order (n = 0) except for volatilization reactions, which are first order (n = 1).[189] Therefore, within the framework of this specific model, as temperature increases, volatilization can begin to have more outsized importance. It should naturally follow that with increased volatilization comes increased aerosol intensity. With a microkinetic model composed of reaction families (as in an SEMK scheme), this effect of temperature can be readily captured. If different sets of reaction families are proposed, then experimental kinetic work may also need to determine their nth order dependence on temperature, if modified Arrhenius expressions are to be used.

$$k(T) = AT^n \exp\left(-\frac{E_a}{RT}\right) \quad (4)$$

6.2. Pressure. Work from Zhou et al. using a screen-heater pyrolysis reactor under a vacuum atmosphere with rapid primary product quenching showed that low pressure environments are effective in collecting primary lignin-derived oligomers.[35] To further this idea, Pecha et al. used a similar approach by using a modified pyroprobe reactor to analyze milled wood lignin pyrolysis over a range of low pressures (4, 250, 500, 750, and 1000 $mbar_{abs}$).[42] They found that with respect to reactor pressure, there was no significant impact on the formation of gas yields and monomers; however, there was clear increase in char yields as pressure increased. Further analysis of lignin pyrolysis liquids was done with UV-fluorescence. As reactor pressure increases, UV-fluorescence analysis suggests that fewer heavy oligomers are collected as liquid products. Additionally, following FT-ICR-MS analysis, Pecha et al. show that the actual chemical nature of the remaining heavy oligomeric fraction does not change with respect to pressure.[42] This suggests that these heavy oligomers are released during pyrolysis through controlled evaporation and thermal ejection (as liquids, from bubbling, described in greater detail in Section 7) from a primary liquid phase. In that liquid phase heavy oligomers may also rapidly condense to form large insoluble char precursor products.

It is expected that an increase in pressure will hinder the evaporation or ejection of small oligomers from a liquid phase, although pressure does not appear to have a significant effect on the initial formation of oligomers that make up this phase because it is controlled from solid phase reactions. Therefore, increasing reaction pressure reduces the thermo-physical removal of heavy compounds either through evaporation followed by gas-phase diffusion or convection and/or physical aerosol ejection.[39] In other words, increasing pressure increases the retention (as a liquid intermediate) of lignin-derived oligomers, which are the main precursors to char formation. This result is well explained in a recent experimental and modeling study from Marathe et al. using lignins of varying molecular weights (Figure 8).[30]

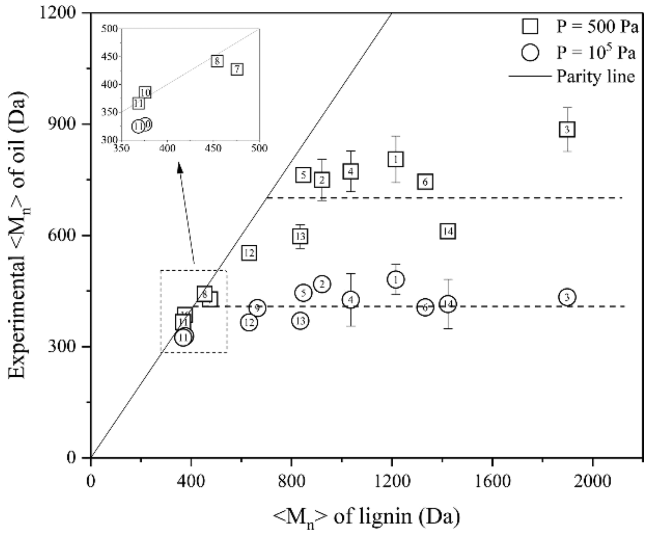

Figure 8. Experimentally obtained molecular weight of oils obtained at different pressure, as a function of starting lignin molecular weight; reproduced from Marathe et al.[30]

In their research, they show that operating a higher pressure (500 vs 10^5 Pa) ultimately results in higher yields of char and gas and lower yields of pyrolysis oil.[30] The higher pressure also results in lighter oils. This result is attributed to the fact that higher pressure alters the transport of molecules away from the pyrolysis reaction front and thereby increases the vapor

https://dx.doi.org/10.1021/acs.iecr.9b05744
Ind. Eng. Chem. Res. 2020, 59, 526−555

residence time. In this way, the vapor residence time and reaction pressure are distinctly coupled, and for this reason, the authors note that pressure is the most influencing process parameter regarding the manipulation of product yields and oil characteristics.[30] The effect of reactor pressure on the outcome of lignin pyrolysis can only be taken into account if liquid−vapor equilibrium is described and if the removal rate is described through flash distillation models with adequate description of mass transfer mechanisms.[62]

6.3. Vapor Residence Time. As previously discussed, the reactions that take place during lignin pyrolysis occur sequentially, beginning with primary depolymerization at ether linkages, followed by secondary reactions such as C−C cracking, polycondensation, and reoligomerization for char and gas formation. For this reason, it is critical to assess the effect of vapor residence time with respect to pyrolysis. Hoekstra et al. report that pyrolysis vapor-phase products (including aerosols) have been shown to continue to be reactive as secondary intermediates even in the absence of catalytic effects.[210] Anca-Couce et al. even suggest that vapor (or volatiles) residence time may be more important than temperature and heating rate on the secondary reactions that can lead to solid residue from pyrolysis in particles with sufficiently large thickness.[211] In order to mitigate the possibility of secondary reactions during analytical pyrolysis studies, researchers typically try to operate with very low vapor residence time at less than approximately 1 s.[35,38,45]

Bai et al. report the possibility that within a residence time of only 0.4 s primary reaction products that are most abundantly lignin monomers and dimers can rapidly reoligomerize.[45] Zhou et al. and Hoekstra et al. showed that the pyrolytic (oligomeric) lignin yields from pyrolysis decrease with both increasing reaction time and temperature in a time span on the order of magnitude of 1 s (Figure 9).[38,210] Their further analysis with UV-fluorescence shows a decrease in spectral intensity with increases in both vapor residence time and temperature. These results, which are consistent with previous work from Zhou et al.,[35,36] show that higher reaction temperature and longer residence time increases the occurrence of secondary pyrolysis reactions. A study from Hosoya et al. over even longer residence times (40−120 s) additionally supports this conclusion regarding secondary reactions.[212] They show significant changes in the characteristics of the lignin-derived benzene ring and side-chain structures as pyrolysis time increases. Guaiacol-type aromatic structures are completely reacted away as time increases, leaving only phenol and cresol types at a time of 120 s, and also at this time, the only remaining side-chain structures are aromatic H and saturated alkyl groups.[212]

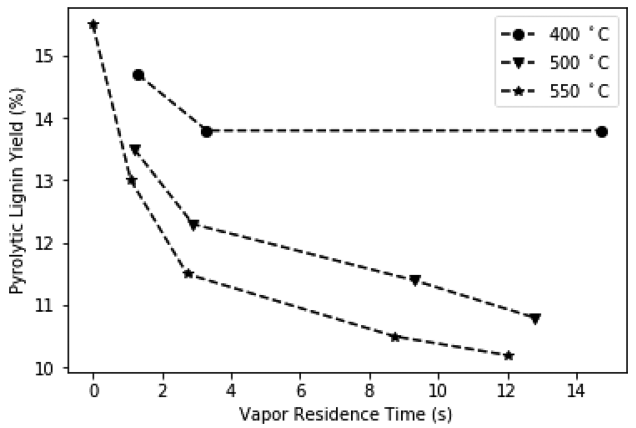

Figure 9. Yield of pyrolytic lignin from whole biomass pyrolysis with respect to vapor residence time and temperature; adapted from Zhou et al. and Hoekstra et al.[38,210]

7. EVAPORATION OF LIGNIN INTERMEDIATES

An important phenomenon that has been proposed to have significant contribution to pyrolysis yields and product characteristics is the direct evaporation of intermediate species. In a recently published study on the pyrolysis of lignins with different molecular weights, Marathe et al. report evidence that low molecular weight lignins are primarily evaporation/sublimating/ejecting during pyrolysis processes, while the extent of reactions (particularly cracking) is low.[30] This suggests that the evaporation temperature (i.e., boiling point) is an important thermo-physical property of pyrolysis intermediates and/or products.

One useful framework for assessing the boiling points of compounds with a known structure is group contribution methods, such as those proposed by Joback and Reid.[213] Table 6 shows the calculated heat of vaporization (at boiling temperature) and the associated boiling points from the Joback method. A corrected boiling point is also given (denoted as "corr." in Table 6), as it has been shown that for large molecules the Joback method-calculated boiling point can have significant deviations from observed experimental data.[214,215] Calculations were performed with the assistance of ARTIST software (DDBST GmbH, Oldenburg, Germany).[216] The structures considered are H, G, and S monomers (p-coumaryl, coniferyl, and sinapyl alcohols) along with their respective dimers, trimers, and tetramers in which interunit links occur through β-O-4 bonds. This type of approach for calculating bulk fluid and vapor−liquid equilibria properties is conceptually similar to earlier work on Fischer−Tropsch liquids from Marano and Holder.[217,218]

Further, with an estimated boiling point (temperature, pressure) and estimated heat of vaporization, it is possible to produce estimated partial pressures at varying temperatures using the Clausius−Clapeyron equation.[219] This allows for modeling of the vaporization curve separating gas and liquid regimes for a given substance. Figure 10 shows the estimated vaporization curves for G monomer, dimer, trimer, and tetramer calculated using the Clausius−Clapeyron equation. These calculations are limited in that they assume a constant heat of vaporization (although heat of vaporization is more accurately a function of temperature). Another limitation is in the usage of parameters derived from group contribution methods; more robust experimental observations/data are needed to completely verify the values presented in Figure 10.

Assessment of experimental number-average molecular weight of lignin pyrolysis oil is done by Marathe et al. at a reactor temperature of 530 °C.[30] At this temperature, based on the calculated estimate for the liquid−gas phase boundary at 100 kPa (Figure 10), the guaiacyl monomer and dimer should be in the gas phase—i.e., capable of evaporating. Trimers and tetramers would hypothetically still remain in the liquid phase. If the reactor pressure is lowered to 500 Pa, then the trimer may also be included as gas phase products. Marathe et al. show that for low molecular weight lignins (<500 Da), there is no apparent reduction in the molecular weight of pyrolysis oil when compared to the parent lignin. A weight of ∼500 Da falls

https://dx.doi.org/10.1021/acs.iecr.9b05744
Ind. Eng. Chem. Res. 2020, 59, 526−555

Table 6. Normal Boiling Point and Heat of Vaporization for Lignin Model Structures Calculated Using Group Contribution Methods[a]

Name (M.W., Da)	H_{vap} at T_b (kJ/mol) (Joback)[213]	Normal T_b (°C) (Joback)[213]	Normal T_b (°C) (Corr.)[214,215]	Name (M.W., Da)	H_{vap} at T_b (kJ/mol) (Joback)[213]	Normal T_b (°C) (Joback)[213]	Normal T_b (°C) (Corr.)[214,215]
H monomer (150)	68	336	295	H trimer (447)	152	1048	643
G monomer (180)	73	386	324	G trimer (537)	168	1199	715
S monomer (210)	78	437	350	S trimer (627)	184	1350	787
H dimer (298)	110	692	472	H tetramer (595)	194	1405	813
G dimer (358)	120	793	520	G tetramer (715)	215	1606	910
S dimer (418)	131	893	568	S tetramer (835)	236	1807	1006

[a]Corr. = corrected Joback calculation.

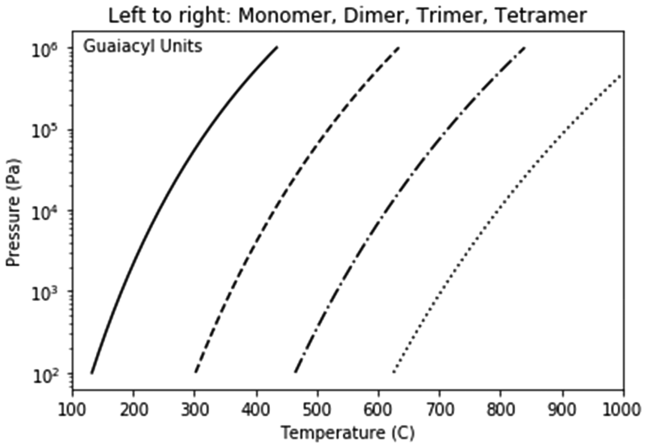

Figure 10. Estimated vapor−liquid phase change boundaries for guaiacyl β-O-4 lignin model units (gas, lower right; liquid, upper left for each curve); calculated based on Clausius−Clapeyron equation using group contribution-derived parameters.

within the trimer mass regime for lignin units (Table 6). The estimates for phase change presented in Figure 10 are therefore consistent with the hypothesis proposed by Marathe et al.,[30] that light lignin units (i.e., monomers, dimers, and some trimers) can preferentially evaporate rather than undergo chemical pyrolysis reactions. Heavier lignin units (tetramers and larger) are unable to evaporate (Figure 10) at pyrolysis reactor temperature (~500 °C), and therefore, they must (1) be ejected as aerosols or continue to react to form (2) smaller molecules capable of evaporation or (3) heavy solid-phase chars.

Within the framework of microkinetic modeling, Yanez et al. used the normal boiling point as the criterion by which to determine when molecular species are "shunted to the vapor phase" from the liquid intermediate.[69] A reasonable understanding of phase-change phenomena (i.e., vaporization) allows for this capability. With respect to Section 7, to date, there is no clear evidence that aerosol ejection/convective expulsion has been incorporated into lignin liquefaction modeling at the microkinetic level. Experimental understanding and mathematical modeling of bubbling and aerosolization as it relates to biomass pyrolysis is still an outstanding problem.[76]

In the coal pyrolysis CPD model,[59,60,65] intermediate products undergo vapor/liquid phase equilibrium on a rapid time scale compared with chemical rates. As a first approximation, the vapor−liquid phase equilibrium was described by the Raoult's law. The partial pressure of large oligomeric molecules used was estimated by the correlation developed by Unger and Suuberg, which is cited in work by Solomon and King.[220,221] To calculate the vapor/liquid ratio in equilibrium conditions a flash distillation model was implemented with appropriate assumptions of the location and amount of material that is in vapor−liquid equilibrium.[60] The theoretical treatment of mass transfer mechanisms for vapors removal was reviewed by Suuberg.[222] Oh et al. develop a model for intraparticle transport of gases and liquid

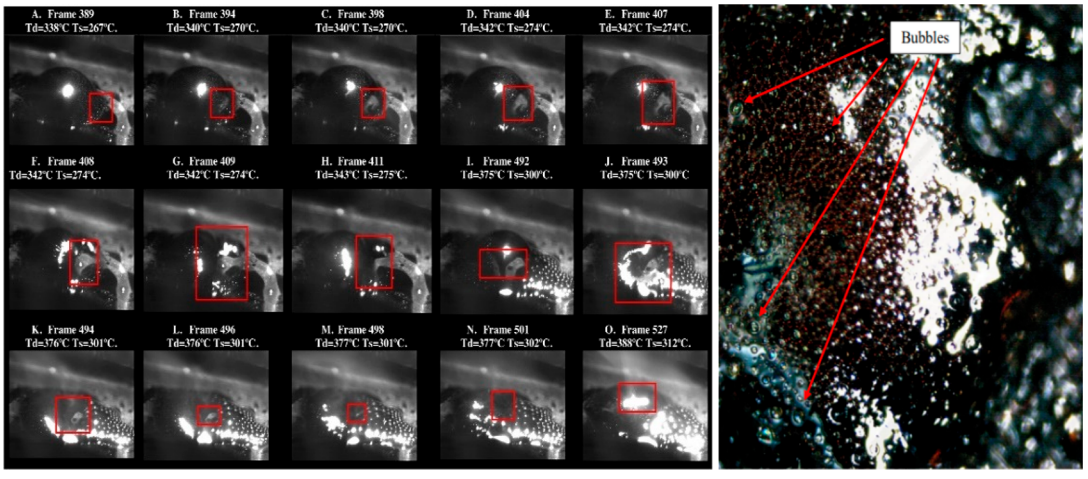

Figure 11. Photographic visualization of the formation and collapse of bubbles within a liquid intermediate phase during organosolv lignin pyrolysis; reproduced from Montoya et al.[39] (left) and Marathe et al.[30] (right).

https://dx.doi.org/10.1021/acs.iecr.9b05744
Ind. Eng. Chem. Res. 2020, 59, 526−555

intermediate products via the growth of bubbles uniformly dispersed in the molten liquid intermediate.[57]

8. THERMAL EJECTION OF AEROSOLS

Previous work has shown that during lignin pyrolysis, a primary liquid intermediate phase is formed, made up of both lower molecular weight monomers and higher molecular weight oligomers.[25,26,36] Using a wire-mesh reactor and fast-speed camera, Zhou et al. was able to visualize the formation of this liquid intermediate.[36] Further, they postulate that within this liquid phase some light molecules can be formed from dehydration and cracking reactions; lighter products are vaporized at sufficiently high reaction temperatures (monomers in Table 1 have normal boiling points between 150 and 300 °C), while other heavier products will be thermally ejected as aerosols.[36] This mechanism of thermal ejection offers an explanation for the presence of high molecular weight oligomers in pyrolysis oil products. A photographic visualization of this phenomenon is shown in Figure 11 from both Marathe et al. and Montya et al.[30,39] Thermal ejection as described herein is distinct from mere evaporation. While evaporation is a phenomenon of phase change from liquid to gas, thermal ejection can be thought of as convective expulsion.[223] This convective expulsion refers solely to viscous liquid-phase species and occurs from the formation and subsequent bursting of fluid bubbles, governed by hydrodynamic/rheological phenomena. Sharma et al. and then Dufour et al. describe bubble formation as "volatiles "pushing" a melted material."[206,224] Further information on *in situ* rheological study of biomass/lignin pyrolysis can be found in their original publication, along with more recent work from Shrestha et al.[208] Similar studies on rheological analysis in coal pyrolysis have also been published.[225−227]

Stankovikj et al. and Pecha et al. used high-resolution FT-ICR-MS to confirm the presence of this oligomeric fraction resulting from convective expulsion.[25,26,42] The mechanism for aerosol ejection can be explained as follows: As molecules within the liquid intermediate are thermally degraded to generate gases or reach their vaporization temperature or boiling point, they form a gas bubble that is surrounded by a thin film of the liquid; upon bubble breaking, this film is ejected as small liquid droplets—or aerosols—that is molecularly composed of whatever liquid-phase compounds are present in the film at the time of bursting.[39,43,228] There is limited understanding of the nature of the gases responsible for intensive bubbling observed during lignin pyrolysis, but the analysis of lignin pyrolysis products suggest that an important fraction of the bubbles are formed from CO_2 and CO derived from lignin.[42,76] Methods for visualizing and quantifying aerosol ejection rate/intensity are described in previous work from Montoya et al.[39−41] A more in-depth description of aerosol ejection for lignin requires the consideration of the formation of a softened viscoelastic phase via glass transition of lignin, as described by Shrestha et al. and Vural et al.[208,229] In this softening mobile phase, at appropriate temperature and pressure, volatile species develop as gases, leading to an internal overpressurization. As the presence of internal gases increase, bubbles begin to form in the viscoelastic phase, and once the internal pressure is sufficiently high, the gas bubbles can burst and eject heavy liquids (that comprise the bubble surface) in the process.

The significance of quantifying the rate of aerosol formation and oligomer ejection during lignin pyrolysis is tied explicitly to the fact that it is not a chemical process but rather a thermophysical one.[28] Both earlier[5,186−188] and more recent[69,189,190] modeling efforts to describe lignin pyrolysis are largely built on elementary chemical reaction kinetics derived from experimental work using simpler lignin model compounds. While these models overall are very complex, they fall short in capturing the final yields of the heavy oligomer fraction that is known to exist in pyrolysis oil. Yanez et al. specifically indicate that their work could further be improved "if an appropriate physical model for the aerosolization rate as a function of the reaction conditions became available".[69] This is because work with model lignin compounds to derive elementary pathways is unable to accurately reproduce the true nature of liquid intermediate formation and aerosol ejection of heavy oligomers during real lignin pyrolysis. It is important to mention that thermal ejection is controlled by the thickness of the film formed. During biomass pyrolysis, the thickness of the liquid intermediate film may be much thinner, and consequently, thermal ejection may be less important than observed in lignin alone tests. For example, Tiarks et al. conducted experiments with very thin lignin films and observed a clear reduction in aerosols formation.[28] Suuberg developed an approach in which they considered the possibility that some liquid intermediate from coal pyrolysis may be entrained with the gases and vapors.[222] Reactor pressure also plays a significant role in modeling bubble formation and growth, as shown in eq 5 (where r_B = bubble radius, P_B = internal bubble pressure, P_e = external pressure, μ = liquid viscosity, σ = surface tension).[40,57] When external pressure on the viscoelastic liquid intermediate phase increases, the rate of bubble expansion decreases. If reactor pressure is large, then the formation and growth of bubbles should be greatly hindered. For a sufficiently reactor high pressure, the coupled phenomena of bubbling and thermal aerosol ejection is expected to become negligible.

$$\frac{dr_B}{dt} = \frac{r_B}{4\mu}\left(P_B - P_e - \frac{2\sigma}{r_B}\right) \quad (5)$$

Montoya et al. developed a mathematical model which coupled mass and energy balances with the chemical reactions during lignin pyrolysis.[40] Aerosols formation is described as a function of bubbles bursting on liquid surface. The ratio (number of aerosols/number of bubbles) was obtained with an empirical correlation reported by Zhang et al.[230]

9. EFFECT OF SOLVENTS

The high-level motivation for pursuing lignin pyrolysis in the presence of solvents—i.e., solvolysis—is centered on the need to account for alternative removal mechanisms that avoid thermal degradation of oligomeric primary products. It is also motivated by the need to capitalize on existing refinery infrastructure, which is largely built to handle the liquid products extracted and produced within the petroleum industry.[231] Utilization of a solvent can also allow for the easier removal of reactive liquid intermediates, thereby increasing final oil yields at the expense of char yields. Two advantages of this type of biomass solvolysis process, from Isa et al., are quoted directly: "(1) The chosen solvent could dilute the concentration of the products and prevent the cross-linked reactions between hydrocarbon and aromatic compounds generating tar compounds, and (2) relative low reaction temperature (less energy consumption) in comparison with other thermochemical processes (pyrolysis and gasifica-

https://dx.doi.org/10.1021/acs.iecr.9b05744
Ind. Eng. Chem. Res. 2020, 59, 526−555

tion)".[232] However, it is noteworthy that most solvolysis research is still limited to batch and semicontinuous processes.[233]

Two recent works on the role of solvents in thermochemical biomass conversion can be found from Castellví Barnés et al. and Shuai and Luterbacher.[67,234] Solvent effects can be divided into two categories: (1) the effect on feedstock solubility and (2) the effect on solvolysis chemical thermodynamics.[234] Organic solvents can be divided into four groups: (1) polar protic (e.g., methanol and acetic acid),[234] (2) polar aprotic (e.g., tetrahydrofuran (THF) and γ-Valerolactone (GVL)),[234] (3) nonpolar (e.g., hexane and dimethyl ether),[234] and (4) ionic liquids (e.g., [mmim][$MeSO_4$] and [bmpy][PF_6]).[235] Solvents can also be aqueous or organic/aqueous mixtures.[234] In a solvolysis process, lignin must first depolymerize into fragments (liquid intermediate), and then, the fragments must undergo dissolution into the solvent. Because of its molecular structural characteristics, lignin has an overall medium polarity, and therefore, solvolysis needs a medium polarity solvent (e.g., acetone, ethanol, THF) rather than a very polar (e.g., water) or nonpolar (e.g., hexane) solvent.[234] One quantifiable metric proposed by Castellví Barnés et al. to govern solvent selection is the Hildebrand parameter.[67] The Hildebrand parameter is one (among other parameters) empirical measure, based on the assumption that there is a correlation between potential energy per unit volume and mutual solubility of a solute in a given solvent.[236]

They show that solvents with a parameter in the range of 25−40 $MPa^{1/2}$ were suitable for their solvolysis system (Figure 12). Further, they report that poor-interacting solvent performance can be improved through employing blends with well-interacting solvents even in minor amounts and that protic solvents (for whole wood) can depress the overall conversion rate—an effect that warrants further study.[67] Overall conversion rate may be limited by solvent mass transfer, so in essence, a "good" solvent can increase swelling in whole biomass and more easily facilitate removal of soluble depolymerization products. The solubility parameter range of 25−40 $MPa^{1/2}$ reported by Castellví Barnés et al.[67] (for whole biomass) is consistent with results from Sameni et al. and Ye et al., who calculated parameters between approximately 26−30 $MPa^{1/2}$ for industrial lignins.[237,238] Thielemans and Wool report a similar parameter value of about 24.5 for pine and hardwood Kraft lignins,[239] and Lê et al. report a value of 25.5 for beech organosolv lignin.[240] The solubility parameters, calculated using group contributon methods,[241,242] for the model monomers and oligomers described previously in Section 7 are given in Table 7; their values range from roughly 25−30 $MPa^{1/2}$, in agreement with previously reported values. Values reported for some organic solvents are given in the Supporting Information.[67,243] While further detailed review on the calculation of liquid-phase properties relevant to lignin depolymerization is beyond our scope, group contribution methods are capable of estimating other physical parameters in liquids.[244,245] Some of these include liquid density,[246−248] liquid viscosity,[249−251] and surface tension[252,253] (of particular interest with respect to bubbling, as in eq 5 and Figure 11). Hwang et al. have published values for these properties for coal liquids.[254] Dufour et al. have also reported order-of-magnitude values for some thermo-physical properties for modeling transport phenomena in biomass pyrolysis.[75]

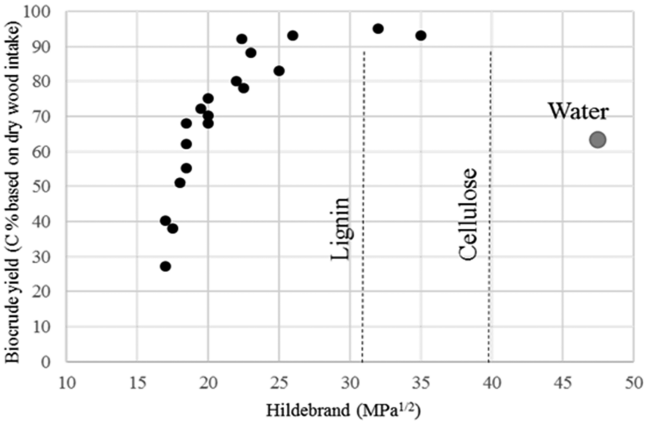

Figure 12. Effect of solvent Hildebrand parameter and yield of oil obtained; reproduced from Castellví Barnés et al.[67]

Additional reading on practical solvent considerations can be found in a recent review from Lange.[231] Lange reports aromatic refinery fractions in the gasoil range, and the gasoil-range fraction of the solvolysis oil itself (heavy fraction of lignin oil), as potential solvents.[16,231] Further, there have been several recent studies in which molecular simulations are employed to computationally model lignin as a platform for more in-depth understanding of solvent effects and chemistry on lignin structure.[3,255−257]

10. REACTIONS RESPONSIBLE FOR SOLID CARBONACEOUS PRODUCT FORMATION

Previous sections have discussed the relevance of several parameters (e.g., temperature, pressure, vapor residence time) on their effect of char formation, and therefore, further investigation into the nature of mechanisms that produce char is warranted. Char is the solid residue from pyrolysis reactions that produce high-molecular weight polyaromatic structures (Figure 13).[205,206,258,259] In literature, the terms "coke" or "soot", in contrast to "char", more typically describe downstream gas-phase formation/deposition of solid carbonaceous

Table 7. Hildebrand Solubility Parameters ($MPa^{1/2}$) for Lignin Model Structures Calculated Using Group Contribution Methods

Name (M.W., Da)	Solubility Parameter (Method: Just et al.)[242]	Solubility Parameter (Method: Fedors)[241]	Name (M.W.)	Solubility Parameter (Method: Just et al.)[242]	Solubility Parameter (Method: Fedors)[241]
H monomer (150)	30.7	30.5	H trimer (447)	28.9	30.2
G monomer (180)	28.6	29.3	G trimer (537)	30.3	28.8
S monomer (210)	29.6	28.4	S trimer (627)	34.5	28.2
H dimer (298)	29.0	30.3	H tetramer (595)	28.9	30.1
G dimer (358)	29.5	29.0	G tetramer (715)	30.8	28.8
S dimer (418)	32.1	28.0	S tetramer (835)	34.1	27.7

https://dx.doi.org/10.1021/acs.iecr.9b05744
Ind. Eng. Chem. Res. 2020, 59, 526−555

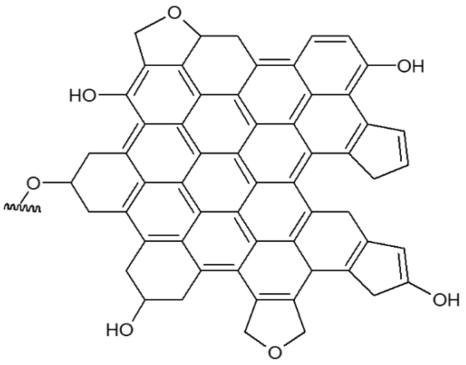

Figure 13. Example of a condensed polyaromatic char structure; adapted from Liu et al.[258]

products.[260] Broadly, it has been shown that lower temperatures tend to yield higher amounts of char,[201−203,205,261] while lower pressure[30,42,207] and vapor residence time tend to yield lower amounts of char.[38,210,212] Higher pressure and correspondingly longer vapor residence time results in reduced mass transfer and an increase in secondary intraparticle char-forming reactions.[30] Bai et al. emphasize the importance of reoligomerization on char formation, especially at temperatures less than 500 °C, where the extent of condensation reactions exceeds that of secondary C−C cracking reactions.[45] They report that the majority of primary lignin pyrolysis products are monomers and dimers,[28,45] while Zhou et al. indicate primary products are largely made up of oligomers.[35,36] However, regardless of differing views on the nature of primary products, there is somewhat of a consensus that secondary condensation reactions in the liquid phase are responsible for the formation of char. With respect to soot/cook, Nowakowska et al. provide an in-depth example of potential mechanism for gas-phase formation of polyaromatic carbonaceous structures from anisole (as a lignin surrogate).[260]

There is also clear evidence that char formation largely relies on the chemistry of methoxy groups and the presence of o-quinone methide species.[205,262−264] In a study of lignin model compounds, Hosoya et al. report that significant char only formed from compounds with guaiacyl units (in comparison to cresols, catechols, and phenols).[262] Additionally, Asmadi et al. show that there is roughly twice as much char produced from pyrolysis of syringol as from guaiacol.[263] They attribute this result to a "double opportunity" of o-quinone methide formation, due to the fact that syringol has two methoxy groups compared to only one in guaiacol.[263] Generally, the pathway to char production first involves the formation of radical species from methoxyl groups, leading to o-quinone methide species and subsequently polycondensation into char (Figure 14). This sequence leading to char formation can be possibly mitigated through several techniques: the addition of hydrogen donors, which stabilize radicals before char formation; minimizing vapor residence time, which correspondingly reduces the frequencies of char-producing reactions; operating at lower pressure, which increases the evaporation and/or thermal ejection of oligomeric lignin-derived species that participate in char-producing reactions; and increasing temperature, which promotes C−C cracking and gas forming secondary reactions over those that produce char.

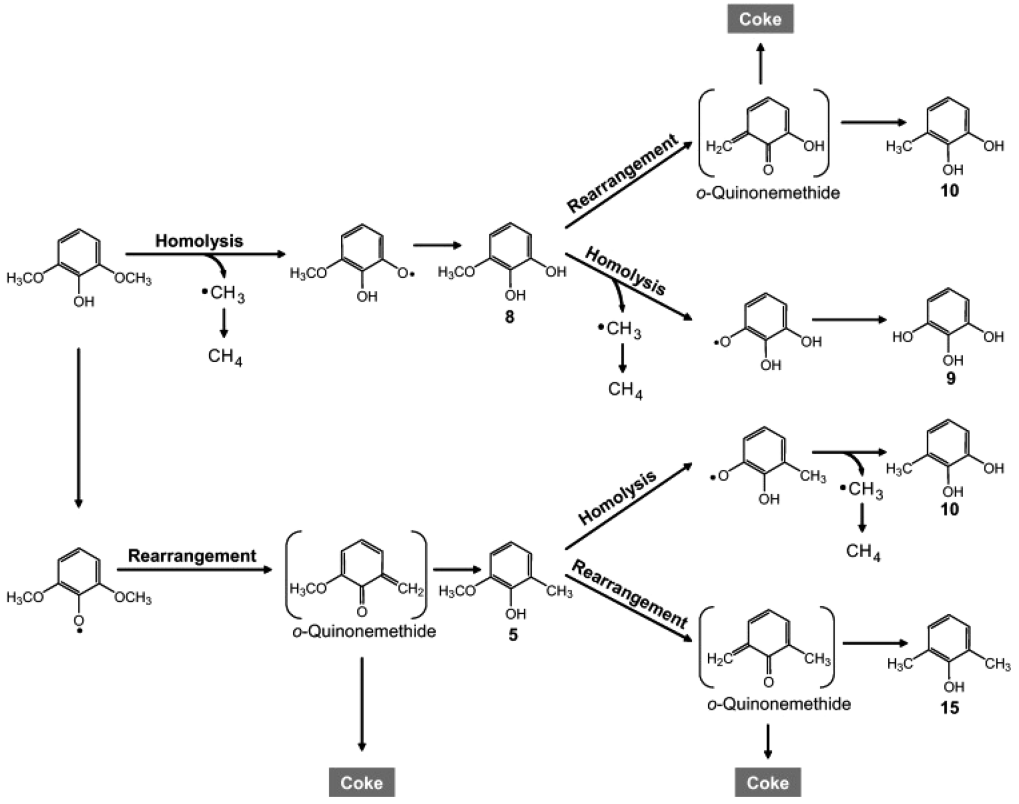

Figure 14. Pyrolysis pathway from syringol to coke, through o-quinonemethide intermediates, with methoxy homolysis and rearrangement as key reactions. Other final products include methyl catechol, pyrogallol, and xylenol; reproduced from Asmadi et al.[263]

https://dx.doi.org/10.1021/acs.iecr.9b05744
Ind. Eng. Chem. Res. 2020, 59, 526−555

Table 8. Reoligomerization Reactions[a]

Description	Reaction
Oligomerization between phenolate and ketone[270]	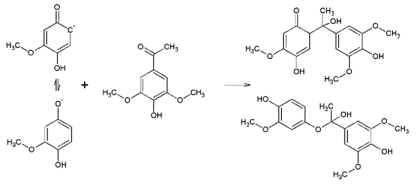
Addition of nucleophile to quinone methide intermediate[88]	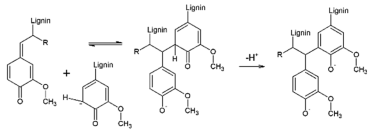
Repolymerization in acidic conditions with the formation of reactive carbon ion[271]	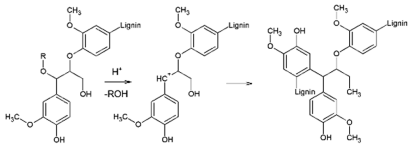
Capping agent (2-naphthol) addition as scavenger for reactive carbon ion[271]	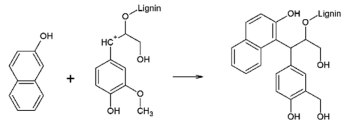

[a]Adapted from given references: 88, 270, 271.

With respect to lignin repolymerization, some of these reactions have been described by Klein et al. as a transformation that leaves lignin aromatic rings intact while altering the propanoid side chains and methoxy groups.[5,187] The terminal (γ) CH_2OH groups of the propanoid side chains readily decompose to formaldehyde. The scission of methoxyl groups during condensation/carbonization reactions results in the formation of methane and methanol. Clusters containing between two and four aromatic rings will result in the formation of oligomers that may be solubilized in a solvent or may remain in the liquid intermediate. If the lignin oligomeric intermediate is exposed to prolonged heating, C−C bonds are formed, generating cross-linked lignin structures. The self-condensation capacity of lignin is typically accelerated in acid environments.[265] It has been broadly shown that low molecular-weight (THF-soluble) portion of lignin undergoes pyrolytic decomposition reactions into volatiles and polymerization reactions into high molecular weight products (that are THF insoluble).[261] The main reactions happening during repolymerization are aldol condensation, rearrangement reactions, demethoxylation, hydrogenation, and hydrodeoxygenation (Table 8) and are responsible for further increasing the molecular weight of intermediate products via overall increase in the average degree of polymerization of these products. In the coal pyrolysis CPD model,[65] a simple one-step Arrhenius rate expression is used to describe cross-linking, accounting for the reattachment of intermediate molecules (liquid) to the infinite char matrix.[266] In this model, the mass of liquid intermediate is updated at each time step. For bituminous coals, cross-linking occurs after tar release. For low-rank coals, significant cross-linking happens before tar release.[267−269]

11. STRATEGIES TO INCREASE THE YIELD OF MONOPHENOLS

The Early Stage Catalytic Conversion of Lignin (ECCL) strategy provides an excellent framework for almost all the emerging technologies for lignin valorization.[8] The main hypothesis of all the strategies in this area is that employing solvents, catalysts, or additives in the liquefaction and fractionation of lignocellulosic materials may result in more easily refined lignin products. The goal is to avoid and circumvent the undesirable sequence of depolymerization (cleavage of weak C−O bonds), repolymerization (formation of strong C−C bonds), and depolymerization (through the cracking of C−C bonds formed in the previous step).[8] All the ECCL technologies are based on careful control of lignin depolymerization reactions and stabilization of lignin fragments to avoid the formation of recalcitrant C−C bonds (for example, reactive aldehydes as intermediates are reduced to alcohols).[8,272] In an extensive review, Kozliak et al. listed more than 40 lignin liquefaction conditions and tried to classify them by the approach used to mitigate undesirable repolymerization reactions (acid or base catalysts, use of protic solvents, ionic liquids, capping agents, redox approaches, short residence time, noble vs non-noble metal catalysts, metal oxides, sulfides and phosphides).[272]

Acid and Base Catalysts. The use of organic acids and bases is a common approach to accelerate depolymerization reactions and mitigate repolymerization. NaOH, boric acid,

https://dx.doi.org/10.1021/acs.iecr.9b05744
Ind. Eng. Chem. Res. 2020, 59, 526−555

Table 9. Summary of Computational and Experimental Modeling Approaches to Describe the Kinetics of Lignin Depolymerization

Authors	Type of Study	Summary
Adam et al.[193]	Experimental lignin pyrolysis and kinetic modeling	Kraft lignin is pyrolyzed in a fluidized bed reactor at temperatures from 450 to 600 °C. Four distinct lumped kinetic parameters are used for modeling pyrolysis: three primary reactions occurring in parallel to yield gases, tar and char from lignin; and one secondary reaction to yield gases from tar cracking. Frequency factors and activation energies for each are used to determine a kinetic constant for the lumped parameters. Good agreement is shown between experiment and modeling.
Farag et al.[278]	Experimental microwave pyrolysis of lignin and kinetic modeling	Kraft lignin is pyrolyzed in a microwave reactor with continuous weight-loss measurement from 20 to 790 °C. Liquid products collected are further analyzed with GC/MS. The authors propose three distinct kinetic models of increasing complexity. The first features parallel lumped reactions from lignin to noncondensable gas, condensable gas, and remaining solid. The second model has parallel reactions from lignin to noncondensable gas, water, oil, and remaining solid. The third model has parallel reactions from lignin to noncondensable gas, water, high molecular weight components (not GC/MS identified), aliphatic, single-ring nonphenolics, phenolics, and remaining solid.
Yong and Matsumura[279,280]	Experimental conversion of lignin in subcritical and supercritical water	Lignin reactions take place in supercritical water[280] (390−450 °C) with short residence times (0.5−10s) to evaluate kinetic parameters. Liquid and gas products were analyzed with HPLC and GC/TCD-FID, respectively. The authors then propose a lumped kinetic scheme for lignin liquefaction which features 10 lumped intermediate/product groups: starting lignin, guaiacol, phenol, catechol, o-cresol, m-cresol, "other liquid products", gas, aromatic hydrocarbons (benzene, naphthalene, toluene), and char. These lumped groups are variously connected by 20 assumed first-order reactions with reported kinetic parameters. Results from this study show good agreement with previously published experimental results on hydrothermal treatment of lignin.[281] Further work also considers lignin conversion in subcritical water.[279]
Gasson et al.;[282] Forchheim et al.[283]	Experimental lignin degradation in ethanol/formic acid and kinetic modeling	Experimental study utilizing Protobind 1000 lignin produced from wheat straw. Reactions employed 0.33 g of lignin in 0.27 g of formic acid and 2.0 g of ethanol under nitrogen in 5 mL batch reactors (part 1).[282] Reaction temperature was 360 °C with durations of 15, 30, 45, 60, 90, 120, 240, 360, 480, and 1180 min. Based on experimental results, the authors derive rate coefficients for 17 distinct lumped reactions between 11 lumped intermediate/final species. These groups include starting lignin, 4-ethylphenols, methoxyphenols, depolymerized lignin, phenols, catechols, 2-ethylphenols, ethanol, formic acid, char, and gas. Further work (part 2)[283] extends this kinetic model to CSTR and temperatures from 360 to 400 °C, reporting good agreement with experiments.
Klein and Virk[5]	Computational simulation of lignin pyrolysis	Freudenberg spruce lignin[96] is parametrized, and its pyrolysis is simulated at 400, 500, and 600 °C based on kinetic parameters derived for 16 model compounds (Table5). Pyrolysis products include gas, aqueous, phenolic, and carbonaceous residue fractions. Yields of simulated lignin pyrolysis at 500 °C are given for carbon monoxide, methane, water, methanol, guaiacol, catechol, phenol, methylguaiacol, methylcatechol, and p-cresol. Simulation results are compared to published experimental data.[284] Simulation shows good agreement with temporally resolved weight-loss during lignin pyrolysis, particularly for reaction temperature of 500 °C.
Yanez et al.[69]	Computational simulation of lignin pyrolysis	A stochastic model lignin library is used at the starting "feedstock" for wheat straw lignin pyrolysis. Kinetic parameters from Klein and Virk[5] are used as initial estimates, and frequency factors are optimized against experimental data.[191] Higher granularity is achieved in the molecular fingerprinting of pyrolysis products through the consideration of ∼4000 reactions and ∼1500 distinct species that result from the application of kinetic reaction families to the starting lignin library. Temporally resolved simulation yields of gases, aromatics, char, and aqueous fractions, as well as molecular weight distribution, are reported. There is good agreement between the model and experimental data[191] for the yields of the following product families: gases, oxygenates, water, char, phenols, ethyl phenols, vinyl phenols, propenyls, benzaldehydes, acetophenones, monolignols, and other aromatics.
Faravelli et al.[188]	Computational simulation of lignin pyrolysis	Three hypothetical structures termed "LIG-C ($C_{17}H_{17}O_5$)", "LIG-O ($C_{16}H_{11}O_6(OCH_3)_4$)", and "LIG-H ($C_{18}H_{17}O_5(OCH_3)_4$)" are used as reference units for lignin overall. These three model units are utilized such that their weighted sum has the same elemental composition (carbon, hydrogen, oxygen wt %) as a real lignin feedstock. Estimated kinetic rate parameters are applied to a variety of reactions lumped into higher groups. The reaction groups include initiation (11 total), decomposition (21 total), molecular (2 total), substitutive addition (20 total), recombination (32 total), volatilization (10 total), char devolatilization (10 total), and H-abstraction reactions (14 total). There is good agreement reported for temporally resolved model predictions and experimental data from a variety of sources/lignins.[285−287]
Hough et al.[189]	Computational simulation of lignin pyrolysis	Following a similar approach to Faravelli et al.,[188] the authors use LIG-C, LIG-O, and LIG-H model structures as reference units for starting pyrolysis. They also follow the same reaction framework as Faravelli et al. although with an updated kinetic scheme that includes ∼400 reactions and ∼100 species and justification for the applied modifications. The model shows good agreement with temporally resolved thermogravimetric experimental data for many milled wood lignins. Further, their simulation results also compare well with experimental[202] yields of light oil, heavy oil, char, and gas, as well as ^{13}C NMR characteristics, for the following functional groups: C═O, aromatic C−O, aromatic C−C, aromatic C−H, aliphatic C−O, methoxyl and aliphatic C−C. The Python code for this model is freely available for use, with details available in the original publication. Further work explored the application of machine learning to reduce model solution time.[288]

https://dx.doi.org/10.1021/acs.iecr.9b05744
Ind. Eng. Chem. Res. 2020, 59, 526−555

and CO_2 are known to facilitate the cleavage of ether bonds.[272] Lewis acids ($NiCl_2$, $FeCl_3$) also favor depolymerization reactions.[273] Kumar et al. studied the effect of acid and base catalysts (sulfuric acid, acetic acid, formic acid, KOH, $KHCO_3$, CH_3COONa, CH_3COOK) on the formation of heavy oligomers during biomass liquefaction in phenolic solvents. The authors found that H_2SO_4 had a negative effect; all the bases studied reduced the formation of heavy components.[274] Walker et al. recently published universal kinetic solvent effects in acid-catalyzed reactions of biomass-derived oxygenates which has potential to be very useful for the development of generalized microkinetic models for lignin liquefaction technologies.[68]

Capping and Protecting Agents. These are agents that form a product with reduced reactivity toward repolymerization. Boric acid is believed to complex phenolic anions of lignin intermediates, reducing in this way its electron density and reactivity toward carbonyl moieties.[272] Organic protic solvents such as alcohols activate ether-bond depolymerization and slow product repolymerization.[275] In the case of methanol, it suppresses repolymerization by methylation of the intermediate products during lignin hydrogenolysis.[276] Shuai et al. reported that adding formaldehyde during biomass pretreatment produces a lignin soluble fraction that results in high yields of monomers. Formaldehyde prevents lignin condensation by forming 1,3-dioxane structures with lignin hydroxyl side groups.[277]

12. FROM MICROKINETICS TO PSEUDOKINETICS

One of the major challenges when using microkinetics is that the results of this type of modeling approach are difficult to integrate with data or results at higher scales. In the area of lignin pyrolysis/solvolysis, pseudokinetic models utilizing lumped parameters and families of representative reactions with associated kinetic values have been proposed. Some of these are summarized in Table 9. In general, computational studies are able to rely on a wider range of molecularly derived reaction simulations, while experimental work tends to be limited to more broad lumped schemes, as previously outlined in Section 5.

Although it has been shown that molecular-level detail is achievable with computational study, experimental work is rarely able to capture the fine nature of lignin depolymerization, largely due to the heterogeneity of the starting material and diversity among the large number of reactions that are taking place. There still remain significant challenges at every scale for effective modeling of char formation.[289] However, as shown among some computational studies, results for lignin depolymerization can still be abstracted *post hoc* into lumped parameters following more highly detailed simulation.[232−238,62,177,178] In this way, it is possible to employ computational microkinetic algorithms/simulations, with a tremendously high level of detail, to derive pseudokinetic lumped parameters that are verifiable using experimental techniques for both pyrolytic and solvolytic lignin liquefaction.

One actionable approach that shows promise for developing the microkinetics of lignin liquefaction is through the implementation of automated generators to discern reaction networks, as described in perspectives from Van de Vijver et al. and Vernuccio and Broadbelt.[290,291] The advantage of using an automated reaction network generators lies in the fact that model complexity grows with the number of species included.[290] Because of lignin's heterogeneity and high molecular weight (relative to, for example, light aliphatic hydrocarbons), any pyrolysis reaction network must be very large, featuring thousands of reactions with varying degrees of interconnectivity. To generate "by hand" a mechanistic model at this level of complexity is nearly impossible.[291] Among the ∼200 references detailed in Vernuccio and Broadbelt's perspective on automated reaction network generators, only five explicitly cover microkinetic pyrolysis modeling of biomass polymers: glucose-based carbohydrates,[292−294] hemicellulose,[295] and lignin[69] (from Yanez et al., cited frequently herein). Because of the relative paucity of available work in this area on biomass in general and lignin specifically, there is significant room for growth. Once a reaction network is developed, it can then be constrained by SEMK-style classification into reaction families and/or a seeding technique,[296,297] thereby reducing its size and making it of reasonable scale with which to work computationally and validate experimentally.

Additionally, the lab-scale depolymerization kinetics study of lignin model compounds larger than dimers is challenging. It can be significantly labor intensive[172] to synthesize (in sufficient quantity), characterize, and experiment with such compounds, especially in light of the diversity among lignin monomers and interunit linkages. For example, Forsythe et al. report a method by which gram-scale quantities of lignin oligomers can be synthesized; however, even this work is limited to featuring β-O-4, β-5, and 5-5 bonds.[298] For this reason, it is appropriate to turn to truer *ab initio* computational methods to gain a deeper understanding of lignin model compound depolymerization. Two successful approaches from Kulik and co-workers feature the use of density functional theory and molecular dynamics to study relevant lignin bond cleavages.[299,300] Further development of a computational first-principles understanding of lignin depolymerization in this way can then be used to enrich and inform future microkinetic models.

13. SUMMARY AND OUTLOOK

Effective research and utilization of lignin and lignin-based feedstocks are critical for future growth in engineering developments to support a renewable and sustainable biobased economy for fuels, chemicals, and other high value materials. One concrete step that can be taken with respect to our fundamental understanding of thermochemical lignin conversion lies in the development of a microkinetic model. In this review, some of the necessary experimental data-driven inputs to such a model are discussed, including structural characterization, reaction kinetics, effect of reactor parameters, and product removal mechanisms from intermediate phase (i.e., vaporization, aerosoliziation, solubilization, carbonization/char forming reactions).

Using experimental techniques—analytical pyrolysis coupled with GC/MS, DFRC method, range of NMR approaches, GPC, and others—the necessary parameters can be determined for building a structural lignin model. These parameters are relative monomer percent (p-hydroxyphenyl, guaiacyl, syringyl), bond-type distribution (β-O-4, α-O-4, β-1, β-5, $\beta-\beta$, 4-O-5, 5-5), molecular weight characteristics (number-averaged and weight-averaged), and degree of branching. It was shown here that branching can be calculated from the molecular weight characteristics and is therefore not a parameter that needs to be independently determined; however, there is significant room to grow in the under-

https://dx.doi.org/10.1021/acs.iecr.9b05744
Ind. Eng. Chem. Res. 2020, 59, 526−555

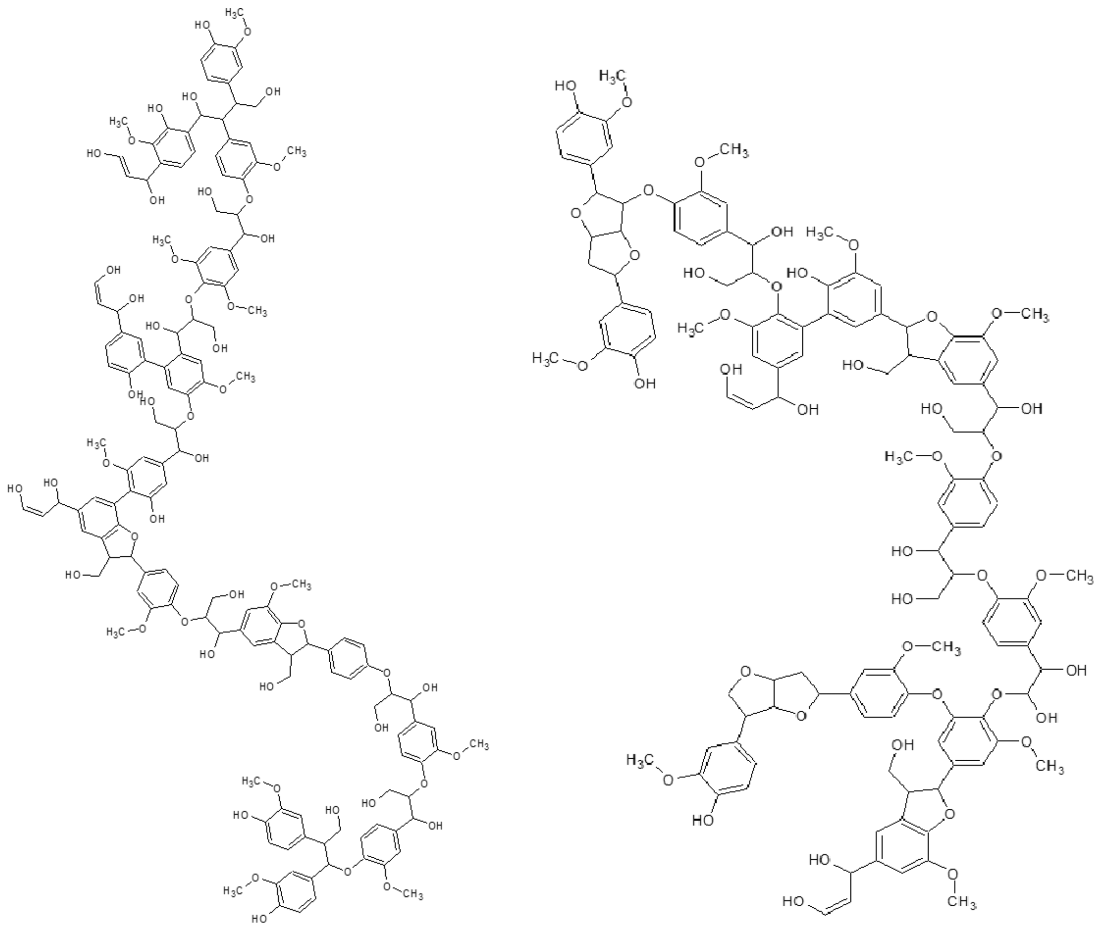

Figure 15. Lignin fragments developed from stochastic modeling; adapted from Dellon et al.[71]

standing of lignin branching (if it exists at all) and in the development of experimental or analytical techniques to probe the degree of branching directly. From a well-defined set of data, lignin structure libraries can be built.[70,71] Two fragments from such a library are given in Figure 15. The advantage of starting with a realistic structure is that there is potential for also simulating the analytical characterization of the stochastically derived lignins; for example, good results have been reported for the computational simulation of NMR chemical shifts for model lignin monomers and dimers.[301,302] An alternative approach is to use the LIG-O/C/H model units proposed by Faravelli et al.[51]

With a foundational structure space built, elementary reaction kinetics can be applied to the polymeric lignin macromolecule to analyze the nature of its decomposition. The bulk of elementary reaction kinetics have been and continue to be assessed through experimental work with model compounds and more recently with computational approaches like molecular dynamics[299,303,304] and/or density functional theory.[189,300,305] This work helps to develop the necessary kinetic parameters for lignin decomposition reactions (i.e., activation energy, pre-exponential factor, or kinetic rate constant). Using this type of model-compound work, coupled with results from experimental analysis of the effect of reaction parameters (temperature, pressure, residence time), allows for conjecturing and/or automatically generating reaction mechanisms and elucidating computationally efficient yet sufficiently rich pathways to describe lignin depolymerization at the molecular level. While there are limitations in using monomeric model compounds as surrogates for lignin, the potential for high-resolution mass spectrometry characterization of oligomeric models[306] and whole lignin[42,208] pyrolysis shows promise.

Finally, there is room for further growth in the understanding of physical and thermal transport phenomena that occur outside of the realm of chemical kinetics within lignin pyrolysis. These transport effects have a significant impact on final product formation and particularly on the fate of primary and intermediate lignin-derived oligomers. Clausius−Clapeyron relations can be employed to describe vaporization of light molecules (up to oligomers). It is also distinctly possible that group contribution methods can be used to estimate thermophysical parameters or potentially build lignin oligomer phase diagrams based on a well-characterized starting structure (or library of structures). Using carefully designed experiments, future research can experimentally measure the physical rates of aerosol ejection or assess the rate and nature of product dissolution in a lignin solvolysis system. With appropriate metrics developed to quantify product removal mechanisms and the effect of additives and/or catalysts, ultimately a more-precise computational microkinetic model can be built and verified or validated with experimental study.

■ ASSOCIATED CONTENT

Supporting Information

The Supporting Information is available free of charge at https://pubs.acs.org/doi/10.1021/acs.iecr.9b05744.

https://dx.doi.org/10.1021/acs.iecr.9b05744
Ind. Eng. Chem. Res. 2020, 59, 526−555

Example Py-GC/MS monomers, example lignin NMR spectra (simulated), some lignin-relevant organic solvents, and their solubility parameters (PDF)

AUTHOR INFORMATION

Corresponding Author

Manuel Garcia-Perez − *Washington State University, Pullman, Washington;* orcid.org/0000-0002-9386-2632; Phone: 509-335-7758; Email: mgarcia-perez@wsu.edu

Other Authors

Evan Terrell − *Washington State University, Pullman, Washington;* orcid.org/0000-0002-1079-4110

Lauren D. Dellon − *Northwestern University, Evanston, Illinois*

Anthony Dufour − *Universite de Lorraine, Nancy, France*

Erika Bartolomei − *Universite de Lorraine, Nancy, France*

Linda J. Broadbelt − *Northwestern University, Evanston, Illinois;* orcid.org/0000-0003-4253-592X

Complete contact information is available at: https://pubs.acs.org/10.1021/acs.iecr.9b05744

Notes

The authors declare no competing financial interest.

ACKNOWLEDGMENTS

The authors acknowledge the financial contributions received from the U.S. Department of Energy (DE-EE0008505) and the U.S. National Science Foundation (NSF-CBET 1926412). The authors are very thankful to the Washington State Department of Ecology and the Federal Aviation Administration for their partial financial support to collect information contained in this review. Anamaria Paiva Pinheiro Pires is especially acknowledged for fruitful discussions, particularly with regard to kinetics and group contribution. Dr. Garcia-Perez is also very thankful to the U.S. Department of Agriculture's National Institute of Food and Agriculture through the Hatch Project (WNP00701) for funding his research program. This project received funding from ARENA as part of ARENA's Emerging Renewables Program. This material is based upon research supported by the Chateaubriand Fellowship of the Office of Science & Technology of the Embassy of France in the United States.

REFERENCES

(1) Ragauskas, A. J.; Beckham, G. T.; Biddy, M. J.; Chandra, R.; Chen, F.; Davis, M. F.; Davison, B. H.; Dixon, R. A.; Gilna, P.; Keller, M.; Langan, P.; Naskar, A. K.; Saddler, J. N.; Tschaplinski, T. J.; Tuskan, G. A.; Wyman, C. E. Lignin Valorization: Improving Lignin Processing in the Biorefinery. *Science (Washington, DC, U. S.)* **2014**, *344* (6185), 1246843.

(2) Wang, H.; Pu, Y.; Ragauskas, A.; Yang, B. From Lignin to Valuable Products−Strategies, Challenges, and Prospects. *Bioresour. Technol.* **2019**, *271* (July 2018), 449−461.

(3) Vermaas, J. V.; Dellon, L. D.; Broadbelt, L. J.; Beckham, G. T.; Crowley, M. F. Automated Transformation of Lignin Topologies into Atomic Structures with LigninBuilder. *ACS Sustainable Chem. Eng.* **2019**, *7* (3), 3443−3453.

(4) Erickson, B.; Nelson; Winters, P. Perspective on Opportunities in Industrial Biotechnology in Renewable Chemicals. *Biotechnol. J.* **2012**, *7* (2), 176−185.

(5) Klein, M. T.; Virk, P. S. Modeling of Lignin Thermolysis. *Energy Fuels* **2008**, *22* (4), 2175−2182.

(6) Hatcher, P. G.; Faulon, J. L.; Wenzel, K. A.; Cody, G. D. A Structural Model for Lignin-Derived Vitrinite from High-Volatile Bituminous Coal (Coalified Wood). *Energy Fuels* **1992**, *6* (6), 813−820.

(7) Mathews, J. P.; Chaffee, A. L. The Molecular Representations of Coal - A Review. *Fuel* **2012**, *96*, 1−14.

(8) Rinaldi, R.; Jastrzebski, R.; Clough, M. T.; Ralph, J.; Kennema, M.; Bruijnincx, P. C. A.; Weckhuysen, B. M. Paving the Way for Lignin Valorisation: Recent Advances in Bioengineering, Biorefining and Catalysis. *Angew. Chem., Int. Ed.* **2016**, *55* (29), 8164−8215.

(9) Laird, D. A.; Brown, R. C.; Amonette, J. E.; Lehmann, J. Review of the Pyrolysis Platform for Coproducing Bio-Oil and Biochar. *Biofuels, Bioprod. Biorefin.* **2009**, *3*, 547−562.

(10) Bridgwater, A. V. Review of Fast Pyrolysis of Biomass and Product Upgrading. *Biomass Bioenergy* **2012**, *38*, 68−94.

(11) Kersten, S.; Garcia-Perez, M. Recent Developments in Fast Pyrolysis of Ligno-Cellulosic Materials. *Curr. Opin. Biotechnol.* **2013**, *24* (3), 414−420.

(12) Mohan, D.; Pittman, C. U.; Steele, P. H. Pyrolysis of Wood/Biomass for Bio-Oil: A Critical Review. *Energy Fuels* **2006**, *20* (3), 848−889.

(13) Alam, D.; Lui, M. Y.; Yuen, A.; Maschmeyer, T.; Haynes, B. S.; Montoya, A. Reaction Analysis of Diaryl Ether Decomposition under Hydrothermal Conditions. *Ind. Eng. Chem. Res.* **2018**, *57* (6), 2014−2022.

(14) Jensen, M. M.; Djajadi, D. T.; Torri, C.; Rasmussen, H. B.; Madsen, R. B.; Venturini, E.; Vassura, I.; Becker, J.; Iversen, B. B.; Meyer, A. S.; Jørgensen, H.; Fabbri, D.; Glasius, M. Hydrothermal Liquefaction of Enzymatic Hydrolysis Lignin: Biomass Pretreatment Severity Affects Lignin Valorization. *ACS Sustainable Chem. Eng.* **2018**, *6* (5), 5940−5949.

(15) Arturi, K. R.; Strandgaard, M.; Nielsen, R. P.; Søgaard, E. G.; Maschietti, M. Hydrothermal Liquefaction of Lignin in Near-Critical Water in a New Batch Reactor: Influence of Phenol and Temperature. *J. Supercrit. Fluids* **2017**, *123*, 28−39.

(16) Meier, D.; Berns, J.; Faix, O.; Balfanz, U.; Baldauf, W. Hydrocracking of Organocell Lignin for Phenol Production. *Biomass Bioenergy* **1994**, *7* (1−6), 99−105.

(17) Løhre, C.; Barth, T.; Kleinert, M. The Effect of Solvent and Input Material Pretreatment on Product Yield and Composition of Bio-Oils from Lignin Solvolysis. *J. Anal. Appl. Pyrolysis* **2016**, *119*, 208−216.

(18) Løhre, C.; Laugerud, G. A. A.; Huijgen, W. J. J.; Barth, T. Lignin-to-Liquid-Solvolysis (LtL) of Organosolv Extracted Lignin. *ACS Sustainable Chem. Eng.* **2018**, *6* (3), 3102−3112.

(19) Liu, Q.; Li, P.; Liu, N.; Shen, D. Lignin Depolymerization to Aromatic Monomers and Oligomers in Isopropanol Assisted by Microwave Heating. *Polym. Degrad. Stab.* **2017**, *135*, 54−60.

(20) Jones, S.; Valkenburg, C.; Walton, C.; Elliott, D.; Holladay, J.; Stevens, D.; Kinchin, C.; Czernik, S. *Production of Gasoline and Diesel from Biomass via Fast Pyrolysis, Hydrotreating and Hydrocracking: A Design Case* **2009**, DOI: 10.2172/1218327.

(21) Jones, S.; Snowden-Swan, L. *Production of Gasoline and Diesel from Biomass via Fast Pyrolysis, Hydrotreating and Hydrocracking: 2012 State of Technology and Projections to 2017* **2013**, DOI: 10.2172/1111230.

(22) Gayubo, A. G.; Valle, B.; Aguayo, A. T.; Olazar, M.; Bilbao, J. Pyrolytic Lignin Removal for the Valorization of Biomass Pyrolysis Crude Bio-Oil by Catalytic Transformation. *J. Chem. Technol. Biotechnol.* **2010**, *85* (1), 132−144.

(23) Schutyser, W.; Renders, T.; Van Den Bosch, S.; Koelewijn, S. F.; Beckham, G. T.; Sels, B. F. Chemicals from Lignin: An Interplay of Lignocellulose Fractionation, Depolymerisation, and Upgrading. *Chem. Soc. Rev.* **2018**, *47* (3), 852−908.

(24) Lange, J. P. Renewable Feedstocks: The Problem of Catalyst Deactivation and Its Mitigation. *Angew. Chem., Int. Ed.* **2015**, *54* (45), 13186−13197.

(25) Stankovikj, F.; McDonald, A. G.; Helms, G. L.; Garcia-Perez, M. Quantification of Bio-Oil Functional Groups and Evidences of the Presence of Pyrolytic Humins. *Energy Fuels* **2016**, *30* (8), 6505−6524.
(26) Stankovikj, F.; McDonald, A. G.; Helms, G. L.; Olarte, M. V.; Garcia-Perez, M. Characterization of the Water-Soluble Fraction of Woody Biomass Pyrolysis Oils. *Energy Fuels* **2017**, *31* (2), 1650−1664.
(27) Pinheiro Pires, A. P.; Arauzo, J.; Fonts, I.; Domine, M. E.; Fernández Arroyo, A.; Garcia-Perez, M. E.; Montoya, J.; Chejne, F.; Pfromm, P.; Garcia-Perez, M. Challenges and Opportunities for Bio-Oil Refining: A Review. *Energy Fuels* **2019**, *33* (6), 4683−4720.
(28) Tiarks, J. A.; Dedic, C. E.; Meyer, T. R.; Brown, R. C.; Michael, J. B. Visualization of Physicochemical Phenomena during Biomass Pyrolysis in an Optically Accessible Reactor. *J. Anal. Appl. Pyrolysis* **2019**, *143* (August), 104667.
(29) Iisa, K.; Johansson, A. C.; Pettersson, E.; French, R. J.; Orton, K. A.; Wiinikka, H. Chemical and Physical Characterization of Aerosols from Fast Pyrolysis of Biomass. *J. Anal. Appl. Pyrolysis* **2019**, *142* (April), 104606.
(30) Marathe, P. S.; Westerhof, R. J. M.; Kersten, S. R. A. Fast Pyrolysis of Lignins with Different Molecular Weight: Experiments and Modelling. *Appl. Energy* **2019**, *236* (December 2018), 1125−1137.
(31) Pelaez-Samaniego, M. R.; Yadama, V.; Garcia-Perez, M.; Lowell, E.; McDonald, A. G. Effect of Temperature during Wood Torrefaction on the Formation of Lignin Liquid Intermediates. *J. Anal. Appl. Pyrolysis* **2014**, *109*, 222−233.
(32) Pelaez-Samaniego, M. R.; Yadama, V.; Garcia-Perez, M.; Lowell, E. Abundance and Characteristics of Lignin Liquid Intermediates in Wood (Pinus Ponderosa Dougl. Ex Laws.) during Hot Water Extraction. *Biomass Bioenergy* **2015**, *81*, 117−128.
(33) Hilbers, T. J.; Wang, Z.; Pecha, B.; Westerhof, R. J. M.; Kersten, S. R. A.; Pelaez-Samaniego, M. R.; Garcia-Perez, M. Cellulose-Lignin Interactions during Slow and Fast Pyrolysis. *J. Anal. Appl. Pyrolysis* **2015**, *114*, 197−207.
(34) Zhou, S.; Mourant, D.; Lievens, C.; Wang, Y.; Li, C. Z.; Garcia-Perez, M. Effect of Sulfuric Acid Concentration on the Yield and Properties of the Bio-Oils Obtained from the Auger and Fast Pyrolysis of Douglas Fir. *Fuel* **2013**, *104*, 536−546.
(35) Zhou, S.; Garcia-Perez, M.; Pecha, B.; Kersten, S. R. A.; McDonald, A. G.; Westerhof, R. J. M. Effect of the Fast Pyrolysis Temperature on the Primary and Secondary Products of Lignin. *Energy Fuels* **2013**, *27* (10), 5867−5877.
(36) Zhou, S.; Pecha, B.; van Kuppevelt, M.; McDonald, A. G.; Garcia-Perez, M. Slow and Fast Pyrolysis of Douglas-Fir Lignin: Importance of Liquid-Intermediate Formation on the Distribution of Products. *Biomass Bioenergy* **2014**, *66*, 398−409.
(37) Zhou, S.; Garcia-Perez, M.; Pecha, B.; McDonald, A. G.; Westerhof, R. J. M. Effect of Particle Size on the Composition of Lignin Derived Oligomers Obtained by Fast Pyrolysis of Beech Wood. *Fuel* **2014**, *125*, 15−19.
(38) Zhou, S.; Garcia-Perez, M.; Pecha, B.; McDonald, A. G.; Kersten, S. R. A.; Westerhof, R. J. M. Secondary Vapor Phase Reactions of Lignin-Derived Oligomers Obtained by Fast Pyrolysis of Pine Wood. *Energy Fuels* **2013**, *27* (3), 1428−1438.
(39) Montoya, J.; Pecha, B.; Janna, F. C.; Garcia-Perez, M. Micro-Explosion of Liquid Intermediates during the Fast Pyrolysis of Sucrose and Organosolv Lignin. *J. Anal. Appl. Pyrolysis* **2016**, *122*, 106−121.
(40) Montoya, J.; Pecha, B.; Janna, F. C.; Garcia-Perez, M. Single Particle Model for Biomass Pyrolysis with Bubble Formation Dynamics inside the Liquid Intermediate and Its Contribution to Aerosol Formation by Thermal Ejection. *J. Anal. Appl. Pyrolysis* **2017**, *124*, 204−218.
(41) Montoya, J.; Pecha, B.; Janna, F. C.; Garcia-Perez, M. Methodology for Estimation of Thermal Ejection Droplet Size Distribution and Intensity during the Pyrolysis of Sugarcane Bagasse and Model Compounds. *J. Anal. Appl. Pyrolysis* **2017**, *125* (May), 69−82.
(42) Pecha, M. B.; Terrell, E.; Montoya, J. I.; Stankovikj, F.; Broadbelt, L. J.; Chejne, F.; Garcia-Perez, M. Effect of Pressure on Pyrolysis of Milled Wood Lignin and Acid-Washed Hybrid Poplar Wood. *Ind. Eng. Chem. Res.* **2017**, *56* (32), 9079.
(43) Piskorz, J.; Majerski, P.; Radlein, D. Pyrolysis of Biomass - Aerosol Generation: Properties, Applications, and Significance for Process Engineers. In *Biomass Conference of the Americas*; Oakland, CA, 1999.
(44) Fratini, E.; Bonini, M.; Oasmaa, A.; Solantausta, Y.; Teixeira, J.; Baglioni, P. SANS Analysis of the Microstructural Evolution during the Aging of Pyrolysis Oils from Biomass. *Langmuir* **2006**, *22* (1), 306−312.
(45) Bai, X.; Kim, K. H.; Brown, R. C.; Dalluge, E.; Hutchinson, C.; Lee, Y. J.; Dalluge, D. Formation of Phenolic Oligomers during Fast Pyrolysis of Lignin. *Fuel* **2014**, *128*, 170−179.
(46) Dumesic, J. A.; Rudd, D. F.; Aparicio, L. M.; Rekoske, J. E.; Trevino, A. A. *The Microkinetics of Heterogeneous Catalysis*; American Chemical Society: Washington, DC, 1993.
(47) Davis, M. E.; Davis, R. J. Microkinetic Analysis of Catalytic Reactions. In *Fundamentals of Chemical Reaction Engineering*; McGraw-Hill: New York, 2003; Chapter 7.
(48) Choksi, T.; Greeley, J. Partial Oxidation of Methanol on MoO3 (010): A DFT and Microkinetic Study. *ACS Catal.* **2016**, *6* (11), 7260−7277.
(49) Koehle, M.; Mhadeshwar, A. Microkinetic Modeling and Analysis of Ethanol Partial Oxidation and Reforming Reaction Pathways on Platinum at Short Contact Times. *Chem. Eng. Sci.* **2012**, *78*, 209−225.
(50) Kraus, P.; Lindstedt, R. P. Microkinetic Mechanisms for Partial Oxidation of Methane over Platinum and Rhodium. *J. Phys. Chem. C* **2017**, *121* (17), 9442−9453.
(51) Ranzi, E.; Frassoldati, A.; Granata, S.; Faravelli, T. Wide-Range Kinetic Modeling Study of the Pyrolysis, Partial Oxidation, and Combustion of Heavy n-Alkanes. *Ind. Eng. Chem. Res.* **2005**, *44* (14), 5170−5183.
(52) Moss, J. T.; Berkowitz, A. M.; Oehlschlaeger, M. A.; Biet, J.; Warth, V.; Glaude, P.-A.; Battin-Leclerc, F. An Experimental and Kinetic Modeling Study of the Oxidation of the Four Isomers of Butanol. *J. Phys. Chem. A* **2008**, *112* (43), 10843−10855.
(53) Oakley, L. H.; Casadio, F.; Shull, P. K. R.; Broadbelt, P. L. J. Modeling the Evolution of Crosslinked and Extractable Material in an Oil-Based Paint Model System. *Angew. Chem., Int. Ed.* **2018**, *57* (25), 7413−7417.
(54) Oakley, L. H.; Casadio, F.; Shull, K. R.; Broadbelt, L. J. Examination of Mechanisms for Formation of Volatile Aldehydes from Oxidation of Oil-Based Systems. *Ind. Eng. Chem. Res.* **2018**, *57* (1), 139−149.
(55) Solomon, P. R.; Fletcher, T. H.; Pugmire, R. J. Progress in Coal Pyrolysis. *Fuel* **1993**, *72* (5), 587−597.
(56) Solomon, P. R.; Serio, M. A.; Suuberg, E. M. Coal Pyrolysis: Experiments, Kinetic Rates and Mechanisms. *Prog. Energy Combust. Sci.* **1992**, *18* (2), 133−220.
(57) Oh, M. S.; Peters, W. A.; Howard, J. B. An Experimental and Modeling Study of Softening Coal Pyrolysis. *AIChE J.* **1989**, *35* (5), 775−792.
(58) Grant, D. M.; Pugmire, R. J.; Fletcher, T. H.; Kerstein, A. R. Chemical Model of Coal Devolatilization Using Percolation Lattice Statistics. *Energy Fuels* **1989**, *3* (2), 175−186.
(59) Fletcher, T. H.; Kerstein, A. R.; Pugmire, R. J.; Grant, D. M. Chemical Percolation Model for Devolatilization. 2. Temperature and Heating Rate Effects on Product Yields. *Energy Fuels* **1990**, *4* (1), 54−60.
(60) Fletcher, T. H.; Kerstein, A. R.; Pugmire, R. J.; Solum, M. S.; Grant, D. M. Chemical Percolation Model for Devolatilization. 3. Direct Use of 13C NMR Data To Predict Effects of Coal Type. *Energy Fuels* **1992**, *6* (4), 414−431.
(61) Genetti, D.; Fletcher, T. H.; Pugmire, R. J. Development and Application of a Correlation Of13C NMR Chemical Structural

Analyses of Coal Based on Elemental Composition and Volatile Matter Content. *Energy Fuels* **1999**, *13* (1), 60−68.
(62) Hsu, J. *Swelling, Mass Transport, and Chemical Kinetics in Bituminous Coal Pyrolysis*; Massachusetts Institue of Technology, 1989.
(63) Brebu, M.; Tamminen, T.; Spiridon, I. Thermal Degradation of Various Lignins by TG-MS/FTIR and Py-GC-MS. *J. Anal. Appl. Pyrolysis* **2013**, *104*, 531−539.
(64) ChemSpider. www.chemspider.com (accessed Oct 13, 2019).
(65) Fletcher, T. H. Review of 30 Years of Research Using the Chemical Percolation Devolatilization Model. *Energy Fuels* **2019**, *33* (12), 12123−12153.
(66) Buendia-Kandia, F.; Mauviel, G.; Guedon, E.; Rondags, E.; Petitjean, D.; Dufour, A. Decomposition of Cellulose in Hot-Compressed Water: Detailed Analysis of the Products and Effect of Operating Conditions. *Energy Fuels* **2018**, *32* (4), 4127−4138.
(67) Castellví Barnés, M.; Oltvoort, J.; Kersten, S. R. A.; Lange, J. P. Wood Liquefaction: Role of Solvent. *Ind. Eng. Chem. Res.* **2017**, *56* (3), 635−644.
(68) Walker, T. W.; Chew, A. K.; Li, H.; Demir, B.; Zhang, Z. C.; Huber, G. W.; Van Lehn, R. C.; Dumesic, J. A. Universal Kinetic Solvent Effects in Acid-Catalyzed Reactions of Biomass-Derived Oxygenates. *Energy Environ. Sci.* **2018**, *11* (3), 617−628.
(69) Yanez, A. J.; Natarajan, P.; Li, W.; Mabon, R.; Broadbelt, L. J. Coupled Structural and Kinetic Model of Lignin Fast Pyrolysis. *Energy Fuels* **2018**, *32* (2), 1822−1830.
(70) Yanez, A. J.; Li, W.; Mabon, R.; Broadbelt, L. J. A Stochastic Method to Generate Libraries of Structural Representations of Lignin. *Energy Fuels* **2016**, *30* (7), 5835−5845.
(71) Dellon, L. D.; Yanez, A. J.; Li, W.; Mabon, R.; Broadbelt, L. J. Computational Generation of Lignin Libraries from Diverse Biomass Sources. *Energy Fuels* **2017**, *31* (8), 8263−8274.
(72) Banoub, J.; Delmas, G. H.; Joly, N.; Mackenzie, G.; Cachet, N.; Benjelloun-Mlayah, B.; Delmas, M. A Critique on the Structural Analysis of Lignins and Application of Novel Tandem Mass Spectrometric Strategies to Determine Lignin Sequencing. *J. Mass Spectrom.* **2015**, *50* (1), 5−48.
(73) Kiyota, E.; Mazzafera, P.; Sawaya, A. C. H. F. Analysis of Soluble Lignin in Sugarcane by Ultrahigh Performance Liquid Chromatography-Tandem Mass Spectrometry with a Do-It-Yourself Oligomer Database. *Anal. Chem.* **2012**, *84* (16), 7015−7020.
(74) Araújo, P.; Ferreira, M. S.; De Oliveira, D. N.; Pereira, L.; Sawaya, A. C. H. F.; Catharino, R. R.; Mazzafera, P. Mass Spectrometry Imaging: An Expeditious and Powerful Technique for Fast in Situ Lignin Assessment in Eucalyptus. *Anal. Chem.* **2014**, *86* (7), 3415−3419.
(75) Dufour, A.; Ouartassi, B.; Bounaceur, R.; Zoulalian, A. Modelling Intra-Particle Phenomena of Biomass Pyrolysis. *Chem. Eng. Res. Des.* **2011**, *89* (10), 2136−2146.
(76) Pecha, M. B.; Arbelaez, J. I. M.; Garcia-Perez, M.; Chejne, F.; Ciesielski, P. N. *Progress in Understanding the Four Dominant Intra-Particle Phenomena of Lignocellulose Pyrolysis: Chemical Reactions, Heat Transfer, Mass Transfer, and Phase Change*; Royal Society of Chemistry, 2019; Vol. *21*. DOI: 10.1039/c9gc00585d.
(77) Vanholme, R.; De Meester, B.; Ralph, J.; Boerjan, W. Lignin Biosynthesis and Its Integration into Metabolism. *Curr. Opin. Biotechnol.* **2019**, *56*, 230−239.
(78) Ralph, J.; Lapierre, C.; Boerjan, W. Lignin Structure and Its Engineering. *Curr. Opin. Biotechnol.* **2019**, *56*, 240−249.
(79) Vanholme, R.; Demedts, B.; Morreel, K.; Ralph, J.; Boerjan, W. Lignin Biosynthesis and Structure. *Plant Physiol.* **2010**, *153* (3), 895−905.
(80) Vogel, J. Unique Aspects of the Grass Cell Wall. *Curr. Opin. Plant Biol.* **2008**, *11* (3), 301−307.
(81) Besombes, S.; Robert, D.; Utille, J. P.; Taravel, F. R.; Mazeau, K. Molecular Modeling of Syringyl and P-Hydroxyphenyl β-O-4 Dimers. Comparative Study of the Computed and Experimental Conformational Properties of Lignin β-O-4 Model Compounds. *J. Agric. Food Chem.* **2003**, *51* (1), 34−42.
(82) Ralph, J.; Lundquist, K.; Brunow, G.; Lu, F.; Kim, H.; Schatz, P. F.; Marita, J. M.; Hatfield, R. D.; Ralph, S. A.; Christensen, J. H.; Boerjan, W. Lignins: Natural Polymers from Oxidative Coupling of 4-Hydroxyphenyl- Propanoids. *Phytochem. Rev.* **2004**, *3* (1−2), 29−60.
(83) Hatfield, R. D.; Rancour, D. M.; Marita, J. M. Grass Cell Walls: A Story of Cross-Linking. *Front. Plant Sci.* **2017**, *7* (January), na DOI: 10.3389/fpls.2016.02056.
(84) Tobimatsu, Y.; Schuetz, M. Lignin Polymerization: How Do Plants Manage the Chemistry so Well? *Curr. Opin. Biotechnol.* **2019**, *56*, 75−81.
(85) Holtman, K. M.; Chen, N.; Chappell, M. A.; Kadla, J. F.; Xu, L.; Mao, J. Chemical Structure and Heterogeneity Differences of Two Lignins from Loblolly Pine as Investigated by Advanced Solid-State NMR Spectroscopy. *J. Agric. Food Chem.* **2010**, *58* (18), 9882−9892.
(86) Behling, R.; Valange, S.; Chatel, G. Heterogeneous Catalytic Oxidation for Lignin Valorization into Valuable Chemicals: What Results? What Limitations? What Trends? *Green Chem.* **2016**, *18* (7), 1839−1854.
(87) Albishi, T.; Mikhael, A.; Shahidi, F.; Fridgen, T. D.; Delmas, M.; Banoub, J. Top-down Lignomic Matrix-Assisted Laser Desorption/Ionization Time-of-Flight Tandem Mass Spectrometry Analysis of Lignin Oligomers Extracted from Date Palm Wood. *Rapid Commun. Mass Spectrom.* **2019**, *33* (6), 539−560.
(88) Chakar, F. S.; Ragauskas, A. J. Review of Current and Future Softwood Kraft Lignin Process Chemistry. *Ind. Crops Prod.* **2004**, *20* (2), 131−141.
(89) Boerjan, W.; Ralph, J.; Baucher, M. Lignin Biosynthesis. *Annu. Rev. Plant Biol.* **2003**, *54* (1), 519−546.
(90) Vanholme, R.; Demedts, B.; Morreel, K.; Ralph, J.; Boerjan, W. Lignin Biosynthesis and Structure. *Plant Physiol.* **2010**, *153* (3), 895−905.
(91) Dolk, M.; Pla, F.; Yan, J. F.; McCarthy, J. L. Lignin. 22. Macromolecular Characteristics of Alkali Lignin from Western Hemlock Wood1a. *Macromolecules* **1986**, *19* (5), 1464−1470.
(92) Pla, F.; Dolk, M.; Yan, J. F.; McCarthy, J. L. Lignin. 23. Macromolecular Characteristics of Alkali Lignin and Organosolv Lignin from Black Cottonwood. *Macromolecules* **1986**, *19* (5), 1471−1477.
(93) Pla, F.; Yan, J. F. Branching and Functionality of Lignin Molecules. *J. Wood Chem. Technol.* **1984**, *4* (3), 285−299.
(94) Pla, F.; Yan, J. F. Viscosity and Functionality of Alkali and Organosolv Lignins. *Holzforschung* **1991**, *45* (2), 121−126.
(95) Crestini, C.; Melone, F.; Sette, M.; Saladino, R. Milled Wood Lignin: A Linear Oligomer. *Biomacromolecules* **2011**, *12* (11), 3928−3935.
(96) Freudenberg, K. Lignin: Its Constitution and Formation from p-Hydroxycinnamyl Alcohols. *Science (Washington, DC, U. S.)* **1965**, *148* (3670), 595−600.
(97) Sakakibara, A. A Structural Model of Softwood Lignin. *Wood Sci. Technol.* **1980**, *14* (2), 89−100.
(98) Adler, E. Structural Elements of Lignin. *Ind. Eng. Chem.* **1957**, *49* (9), 1377−1383.
(99) Glasser, W. G.; Glasser, H. R.; Morohoshi, N. Simulation of Reactions with Lignin by Computer (Simrel). 6. Interpretation of Primary Experimental Analysis Data ("Analysis Program"). *Macromolecules* **1981**, *14* (2), 253−262.
(100) Lange, H.; Schiffels, P.; Sette, M.; Sevastyanova, O.; Crestini, C. Fractional Precipitation of Wheat Straw Organosolv Lignin: Macroscopic Properties and Structural Insights. *ACS Sustainable Chem. Eng.* **2016**, *4* (10), 5136−5151.
(101) Faulon, J. L. Stochastic Generator of Chemical Structure. 1. Application to the Structure Elucidation of Large Molecules. *J. Chem. Inf. Model.* **1994**, *34* (5), 1204−1218.
(102) Crestini, C.; Lange, H.; Sette, M.; Argyropoulos, D. S. On the Structure of Softwood Kraft Lignin. *Green Chem.* **2017**, *19* (17), 4104−4121.
(103) McDonough, T. J. *The Chemistry of Organosolv Delignification*; TAPPI Press: Atlanta, GA, 1992.

(104) Pan, X.; Kadla, J. F.; Ehara, K.; Gilkes, N.; Saddler, J. N. Organosolv Ethanol Lignin from Hybrid Poplar as a Radical Scavenger: Relationship between Lignin Structure, Extraction Conditions, and Antioxidant Activity. *J. Agric. Food Chem.* **2006**, *54* (16), 5806−5813.
(105) Zhang, J.; Kim, K. H.; Choi, Y. S.; Motagamwala, A. H.; Dumesic, J. A.; Brown, R. C.; Shanks, B. H. Comparison of Fast Pyrolysis Behavior of Cornstover Lignins Isolated by Different Methods. *ACS Sustainable Chem. Eng.* **2017**, *5* (7), 5657−5661.
(106) Björkman, A. Lignin and Lignin-Carbohydrate Complexes Extraction from Wood Meal with Neutral Solvents. *Ind. Eng. Chem.* **1957**, *49* (9), 1395−1398.
(107) Obst, J. R.; Kirk, T. K. Isolation of Lignin. *Methods Enzymol.* **1985**, *161*, 3−12.
(108) Lupoi, J. S.; Singh, S.; Parthasarathi, R.; Simmons, B. A.; Henry, R. J. Recent Innovations in Analytical Methods for the Qualitative and Quantitative Assessment of Lignin. *Renewable Sustainable Energy Rev.* **2015**, *49*, 871−906.
(109) Hou, Z.; Bennett, C. A.; Klein, M. T.; Virk, P. S. Approaches and Software Tools for Modeling Lignin Pyrolysis. *Energy Fuels* **2010**, *24* (1), 58−67.
(110) Chua, Y. W.; Wu, H.; Yu, Y. Interactions between Low-and High-Molecular-Weight Portions of Lignin during Fast Pyrolysis at Low Temperatures. *Energy Fuels* **2019**, *33*, 11173−11180.
(111) Sonoda, T.; Ona, T.; Yokoi, H.; Ishida, Y.; Ohtani, H.; Tsuge, S. Quantitative Analysis of Detailed Lignin Monomer Composition by Pyrolysis-Gas Chromatography Combined with Preliminary Acetylation of the Samples. *Anal. Chem.* **2001**, *73* (22), 5429−5435.
(112) Chen, L.; Wang, X.; Yang, H.; Lu, Q.; Li, D.; Yang, Q.; Chen, H. Study on Pyrolysis Behaviors of Non-Woody Lignins with TG-FTIR and Py-GC/MS. *J. Anal. Appl. Pyrolysis* **2015**, *113*, 499−507.
(113) del Río, J. C.; Gutiérrez, A.; Rodríguez, I. M.; Ibarra, D.; Martínez, Á. T. Composition of Non-Woody Plant Lignins and Cinnamic Acids by Py-GC/MS, Py/TMAH and FT-IR. *J. Anal. Appl. Pyrolysis* **2007**, *79*, 39−46.
(114) Lourenço, A.; Gominho, J.; Marques, A. V.; Pereira, H. Comparison of Py-GC/FID and Wet Chemistry Analysis for Lignin Determination in Wood and Pulps from Eucalyptus Globulus. *BioResources* **2013**, *8* (2), 2967−2980.
(115) Moghaddam, L.; Rencoret, J.; Maliger, V. R.; Rackemann, D. W.; Harrison, M. D.; Gutiérrez, A.; Del Río, J. C.; Doherty, W. O. S. Structural Characteristics of Bagasse Furfural Residue and Its Lignin Component. An NMR, Py-GC/MS, and FTIR Study. *ACS Sustainable Chem. Eng.* **2017**, *5* (6), 4846−4855.
(116) Del Río, J. C.; Rencoret, J.; Prinsen, P.; Martínez, Á. T.; Ralph, J.; Gutiérrez, A. Structural Characterization of Wheat Straw Lignin as Revealed by Analytical Pyrolysis, 2D-NMR, and Reductive Cleavage Methods. *J. Agric. Food Chem.* **2012**, *60* (23), 5922−5935.
(117) Jia, L.; Buendia-Kandia, F.; Dumarcay, S.; Poirot, H.; Mauviel, G.; Gérardin, P.; Dufour, A. Fast Pyrolysis of Heartwood, Sapwood, and Bark: A Complementary Application of Online Photoionization Mass Spectrometry and Conventional Pyrolysis Gas Chromatography/Mass Spectrometry. *Energy Fuels* **2017**, *31* (4), 4078−4089.
(118) Lu, F.; Ralph, J. DFRC Method for Lignin Analysis. 1. New Method for β-Aryl Ether Cleavage: Lignin Model Studies. *J. Agric. Food Chem.* **1997**, *45* (12), 4655−4660.
(119) Lu, F.; Ralph, J. The DFRC Method for Lignin Analysis. 2. Monomers from Isolated Lignins. *J. Agric. Food Chem.* **1998**, *46* (2), 547−552.
(120) Yuan, T. Q.; Sun, S. N.; Xu, F.; Sun, R. C. Characterization of Lignin Structures and Lignin-Carbohydrate Complex (LCC) Linkages by Quantitative 13C and 2D HSQC NMR Spectroscopy. *J. Agric. Food Chem.* **2011**, *59* (19), 10604−10614.
(121) Bauer, S.; Sorek, H.; Mitchell, V. D.; Ibáñez, A. B.; Wemmer, D. E. Characterization of Miscanthus Giganteus Lignin Isolated by Ethanol Organosolv Process under Reflux Condition. *J. Agric. Food Chem.* **2012**, *60* (33), 8203−8212.
(122) Foston, M.; Samuel, R.; He, J.; Ragauskas, A. J. A Review of Whole Cell Wall NMR by the Direct-Dissolution of Biomass. *Green Chem.* **2016**, *18* (3), 608−621.
(123) Saito, K.; Kaiho, A.; Sakai, R.; Nishimura, H.; Okada, H.; Watanabe, T. Characterization of the Interunit Bonds of Lignin Oligomers Released by Acid-Catalyzed Selective Solvolysis of Cryptomeria Japonica and Eucalyptus Globulus Woods via Thioacidolysis and 2D-NMR. *J. Agric. Food Chem.* **2016**, *64* (48), 9152−9160.
(124) Le Brech, Y.; Delmotte, L.; Raya, J.; Brosse, N.; Gadiou, R.; Dufour, A. High Resolution Solid State 2D NMR Analysis of Biomass and Biochar. *Anal. Chem.* **2015**, *87* (2), 843−847.
(125) Yue, F.; Lu, F.; Ralph, S.; Ralph, J. Identification of 4-O-5-Units in Softwood Lignins via Definitive Lignin Models and NMR. *Biomacromolecules* **2016**, *17* (6), 1909−1920.
(126) Rencoret, J.; Marques, G.; Gutiérrez, A.; Nieto, L.; Jiménez-Barbero, J.; Martínez, Á. T.; del Río, J. C. Isolation and Structural Characterization of the Milled-Wood Lignin from Paulownia Fortunei Wood. *Ind. Crops Prod.* **2009**, *30* (1), 137−143.
(127) Samuel, R.; Pu, Y.; Raman, B.; Ragauskas, A. J. Structural Characterization and Comparison of Switchgrass Ball-Milled Lignin before and after Dilute Acid Pretreatment. *Appl. Biochem. Biotechnol.* **2010**, *162* (1), 62−74.
(128) Rencoret, J.; Marques, G.; Gutiérrez, A.; Ibarra, D.; Li, J.; Gellerstedt, G.; Santos, J. I.; Jiménez-Barbero, J.; Martínez, Á. T.; Del Río, J. C. Structural Characterization of Milled Wood Lignins from Different Eucalypt Species. *Holzforschung* **2008**, *62* (5), 514−526.
(129) Capanema, E. A.; Balakshin, M. Y.; Kadla, J. F. A Comprehensive Approach for Quantitative Lignin Characterization by NMR Spectroscopy. *J. Agric. Food Chem.* **2004**, *52* (7), 1850−1860.
(130) Balakshin, M. Y.; Capanema, E. A. Comprehensive Structural Analysis of Biorefinery Lignins with a Quantitative 13C NMR Approach. *RSC Adv.* **2015**, *5* (106), 87187−87199.
(131) Capanema, E. A.; Balakshin, M. Y.; Kadla, J. F. Quantitative Characterization of a Hardwood Milled Wood Lignin by Nuclear Magnetic Resonance Spectroscopy. *J. Agric. Food Chem.* **2005**, *53* (25), 9639−9649.
(132) Ralph, J.; Marita, J. M.; Ralph, S. A.; Hatfield, R. D.; Lu, F. L.; Ede, R. M.; Peng, J.; Landucci, L. L. Solution State NMR of Lignins. In *Advances in Lignocellulosics Characterization*; TAPPI Press: Atlanta, GA, 1999; pp 55−108.
(133) Ralph, S.; Ralph, J. *NMR Database of Lignin and Cell Wall Model Compounds*; FPL/DFRC NMR Database, 2009.
(134) Crestini, C.; Argyropoulos, D. S. Structural Analysis of Wheat Straw Lignin by Quantitative 31P and 2D NMR Spectroscopy. The Occurrence of Ester Bonds and α-O-4 Substructures. *J. Agric. Food Chem.* **1997**, *45* (4), 1212−1219.
(135) Granata, A.; Argyropoulos, D. S. 2-Chloro-4,4,5,5-Tetramethyl-1,3,2-Dioxaphospholane, a Reagent for the Accurate Determination of the Uncondensed and Condensed Phenolic Moieties in Lignins. *J. Agric. Food Chem.* **1995**, *43* (6), 1538−1544.
(136) Pu, Y.; Cao, S.; Ragauskas, A. J. Application of Quantitative 31 P NMR in Biomass Lignin and Biofuel Precursors Characterization. *Energy Environ. Sci.* **2011**, *4* (9), 3154−3166.
(137) Castillo, A. M.; Patiny, L.; Wist, J. Fast and Accurate Algorithm for the Simulation of NMR Spectra of Large Spin Systems. *J. Magn. Reson.* **2011**, *209* (2), 123−130.
(138) Steinbeck, C.; Krause, S.; Kuhn, S. NMRShiftDB - Constructing a Free Chemical Information System with Open-Source Components. *J. Chem. Inf. Comput. Sci.* **2003**, *43* (6), 1733−1739.
(139) Sette, M.; Wechselberger, R.; Crestini, C. Elucidation of Lignin Structure by Quantitative 2D NMR. *Chem. - Eur. J.* **2011**, *17* (34), 9529−9535.
(140) Guerra, A.; Filpponen, I.; Lucia, L. A.; Argyropoulos, D. S. Comparative Evaluation of Three Lignin Isolation Protocols for Various Wood Species. *J. Agric. Food Chem.* **2006**, *54* (26), 9696−9705.

https://dx.doi.org/10.1021/acs.iecr.9b05744
Ind. Eng. Chem. Res. 2020, 59, 526−555

(141) Lange, H.; Rulli, F.; Crestini, C. Gel Permeation Chromatography in Determining Molecular Weights of Lignins: Critical Aspects Revisited for Improved Utility in the Development of Novel Materials. *ACS Sustainable Chem. Eng.* **2016**, *4* (10), 5167−5180.
(142) Hu, J.; Shen, D.; Xiao, R.; Wu, S.; Zhang, H. Free-Radical Analysis on Thermochemical Transformation of Lignin to Phenolic Compounds. *Energy Fuels* **2013**, *27* (1), 285−293.
(143) Zeng, J.; Tong, Z.; Wang, L.; Zhu, J. Y.; Ingram, L. Isolation and Structural Characterization of Sugarcane Bagasse Lignin after Dilute Phosphoric Acid plus Steam Explosion Pretreatment and Its Effect on Cellulose Hydrolysis. *Bioresour. Technol.* **2014**, *154*, 274−281.
(144) Cui, C.; Sun, R.; Argyropoulos, D. S. Fractional Precipitation of Softwood Kraft Lignin: Isolation of Narrow Fractions Common to a Variety of Lignins. *ACS Sustainable Chem. Eng.* **2014**, *2* (4), 959−968.
(145) Ziebell, A.; Gracom, K.; Katahira, R.; Chen, F.; Pu, Y.; Ragauskas, A.; Dixon, R. A.; Davis, M. Increase in 4-Coumaryl Alcohol Units during Lignification in Alfalfa (Medicago Sativa) Alters the Extractability and Molecular Weight of Lignin. *J. Biol. Chem.* **2010**, *285* (50), 38961−38968.
(146) Chan, J. M. W.; Bauer, S.; Sorek, H.; Sreekumar, S.; Wang, K.; Toste, F. D. Studies on the Vanadium-Catalyzed Nonoxidative Depolymerization of Miscanthus Giganteus-Derived Lignin. *ACS Catal.* **2013**, *3* (6), 1369−1377.
(147) Tolbert, A.; Akinosho, H.; Khunsupat, R.; Naskar, A. K.; Ragauskas, A. J. Characterization and Analysis of the Molecualr Weight of Lignin for Biorefining Studies. *Biofuels, Bioprod. Biorefin.* **2014**, *8*, 836−856.
(148) Zinovyev, G.; Sulaeva, I.; Podzimek, S.; Rössner, D.; Kilpeläinen, I.; Sumerskii, I.; Rosenau, T.; Potthast, A. Getting Closer to Absolute Molar Masses of Technical Lignins. *ChemSusChem* **2018**, *11* (18), 3259−3268.
(149) Hoekstra, E.; Kersten, S. R. A.; Tudos, A.; Meier, D.; Hogendoorn, K. J. A. Possibilities and Pitfalls in Analyzing (Upgraded) Pyrolysis Oil by Size Exclusion Chromatography (SEC). *J. Anal. Appl. Pyrolysis* **2011**, *91* (1), 76−88.
(150) McClelland, D. J.; Motagamwala, A. H.; Li, Y.; Rover, M. R.; Wittrig, A. M.; Wu, C.; Buchanan, J. S.; Brown, R. C.; Ralph, J.; Dumesic, J. A.; Huber, G. W. Functionality and Molecular Weight Distribution of Red Oak Lignin before and after Pyrolysis and Hydrogenation. *Green Chem.* **2017**, *19* (5), 1378−1389.
(151) Wen, J. L.; Yuan, T. Q.; Sun, S. L.; Xu, F.; Sun, R. C. Understanding the Chemical Transformations of Lignin during Ionic Liquid Pretreatment. *Green Chem.* **2014**, *16* (1), 181−190.
(152) Wayman, M.; Chua, M. G. S. Characterization of Autohydrolysis Aspen (P. Tremuloides) Lignins. Part 4. Residual Autohydrolysis Lignin. *Can. J. Chem.* **1979**, *57* (19), 2612−2616.
(153) Xiao, L. P.; Shi, Z. J.; Xu, F.; Sun, R. C. Characterization of Lignins Isolated with Alkaline Ethanol from the Hydrothermal Pretreated Tamarix Ramosissima. *BioEnergy Res.* **2013**, *6* (2), 519−532.
(154) Hu, G.; Cateto, C.; Pu, Y.; Samuel, R.; Ragauskas, A. J. Structural Characterization of Switchgrass Lignin after Ethanol Organosolv Pretreatment. *Energy Fuels* **2012**, *26* (1), 740−745.
(155) Lu, X.; Zheng, X.; Li, X.; Zhao, J. Adsorption and Mechanism of Cellulase Enzymes onto Lignin Isolated from Corn Stover Pretreated with Liquid Hot Water. *Biotechnol. Biofuels* **2016**, *9* (1), 1−12.
(156) Buranov, A. U.; Mazza, G. Lignin in Straw of Herbaceous Crops. *Ind. Crops Prod.* **2008**, *28* (3), 237−259.
(157) Kang, S.; Xiao, L.; Meng, L.; Zhang, X.; Sun, R. Isolation and Structural Characterization of Lignin from Cotton Stalk Treated in an Ammonia Hydrothermal System. *Int. J. Mol. Sci.* **2012**, *13* (11), 15209−15226.
(158) Phongpreecha, T.; Hool, N. C.; Stoklosa, R. J.; Klett, A. S.; Foster, C. E.; Bhalla, A.; Holmes, D.; Thies, M. C.; Hodge, D. B. Predicting Lignin Depolymerization Yields from Quantifiable Properties Using Fractionated Biorefinery Lignins. *Green Chem.* **2017**, *19* (21), 5131−5143.
(159) Flory, P. J. *Principles of Polymer Chemistry*; Cornell University Press: Ithaca and London, 1953.
(160) Flory, P. J. Fundamental Principles of Condensation Polymerization. *Chem. Rev.* **1946**, *39* (1), 137−197.
(161) El Hage, R.; Brosse, N.; Chrusciel, L.; Sanchez, C.; Sannigrahi, P.; Ragauskas, A. Characterization of Milled Wood Lignin and Ethanol Organosolv Lignin from Miscanthus. *Polym. Degrad. Stab.* **2009**, *94* (10), 1632−1638.
(162) Flory, P. J. Molecular Size Distribution in Three Dimensional Polymers. I. Gelation. *J. Am. Chem. Soc.* **1941**, *63* (11), 3083−3090.
(163) Stockmayer, W. H. Theory of Molecular Size Distribution and Gel Formation in Branched-Chain Polymers. *J. Chem. Phys.* **1943**, *11* (2), 45−55.
(164) Garcìa-Pèrez, M.; Chaala, A.; Pakdel, H.; Kretschmer, D.; Rodrigue, D.; Roy, C. Evaluation of the Influence of Stainless Steel and Copper on the Aging Process of Bio-Oil. *Energy Fuels* **2006**, *20* (2), 786−795.
(165) Zeng, J.; Helms, G. L.; Gao, X.; Chen, S. Quantification of Wheat Straw Lignin Structure by Comprehensive NMR Analysis. *J. Agric. Food Chem.* **2013**, *61* (46), 10848−10857.
(166) Lan, W.; Lu, F.; Regner, M.; Zhu, Y.; Rencoret, J.; Ralph, S. A.; Zakai, U. I.; Morreel, K.; Boerjan, W.; Ralph, J. Tricin, a Flavonoid Monomer in Monocot Lignification. *Plant Physiol.* **2015**, *167* (4), 1284−1295.
(167) Andrianova, A. A.; DiProspero, T.; Geib, C.; Smoliakova, I. P.; Kozliak, E. I.; Kubátová, A. Electrospray Ionization with High-Resolution Mass Spectrometry as a Tool for Lignomics: Lignin Mass Spectrum Deconvolution. *J. Am. Soc. Mass Spectrom.* **2018**, *29* (5), 1044−1059.
(168) Kosyakov, D. S.; Ul'yanovskii, N. V.; Sorokina, E. A.; Gorbova, N. S. Optimization of Sample Preparation Conditions in the Study of Lignin by MALDI Mass Spectrometry. *J. Anal. Chem.* **2014**, *69* (14), 1344−1350.
(169) Morreel, K.; Dima, O.; Kim, H.; Lu, F.; Niculaes, C.; Vanholme, R.; Dauwe, R.; Goeminne, G.; Inzé, D.; Messens, E.; Ralph, J.; Boerjan, W. Mass Spectrometry-Based Sequencing of Lignin Oligomers. *Plant Physiol.* **2010**, *153* (4), 1464−1478.
(170) Prothmann, J.; Spégel, P.; Sandahl, M.; Turner, C. Identification of Lignin Oligomers in Kraft Lignin Using Ultra-High-Performance Liquid Chromatography/High-Resolution Multiple-Stage Tandem Mass Spectrometry (UHPLC/HRMS N). *Anal. Bioanal. Chem.* **2018**, *410* (29), 7803−7814.
(171) Richel, A.; Vanderghem, C.; Simon, M.; Wathelet, B.; Paquot, M. Evaluation of Matrix-Assisted Laser Desorption/Ionization Mass Spectrometry for Second-Generation Lignin Analysis. *Anal. Chem. Insights* **2012**, *7* (1), 79−89.
(172) Morreel, K.; Ralph, J.; Kim, H.; Lu, F.; Goeminne, G.; Ralph, S.; Messens, E.; Boerjan, W. Profiling of Oligolignols Reveals Monolignol Coupling Conditions in Lignifying Poplar Xylem. *Plant Physiol.* **2004**, *136* (3), 3537−3549.
(173) Metzger, J. O.; Bicke, C.; Faix, O.; Tuszynski, W.; Angermann, R.; Karas, M.; Strupat, K. Matrix-Assisted Laser Desorption Mass Spectrometry of Lignins**. *Angew. Chem., Int. Ed. Engl.* **1992**, *31* (6), 762−764.
(174) Jegers, H. E.; Klein, M. T. Primary and Secondary Lignin Pyrolysis Reaction Pathways. *Ind. Eng. Chem. Process Des. Dev.* **1985**, *24* (1), 173−183.
(175) Nunn, T. R.; Howard, J. B.; Longwell, J. P.; Peters, W. A. Product Compositions and Kinetics in the Rapid Pyrolysis of Milled Wood Lignin. *Ind. Eng. Chem. Process Des. Dev.* **1985**, *24* (3), 844−852.
(176) Ojha, D. K.; Viju, D.; Vinu, R. Fast Pyrolysis Kinetics of Alkali Lignin: Evaluation of Apparent Rate Parameters and Product Time Evolution. *Bioresour. Technol.* **2017**, *241*, 142−151.
(177) Kawamoto, H.; Horigoshi, S.; Saka, S. Pyrolysis Reactions of Various Lignin Model Dimers. *J. Wood Sci.* **2007**, *53* (2), 168−174.

https://dx.doi.org/10.1021/acs.iecr.9b05744
Ind. Eng. Chem. Res. 2020, 59, 526−555

(178) Asmadi, M.; Kawamoto, H.; Saka, S. Thermal Reactivities of Catechols/Pyrogallols and Cresols/Xylenols as Lignin Pyrolysis Intermediates. *J. Anal. Appl. Pyrolysis* **2011**, *92* (1), 76−87.
(179) Nakamura, T.; Kawamoto, H.; Saka, S. Pyrolysis Behavior of Japanese Cedar Wood Lignin Studied with Various Model Dimers. *J. Anal. Appl. Pyrolysis* **2008**, *81* (2), 173−182.
(180) Kotake, T.; Kawamoto, H.; Saka, S. Pyrolysis Reactions of Coniferyl Alcohol as a Model of the Primary Structure Formed during Lignin Pyrolysis. *J. Anal. Appl. Pyrolysis* **2013**, *104*, 573−584.
(181) Custodis, V. B. F.; Hemberger, P.; Ma, Z.; Van Bokhoven, J. A. Mechanism of Fast Pyrolysis of Lignin: Studying Model Compounds. *J. Phys. Chem. B* **2014**, *118* (29), 8524−8531.
(182) Choi, Y. S.; Singh, R.; Zhang, J.; Balasubramanian, G.; Sturgeon, M. R.; Katahira, R.; Chupka, G.; Beckham, G. T.; Shanks, B. H. Pyrolysis Reaction Networks for Lignin Model Compounds: Unraveling Thermal Deconstruction of β-O-4 and α-O-4 Compounds. *Green Chem.* **2016**, *18* (6), 1762−1773.
(183) Wang, S.; Ru, B.; Dai, G.; Shi, Z.; Zhou, J.; Luo, Z.; Ni, M.; Cen, K. Mechanism Study on the Pyrolysis of a Synthetic β-O-4 Dimer as Lignin Model Compound. *Proc. Combust. Inst.* **2017**, *36* (2), 2225−2233.
(184) Asatryan, R.; Bennadji, H.; Bozzelli, J. W.; Ruckenstein, E.; Khachatryan, L. Molecular Products and Fundamentally Based Reaction Pathways in the Gas-Phase Pyrolysis of the Lignin Model Compound p-Coumaryl Alcohol. *J. Phys. Chem. A* **2017**, *121* (18), 3352−3371.
(185) Nguyen, T. T. P.; Mai, T. V. T.; Huynh, L. K. Detailed Kinetic Modeling of Thermal Decomposition of Guaiacol − A Model Compound for Biomass Lignin. *Biomass Bioenergy* **2018**, *112* (June 2016), 45−60.
(186) Hou, Z.; Bennett, C. A.; Klein, M. T.; Virk, P. S. Approaches and Software Tools for Modeling Lignin Pyrolysis. *Energy Fuels* **2010**, *24* (1), 58−67.
(187) Klein, M. T.; Virk, P. S. Model Pathways in Lignin Thermolysis. 1. Phenethyl Phenyl Ether. *Ind. Eng. Chem. Fundam.* **1983**, *22* (1), 35−45.
(188) Faravelli, T.; Frassoldati, A.; Migliavacca, G.; Ranzi, E. Detailed Kinetic Modeling of the Thermal Degradation of Lignins. *Biomass Bioenergy* **2010**, *34* (3), 290−301.
(189) Hough, B. R.; Schwartz, D. T.; Pfaendtner, J. Detailed Kinetic Modeling of Lignin Pyrolysis for Process Optimization. *Ind. Eng. Chem. Res.* **2016**, *55* (34), 9147−9153.
(190) Furutani, Y.; Kudo, S.; Hayashi, J.-i.; Norinaga, K. Predicting Molecular Composition of Primary Product Derived from Fast Pyrolysis of Lignin with Semi-Detailed Kinetic Model. *Fuel* **2018**, *212* (October2017), 515−522.
(191) Patwardhan, P. R.; Brown, R. C.; Shanks, B. H. Understanding the Fast Pyrolysis of Lignin. *ChemSusChem* **2011**, *4* (11), 1629−1636.
(192) Zhang, J.; Choi, Y. S.; Yoo, C. G.; Kim, T. H.; Brown, R. C.; Shanks, B. H. Cellulose-Hemicellulose and Cellulose-Lignin Interactions during Fast Pyrolysis. *ACS Sustainable Chem. Eng.* **2015**, *3* (2), 293−301.
(193) Adam, M.; Ocone, R.; Mohammad, J.; Berruti, F.; Briens, C. Kinetic Investigations of Kraft Lignin Pyrolysis. *Ind. Eng. Chem. Res.* **2013**, *52* (26), 8645−8654.
(194) Anca-Couce, A. Reaction Mechanisms and Multi-Scale Modelling of Lignocellulosic Biomass Pyrolysis. *Prog. Energy Combust. Sci.* **2016**, *53* (2016), 41−79.
(195) Ranzi, E.; Cuoci, A.; Faravelli, T.; Frassoldati, A.; Migliavacca, G.; Pierucci, S.; Sommariva, S. Chemical Kinetics of Biomass Pyrolysis. *Energy Fuels* **2008**, *22* (6), 4292−4300.
(196) Pu, J.; Laurenti, D.; Geantet, C.; Tayakout-Fayolle, M.; Pitault, I. Kinetic Modeling of Lignin Catalytic Hydroconversion in a Semi-Batch Reactor. *Chem. Eng. J.* **2019**, 122067.
(197) SriBala, G.; Carstensen, H. H.; Van Geem, K. M.; Marin, G. B. Measuring Biomass Fast Pyrolysis Kinetics: State of the Art. *WIREs Energy Environ.* **2019**, *8*, e326.
(198) Sutton, J. E.; Vlachos, D. G. Building Large Microkinetic Models with First-Principles' Accuracy at Reduced Computational Cost. *Chem. Eng. Sci.* **2015**, *121*, 190−199.
(199) Thybaut, J. W.; Marin, G. B. Single-Event MicroKinetics: Catalyst Design for Complex Reaction Networks. *J. Catal.* **2013**, *308*, 352−362.
(200) Garcia-Perez, M.; Wang, S.; Shen, J.; Rhodes, M.; Lee, W. J.; Li, C. Z. Effects of Temperature on the Formation of Lignin-Derived Oligomers during the Fast Pyrolysis of Mallee Woody Biomass. *Energy Fuels* **2008**, *22* (3), 2022−2032.
(201) Jiang, G.; Nowakowski, D. J.; Bridgwater, A. V. Effect of the Temperature on the Composition of Lignin Pyrolysis Products. *Energy Fuels* **2010**, *24* (8), 4470−4475.
(202) Ben, H.; Ragauskas, A. J. NMR Characterization of Pyrolysis Oils from Kraft Lignin. *Energy Fuels* **2011**, *25* (5), 2322−2332.
(203) Kotake, T.; Kawamoto, H.; Saka, S. Mechanisms for the Formation of Monomers and Oligomers during the Pyrolysis of a Softwood Lignin. *J. Anal. Appl. Pyrolysis* **2014**, *105*, 309−316.
(204) Collard, F. X.; Blin, J. A Review on Pyrolysis of Biomass Constituents: Mechanisms and Composition of the Products Obtained from the Conversion of Cellulose, Hemicelluloses and Lignin. *Renewable Sustainable Energy Rev.* **2014**, *38*, 594−608.
(205) Kawamoto, H. Lignin Pyrolysis Reactions. *J. Wood Sci.* **2017**, *63* (2), 117−132.
(206) Sharma, R. K.; Wooten, J. B.; Baliga, V. L.; Lin, X.; Chan, W. G.; Hajaligol, M. R. Characterization of Chars from Pyrolysis of Lignin. *Fuel* **2004**, *83* (11−12), 1469−1482.
(207) Jiang, X.; Lu, Q.; Hu, B.; Liu, J.; Dong, C.; Yang, Y. Intermolecular Interaction Mechanism of Lignin Pyrolysis: A Joint Theoretical and Experimental Study. *Fuel* **2018**, *215* (November2017), 386−394.
(208) Shrestha, B.; Le Brech, Y.; Ghislain, T.; Leclerc, S.; Carré, V.; Aubriet, F.; Hoppe, S.; Marchal, P.; Pontvianne, S.; Brosse, N.; Dufour, A. A Multitechnique Characterization of Lignin Softening and Pyrolysis. *ACS Sustainable Chem. Eng.* **2017**, *5* (8), 6940−6949.
(209) Ansari, K. B.; Arora, J. S.; Chew, J. W.; Dauenhauer, P. J.; Mushrif, S. H. Fast Pyrolysis of Cellulose, Hemicellulose, and Lignin: Effect of Operating Temperature on Bio-Oil Yield and Composition and Insights into the Intrinsic Pyrolysis Chemistry. *Ind. Eng. Chem. Res.* **2019**, *58* (35), 15838−15852.
(210) Hoekstra, E.; Westerhof, R. J. M.; Brilman, W.; Van Swaaij, W. P. M.; Kersten, S. R. A.; Hogendoorn, K. J. A.; Windt, M. Heterogeneous and Homogeneous Reactions of Pyrolysis Vapors from Pine Wood. *AIChE J.* **2012**, *58* (9), 2830−2842.
(211) Anca-Couce, A.; Mehrabian, R.; Scharler, R.; Obernberger, I. Kinetic Scheme of Biomass Pyrolysis Considering Secondary Charring Reactions. *Energy Convers. Manage.* **2014**, *87* (2014), 687−696.
(212) Hosoya, T.; Kawamoto, H.; Saka, S. Secondary Reactions of Lignin-Derived Primary Tar Components. *J. Anal. Appl. Pyrolysis* **2008**, *83* (1), 78−87.
(213) Joback, K. G.; Reid, R. C. Estimation of Pure-Component Properties from Group-Contributions. *Chem. Eng. Commun.* **1987**, *57* (1−6), 233−243.
(214) Stein, S. E.; Brown, R. L. Estimation of Normal Boiling Points from Group Contributions. *J. Chem. Inf. Model.* **1994**, *34* (3), 581−587.
(215) Retzekas, E.; Voutsas, E.; Magoulas, K.; Tassios, D. Prediction of Physical Properties of Hydrocarbons, Petroleum, and Coal Liquid Fractions. *Ind. Eng. Chem. Res.* **2002**, *41* (6), 1695−1702.
(216) ARTIST - Thermophysical Properties from Molecular Structure. DDBST GmbH. http://www.ddbst.com/artist-property-estimation.html (accessed Oct 10, 2019).
(217) Marano, J. J.; Holder, G. D. Characterization of Fischer−Tropsch Liquids for Vapor-Liquid Equilibria Calculations. *Fluid Phase Equilib.* **1997**, *138* (1−2), 1−21.
(218) Marano, J. J.; Holder, G. D. Prediction of Bulk Properties of Fischer−Tropsch Derived Liquids. *Ind. Eng. Chem. Res.* **1997**, *36* (6), 2409−2420.

(219) Rösgen, J.; Hinz, H. J. Phase Diagrams: A Graphical Representation of Linkage Relations. *J. Mol. Biol.* **2003**, *328* (1), 255−271.
(220) Unger, P. E.; Suuberg, E. M. Internal and External Mass Transfer Limitations in Coal Pyrolysis. *ACS Div. Fuel Chem. Prepr.* **1983**, *28* (4), 278−291.
(221) Solomon, P. R.; King, H. H. Tar Evolution from Coal and Model Polymers: Theory and Experiments. *Fuel* **1984**, *63* (9), 1302−1311.
(222) Suuberg, E. M. Mass Transfer Effects in Pyrolysis of Coals: A Review of Experimental Evidence and Models. In *Chemistry of Coal Conversion*; Schlosberg, R. H., Ed.; Springer, 1985.
(223) Seery, D. J.; Freihaut, J. D.; Proscia, W. M.; Howard, J. B.; Peters, W.; Hsu, J.; Hajaligol, M.; Sarofim, A.; Jenkins, R.; Mallin, J.; Espindola-Merin, B.; Essenhigh, R.; Misra, M. K. *Kinetics of Coal Pyrolysis*; U.S. Department of Energy, 1989. https://www.osti.gov/servlets/purl/6307052.
(224) Dufour, A.; Castro-Diaz, M.; Marchal, P.; Brosse, N.; Olcese, R.; Bouroukba, M.; Snape, C. In Situ Analysis of Biomass Pyrolysis by High Temperature Rheology in Relations with 1H NMR. *Energy Fuels* **2012**, *26* (10), 6432−6441.
(225) Krzesińska, M.; Szeluga, U.; Czajkowska, S.; Muszyński, J.; Zachariasz, J.; Pusz, S.; Kwiecińska, B.; Koszorek, A.; Pilawa, B. The Thermal Decomposition Studies of Three Polish Bituminous Coking Coals and Their Blends. *Int. J. Coal Geol.* **2009**, *77* (3−4), 350−355.
(226) Yoshida, T.; Takanohashi, T.; Iino, M.; Kumagai, H.; Kato, K. Interactions among Different Fractions in the Thermoplastic State of Goonyella Coking Coal. *Energy Fuels* **2004**, *18* (2), 349−356.
(227) Castro Díaz, M.; Zhao, H.; Kokonya, S.; Dufour, A.; Snape, C. E. The Effect of Biomass on Fluidity Development in Coking Blends Using High-Temperature SAOS Rheometry. *Energy Fuels* **2012**, *26* (3), 1767−1775.
(228) Dauenhauer, P. J.; Colby, J. L.; Balonek, C. M.; Suszynski, W. J.; Schmidt, L. D. Reactive Boiling of Cellulose for Integrated Catalysis through an Intermediate Liquid. *Green Chem.* **2009**, *11* (10), 1555−1561.
(229) Vural, D.; Smith, J. C.; Petridis, L. Dynamics of the Lignin Glass Transition. *Phys. Chem. Chem. Phys.* **2018**, *20* (31), 20504−20512.
(230) Zhang, J.; Chen, J. J. J.; Zhou, N. Characteristics of Jet Droplet Produced by Bubble Bursting on the Free Liquid Surface. *Chem. Eng. Sci.* **2012**, *68* (1), 151−156.
(231) Lange, J. P. Lignocellulose Liquefaction to Biocrude: A Tutorial Review. *ChemSusChem* **2018**, *11* (6), 997−1014.
(232) Isa, K. M.; Abdullah, T. A. T.; Ali, U. F. M. Hydrogen Donor Solvents in Liquefaction of Biomass: A Review. *Renewable Sustainable Energy Rev.* **2018**, *81* (October 2016), 1259−1268.
(233) Bahlo, R. L.; Hursthouse, A. S.; Sievers, A.; Willner, T. Unexplored Areas of Direct Solvolytic Liquefaction of Lignocellulosic Biomass. *Chem. Ing. Tech.* **2018**, *90* (1), 47−55.
(234) Shuai, L.; Luterbacher, J. Organic Solvent Effects in Biomass Conversion Reactions. *ChemSusChem* **2016**, *9* (2), 133−155.
(235) Pu, Y.; Jiang, N.; Ragauskas, A. J. Ionic Liquid as a Green Solvent for Lignin. *J. Wood Chem. Technol.* **2007**, *27* (1), 23−33.
(236) Barton, A. F. M. Solubility Parameters. *Chem. Rev.* **1975**, *75* (6), 731−753.
(237) Sameni, J.; Krigstin, S.; Sain, M. Acetylation & Lignin Solubility. *BioResources* **2016**, *12* (1), 1548−1565.
(238) Ye, Y.; Liu, Y.; Chang, J. Application of Solubility Parameter Theory to Organosolv Extraction of Lignin from Enzymatically Hydrolyzed Cornstalks. *BioResources* **2014**, *9* (2), 3417−3427.
(239) Thielemans, W.; Wool, R. P. Lignin Esters for Use in Unsaturated Thermosets: Lignin Modification and Solubility Modeling. *Biomacromolecules* **2005**, *6* (4), 1895−1905.
(240) Lê, H. Q.; Zaitseva, A.; Pokki, J. P.; Ståhl, M.; Alopaeus, V.; Sixta, H. Solubility of Organosolv Lignin in γ-Valerolactone/Water Binary Mixtures. *ChemSusChem* **2016**, *9* (20), 2939−2947.
(241) Van Krevelen, D. W.; Nijenhuis, K. T. *Properties of Polymers: Their Correlation with Chemical Structure; Their Numerical Estimation and Prediction from Additive Group Contributions*, Fourth ed.; Elsevier: Amsterdam, The Netherlands, 2009.
(242) Just, S.; Sievert, F.; Thommes, M.; Breitkreutz, J. Improved Group Contribution Parameter Set for the Application of Solubility Parameters to Melt Extrusion. *Eur. J. Pharm. Biopharm.* **2013**, *85* (3), 1191−1199.
(243) Buncel, E.; Stairs, R. A. *Solvent Effects in Chemistry*, Second ed.; John Wiley & Sons: Hoboken, NJ, 2016.
(244) Constantinou, L.; Gani, R. New Group Contribution Method for Estimating Properties of Pure Compounds. *AIChE J.* **1994**, *40* (10), 1697−1710.
(245) Gmehling, J. Present Status and Potential of Group Contribution Methods for Process Development. *J. Chem. Thermodyn.* **2009**, *41* (6), 731−747.
(246) Elbro, H. S.; Fredenslund, A.; Rasmussen, P. Group Contribution Method for the Prediction of Liquid Densities as a Function of Temperature for Solvents, Oligomers, and Polymers. *Ind. Eng. Chem. Res.* **1991**, *30* (12), 2576−2582.
(247) Ihmels, E. C.; Gmehling, J. Extension and Revision of the Group Contribution Method GCVOL for the Prediction of Pure Compound Liquid Densities. *Ind. Eng. Chem. Res.* **2003**, *42* (2), 408−412.
(248) Tsibanogiannis, I. N.; Kalospiros, N. S.; Tassios, D. P. Extension of the GCVOL Method and Application to Some Complex Compounds. *Ind. Eng. Chem. Res.* **1994**, *33* (6), 1641−1643.
(249) Palakkal, M.; Kabadi, V. N. Viscosity of Coal-Derived Liquids. 1. A Group Contribution Method for Pure Model Compound Liquids. *Energy Fuels* **1996**, *10* (2), 333−340.
(250) Sastri, S. R. S.; Rao, K. K. A New Group Contribution Method for Predicting Viscosity of Organic Liquids. *Chem. Eng. J.* **1992**, *50* (1), 9−25.
(251) Nannoolal, Y.; Rarey, J.; Ramjugernath, D. Estimation of Pure Component Properties. Part 4: Estimation of the Saturated Liquid Viscosity of Non-Electrolyte Organic Compounds via Group Contributions and Group Interactions. *Fluid Phase Equilib.* **2009**, *281* (2), 97−119.
(252) Sastri, S. R. S.; Rao, K. K. A Simple Method to Predict Surface Tension of Organic Liquids. *Chem. Eng. J. Biochem. Eng. J.* **1995**, *59* (2), 181−186.
(253) Gharagheizi, F.; Eslamimanesh, A.; Mohammadi, A. H.; Richon, D. Use of Artificial Neural Network-Group Contribution Method to Determine Surface Tension of Pure Compounds. *J. Chem. Eng. Data* **2011**, *56* (5), 2587−2601.
(254) Hwang, S. C.; Tsonopoulos, C.; Cunningham, J. R.; Wilson, G. M. Density, Viscosity, and Surface Tension of Coal Liquids at High Temperatures and Pressures. *Ind. Eng. Chem. Process Des. Dev.* **1982**, *21* (1), 127−134.
(255) Vermaas, J. V.; Petridis, L.; Ralph, J.; Crowley, M. F.; Beckham, G. T. Systematic Parameterization of Lignin for the CHARMM Force Field. *Green Chem.* **2019**, *21* (1), 109−122.
(256) Petridis, L.; Schulz, R.; Smith, J. C. Simulation Analysis of the Temperature Dependence of Lignin Structure and Dynamics. *J. Am. Chem. Soc.* **2011**, *133* (50), 20277−20287.
(257) Sangha, A. K.; Petridis, L.; Smith, J. C.; Ziebell, A.; Parks, J. M. Molecular Simulation as a Tool for Studying Lignin. *Environ. Prog. Sustainable Energy* **2012**, *31* (1), 47−54.
(258) Liu, W. J.; Jiang, H.; Yu, H. Q. Thermochemical Conversion of Lignin to Functional Materials: A Review and Future Directions. *Green Chem.* **2015**, *17* (11), 4888−4907.
(259) Smith, M. W.; Pecha, B.; Helms, G.; Scudiero, L.; Garcia-Perez, M. Chemical and Morphological Evaluation of Chars Produced from Primary Biomass Constituents: Cellulose, Xylan, and Lignin. *Biomass Bioenergy* **2017**, *104*, 17−35.
(260) Nowakowska, M.; Herbinet, O.; Dufour, A.; Glaude, P. A. Detailed Kinetic Study of Anisole Pyrolysis and Oxidation to Understand Tar Formation during Biomass Combustion and Gasification. *Combust. Flame* **2014**, *161* (6), 1474−1488.

https://dx.doi.org/10.1021/acs.iecr.9b05744
Ind. Eng. Chem. Res. 2020, 59, 526−555

(261) Chua, Y. W.; Yu, Y.; Wu, H. Structural Changes of Chars Produced from Fast Pyrolysis of Lignin at 100−300 °C. *Fuel* **2019**, *255* (June), 115754.
(262) Hosoya, T.; Kawamoto, H.; Saka, S. Role of Methoxyl Group in Char Formation from Lignin-Related Compounds. *J. Anal. Appl. Pyrolysis* **2009**, *84* (1), 79−83.
(263) Asmadi, M.; Kawamoto, H.; Saka, S. Thermal Reactions of Guaiacol and Syringol as Lignin Model Aromatic Nuclei. *J. Anal. Appl. Pyrolysis* **2011**, *92* (1), 88−98.
(264) Mu, W.; Ben, H.; Ragauskas, A.; Deng, Y. Lignin Pyrolysis Components and Upgrading-Technology Review. *BioEnergy Res.* **2013**, *6* (4), 1183−1204.
(265) Xu, C.; Arancon, R. A. D.; Labidi, J.; Luque, R. Lignin Depolymerisation Strategies: Towards Valuable Chemicals and Fuels. *Chem. Soc. Rev.* **2014**, *43* (22), 7485−7500.
(266) Solomon, P. R.; Hamblen, D. G.; Yu, Z. Z.; Serio, M. A. Network Models of Coal Thermal Decomposition. *Fuel* **1990**, *69* (6), 754−763.
(267) Solomon, P. R.; Serio, M. A.; Kroo, E.; Despande, G. V. Cross-Linking Reactions during Coal Conversion. *Energy Fuels* **1990**, *4* (1), 42−54.
(268) Fletcher, T. H.; Solum, M. S.; Grant, D. M.; Critchfield, S.; Pugmire, R. J. Solid State 13C and 1H NMR Studies of the Evolution of the Chemical Structure of Coal Char and Tar during Devolatilization. *Symp. (Int.) Combust., [Proc.]* **1991**, *23*, 1231−1237.
(269) Pugmire, R. J.; Solum, M. S.; Grant, D. M.; Critchfield, S.; Fletcher, T. H. Structural Evolution of Matched Tar-Char Pairs in Rapid Pyrolysis Experiments. *Fuel* **1991**, *70* (3), 414−423.
(270) Roberts, V. M.; Stein, V.; Reiner, T.; Lemonidou, A.; Li, X.; Lercher, J. A. Towards Quantitative Catalytic Lignin Depolymerization. *Chem. - Eur. J.* **2011**, *17* (21), 5939−5948.
(271) Li, J.; Henriksson, G.; Gellerstedt, G. Lignin Depolymerization/Repolymerization and Its Critical Role for Delignification of Aspen Wood by Steam Explosion. *Bioresour. Technol.* **2007**, *98* (16), 3061−3068.
(272) Kozliak, E. I.; Kubátová, A.; Artemyeva, A. A.; Nagel, E.; Zhang, C.; Rajappagowda, R. B.; Smirnova, A. L. Thermal Liquefaction of Lignin to Aromatics: Efficiency, Selectivity, and Product Analysis. *ACS Sustainable Chem. Eng.* **2016**, *4* (10), 5106−5122.
(273) Hepditch, M. M.; Thring, R. W. Degradation of Solvolysis Lignin Using Lewis Acid Catalysts. *Can. J. Chem. Eng.* **2000**, *78*, 226−231.
(274) Kumar, S.; Lange, J. P.; Van Rossum, G.; Kersten, S. R. A. Liquefaction of Lignocellulose: Do Basic and Acidic Additives Help Out? *Chem. Eng. J.* **2015**, *278*, 99−104.
(275) Singh, R.; Prakash, A.; Dhiman, S. K.; Balagurumurthy, B.; Arora, A. K.; Puri, S. K.; Bhaskar, T. Hydrothermal Conversion of Lignin to Substituted Phenols and Aromatic Ethers. *Bioresour. Technol.* **2014**, *165* (C), 319−322.
(276) Shu, R.; Long, J.; Xu, Y.; Ma, L.; Zhang, Q.; Wang, T.; Wang, C.; Yuan, Z.; Wu, Q. Investigation on the Structural Effect of Lignin during the Hydrogenolysis Process. *Bioresour. Technol.* **2016**, *200*, 14−22.
(277) Shuai, L.; Amiri, M. T.; Questell-Santiago, Y. M.; Heroguel, F.; Li, Y.; Kim, H.; Meilan, R.; Chapple, C.; Ralph, J.; Luterbacher, J. S. Formaldehyde Stabilization Facilitates Lignin Monomer Production during Biomass Depolymerization. *Science (Washington, DC, U. S.)* **2016**, *354* (6310), 329−333.
(278) Farag, S.; Kouisni, L.; Chaouki, J. Lumped Approach in Kinetic Modeling of Microwave Pyrolysis of Kraft Lignin. *Energy Fuels* **2014**, *28* (2), 1406−1417.
(279) Yong, T. L. K.; Matsumura, Y. Kinetic Analysis of Lignin Hydrothermal Conversion in Sub- and Supercritical Water. *Ind. Eng. Chem. Res.* **2013**, *52* (16), 5626−5639.
(280) Yong, T. L. K.; Matsumura, Y. Reaction Kinetics of the Lignin Conversion in Supercritical Water. *Ind. Eng. Chem. Res.* **2012**, *51* (37), 11975−11988.
(281) Zhang, B.; Huang, H. J.; Ramaswamy, S. Reaction Kinetics of the Hydrothermal Treatment of Lignin. *Appl. Biochem. Biotechnol.* **2008**, *147* (1−3), 119−131.
(282) Gasson, J. R.; Forchheim, D.; Sutter, T.; Hornung, U.; Kruse, A.; Barth, T. Modeling the Lignin Degradation Kinetics in an Ethanol/Formic Acid Solvolysis Approach. Part 1. Kinetic Model Development. *Ind. Eng. Chem. Res.* **2012**, *51* (32), 10595−10606.
(283) Forchheim, D.; Gasson, J. R.; Hornung, U.; Kruse, A.; Barth, T. Modeling the Lignin Degradation Kinetics in a Ethanol/Formic Acid Solvolysis Approach. Part 2. Validation and Transfer to Variable Conditions. *Ind. Eng. Chem. Res.* **2012**, *51* (46), 15053−15063.
(284) Iatridis, B.; Gavalas, G. R. Pyrolysis of a Precipitated Kraft Lignin. *Ind. Eng. Chem. Prod. Res. Dev.* **1979**, *18* (2), 127−130.
(285) Jakab, E.; Faix, O.; Till, F.; Székely, T. Thermogravimetry/Mass Spectrometry Study of Six Lignins within the Scope of an International Round Robin Test. *J. Anal. Appl. Pyrolysis* **1995**, *35* (2), 167−179.
(286) Pasquali, C. E. L.; Herrera, H. Pyrolysis of Lignin and IR Analysis of Residues. *Thermochim. Acta* **1997**, *293* (1−2), 39−46.
(287) Williams, P. T.; Besler, S. The Influence of Temperature and Heating Rate on the Slow Pyrolysis of Biomass. *Renewable Energy* **1996**, *7* (3), 233−250.
(288) Hough, B. R.; Beck, D. A. C.; Schwartz, D. T.; Pfaendtner, J. Application of Machine Learning to Pyrolysis Reaction Networks: Reducing Model Solution Time to Enable Process Optimization. *Comput. Chem. Eng.* **2017**, *104*, 56−63.
(289) Westmoreland, P. R. Pyrolysis Kinetics for Lignocellulosic Biomass-to-Oil from Molecular Modeling. *Curr. Opin. Chem. Eng.* **2019**, *23*, 123−129.
(290) Van de Vijver, R.; Vandewiele, N. M.; Bhoorasingh, P. L.; Slakman, B. L.; Khanshan, F. S.; Carstensen, H. H.; Reyniers, M. F.; Marin, G. B.; West, R. H.; Van Geem, K. M. Automatic Mechanism and Kinetic Model Generation for Gas- and Solution-Phase Processes: A Perspective on Best Practices, Recent Advances, and Future Challenges. *Int. J. Chem. Kinet.* **2015**, *47* (4), 199−231.
(291) Vernuccio, S.; Broadbelt, L. J. Discerning Complex Reaction Networks Using Automated Generators. *AIChE J.* **2019**, *65* (8), 1−20.
(292) Zhou, X.; Mayes, H. B.; Broadbelt, L. J.; Nolte, M. W.; Shanks, B. H. Fast Pyrolysis of Glucose-Based Carbohydrates with Added NaCl Part 1: Experiments and Development of a Mechanistic Model. *AIChE J.* **2016**, *62* (3), 766−777.
(293) Zhou, X.; Mayes, H. B.; Broadbelt, L. J.; Nolte, M. W.; Shanks, B. H. Fast Pyrolysis of Glucose-Based Carbohydrates with Added NaCl Part 2: Validation and Evaluation of the Mechanistic Model. *AIChE J.* **2016**, *62* (3), 778−791.
(294) Zhou, X.; Nolte, M. W.; Mayes, H. B.; Shanks, B. H.; Broadbelt, L. J. Experimental and Mechanistic Modeling of Fast Pyrolysis of Neat Glucose-Based Carbohydrates. 1. Experiments and Development of a Detailed Mechanistic Model. *Ind. Eng. Chem. Res.* **2014**, *53* (34), 13274−13289.
(295) Zhou, X.; Li, W.; Mabon, R.; Broadbelt, L. J. A Mechanistic Model of Fast Pyrolysis of Hemicellulose. *Energy Environ. Sci.* **2018**, *11* (5), 1240−1260.
(296) Joshi, P. V.; Freund, H.; Klein, M. T. Directed Kinetic Model Building: Seeding as a Model Reduction Tool. *Energy Fuels* **1999**, *13* (4), 877−880.
(297) Dellon, L. D.; Sung, C. Y.; Robichaud, D. J.; Broadbelt, L. J. 110th Anniversary: Microkinetic Modeling of the Vapor Phase Upgrading of Biomass-Derived Oxygenates. *Ind. Eng. Chem. Res.* **2019**, *58*, 15173−15189.
(298) Forsythe, W. G.; Garrett, M. D.; Hardacre, C.; Nieuwenhuyzen, M.; Sheldrake, G. N. An Efficient and Flexible Synthesis of Model Lignin Oligomers. *Green Chem.* **2013**, *15* (11), 3031−3038.
(299) Mar, B. D.; Kulik, H. J. Depolymerization Pathways for Branching Lignin Spirodienone Units Revealed with Ab Initio Steered Molecular Dynamics. *J. Phys. Chem. A* **2017**, *121* (2), 532−5430.

https://dx.doi.org/10.1021/acs.iecr.9b05744
Ind. Eng. Chem. Res. 2020, 59, 526−555

(300) Mar, B. D.; Qi, H. W.; Liu, F.; Kulik, H. J. Ab Initio Screening Approach for the Discovery of Lignin Polymer Breaking Pathways. *J. Phys. Chem. A* **2015**, *119* (24), 6551−6562.
(301) Watts, H. D.; Mohamed, M. N. A.; Kubicki, J. D. Comparison of Multistandard and TMS-Standard Calculated NMR Shifts for Coniferyl Alcohol and Application of the Multistandard Method to Lignin Dimers. *J. Phys. Chem. B* **2011**, *115* (9), 1958−1970.
(302) Jalali-Heravi, M.; Masoum, S.; Shahbazikhah, P. Simulation Of13C Nuclear Magnetic Resonance Spectra of Lignin Compounds Using Principal Component Analysis and Artificial Neural Networks. *J. Magn. Reson.* **2004**, *171* (1), 176−185.
(303) Zhang, T.; Li, X.; Qiao, X.; Zheng, M.; Guo, L.; Song, W.; Lin, W. Initial Mechanisms for an Overall Behavior of Lignin Pyrolysis through Large-Scale ReaxFF Molecular Dynamics Simulations. *Energy Fuels* **2016**, *30* (4), 3140−3150.
(304) Zhang, T.; Li, X.; Guo, L. Initial Reactivity of Linkages and Monomer Rings in Lignin Pyrolysis Revealed by ReaxFF Molecular Dynamics. *Langmuir* **2017**, *33* (42), 11646−11657.
(305) Elder, T.; Beste, A. Density Functional Theory Study of the Concerted Pyrolysis Mechanism for Lignin Models. *Energy Fuels* **2014**, *28* (8), 5229−5235.
(306) Sheng, H.; Murria, P.; Degenstein, J. C.; Tang, W.; Riedeman, J. S.; Hurt, M. R.; Dow, A.; Klein, I.; Zhu, H.; Nash, J. J.; Abu-Omar, M.; Agrawal, R.; Delgass, W. N.; Ribeiro, F. H.; Kenttamaa, H. I. Initial Products and Reaction Mechanisms for Fast Pyrolysis of Synthetic G-Lignin Oligomers with β-O-4 Linkages via On-Line Mass Spectrometry and Quantum Chemical Calculations. *ChemistrySelect* **2017**, *2* (24), 7185−7193.

https://dx.doi.org/10.1021/acs.iecr.9b05744
Ind. Eng. Chem. Res. 2020, 59, 526−555